

Thermal Spray Coatings Workshop:
Sensors, Modeling and Control Strategies
Summary of a Workshop Held at
National Institute of Standards and Technology

Frank S. Biancaniello
Stephen D. Ridder

U.S. DEPARTMENT OF COMMERCE
Technology Administration
Metallurgy Division
Materials Science and Engineering Laboratory
National Institute of Standards
and Technology
Gaithersburg, MD 20899



U.S. DEPARTMENT OF COMMERCE
Technology Administration
National Institute of Standards and
Technology

Thermal Spray Coatings Workshop:
Sensors, Modeling and Control Strategies
Summary of a Workshop Held at
National Institute of Standards and Technology

Frank S. Biancaniello
Stephen D. Ridder

U.S. DEPARTMENT OF COMMERCE
Technology Administration
Metallurgy Division
Materials Science and Engineering Laboratory
National Institute of Standards
and Technology
Gaithersburg, MD 20899

November 1998



U.S. DEPARTMENT OF COMMERCE
William M. Daley, Secretary

TECHNOLOGY ADMINISTRATION
Gary R. Bachula, Acting Under Secretary
for Technology

NATIONAL INSTITUTE OF STANDARDS
AND TECHNOLOGY
Raymond G. Kammer, Director

TABLE OF CONTENTS

TABLE OF CONTENTS	i
DISCLAIMER	ii
WORKSHOP SUMMARY	1
Purpose	1
WORKSHOP AGENDA	2
PRESENTATIONS	3
Introductory Presentations	3
Workshop Presentations	3
DISCUSSION	4
CONCLUSIONS	5
ATTENDANCE LIST	7
Industry	7
Academia	9
National Labs (non NIST)	10
NIST	11
PRESENTATION SLIDES	13
<i>NIST Ceramic Coatings Program</i>	13
<i>Process Diagnostics</i>	23
<i>Spectroscopy Measurements</i>	29
<i>Thermal Imaging</i>	39
<i>Numerical Simulation of Underexpanded Jets</i>	47
<i>Process Control</i>	53
<i>Sensors and Controls for Thermal Spray: Is there a need?</i>	59
<i>Currently used Sensors</i>	65
<i>Measurement of DC Plasma Arc Fluctuations</i>	83
<i>Enthalpy Probe</i>	87
<i>Impact and Solidification of Molten Nickel Droplets</i>	99
NIST THERMAL SPRAY RESEARCH PROGRAM	109

DISCLAIMER

This report is intended as a record of the presentations and discussions which took place at a NIST Metallurgy Division sponsored workshop. The opinions, conclusions, or recommendations that are expressed herein are those of the organizers or individual presenters and do not necessarily reflect the views of NIST. All references to commercial equipment in this report are for identification purposes only and in no way constitute any endorsement or evaluation of the relative merits of such equipment by NIST.

**[RETURN TO
TABLE OF CONTENTS](#)**

WORKSHOP SUMMARY

Purpose

The NIST Metallurgy Division has initiated a research program to investigate coatings produced by thermal spray (TS) techniques. The focus of this research is the development of measurement tools that will aid in the understanding and/or control of the plasma spray process. This process uses plasma jets (generated by either DC or AC arcs) to melt or soften coating feed-stocks and then propel this material onto various substrates. The geometry and operating parameters of the plasma jet hardware, or “gun”, depend on the intended function of the resulting TS coated part. Currently TS coatings are produced by skilled technicians, however, it is now being adapted for automatic control using robotics. Intelligent Processing incorporating expert systems will probably be employed in most advanced systems. This move to robotics is not only to reduce costs, but to improve the reliability of spray coatings and thus enable the use of coatings in high volume applications such as automotive components and property critical devices such as the proposed high-efficiency gas turbines.

Recently a number of advances have been made in new measurement systems, sensors, and modeling techniques that can lead to improved design and control of thermal spray processes. The objectives of this workshop were to present descriptions of some of these advances and their industrial applications, demonstrate some of the systems currently available or under development at NIST, and provide a forum to allow discussion of the current industrial measurement needs for thermal spray coatings.

**[RETURN TO
TABLE OF CONTENTS](#)**

WORKSHOP AGENDA

9:00	Introduction	J. R. Manning (NIST)
9:05	Overview of NIST Mission	C. A. Handwerker (NIST)
9:10	ATP Programs	R. J. Schaefer (NIST)
9:20	MSEL Programs	S. J. Dapkunas (NIST)
9:30	NIST Prior Expertise in Intelligent Processing	S. D. Ridder (NIST)
9:40	NIST Previous Discussions with Thermal Spray Industry	F. S. Biancaniello (NIST)
9:45	NIST Current Status and Future Plans (intro with SBIR activities)	S. D. Ridder (NIST)
	Diagnostics (high-speed video, cinema, holography, spectroscopy, etc.)	
9:50	High-Speed Video	S. D. Ridder (NIST)
10:00	Spectroscopy Measurements	D. W. Bonnell (NIST)
	Sensors (thermal imaging, velocity, size, etc.)	
10:15	Thermal Imaging	J. E. Craig (Stratonics)
	Modeling (CFD, schlieren, etc.)	
10:30	Numerical Simulation of Underexpanded Jets	A. Johnson (NIST)
	Expert Systems (parameterization, truth tables, etc.)	
10:45	Process Control	S. A. Osella (ICT)
11:00	Break	
11:15	Demonstration of NIST Spray Facility (Industrial Building, Room B122)	SDR and FSB (NIST)
	Importance of Sensors and Diagnostics in controlling Industrial Thermal Spray Processes	
11:45	Overview	C. C. Berndt (SUNY Stony Brook)
12:00	Currently used Sensors	C. Moreau (NRC-CNRC)
12:15	Modeling of Thermal Spray	J. Heberlein (U. of Minnesota)
12:30	Enthalpy Probe	M. Boulos (U. of Sherbrooke)
12:45	Imaging for Rapid Prototyping	W. H. Hofmeister (Vanderbilt U.)
1:00	Lunch	
2:00	Industrial Needs as viewed by equipment manufacturers (intro)	D. Crawmer (Praxair)
2:05	Discussion and Suggestions concerning industrial needs	participants
3:30	adjourn	

**[RETURN TO
TABLE OF CONTENTS](#)**

PRESENTATIONS

Introductory Presentations

The program started with an introductory welcome by **J. R. Manning**, group leader for Metallurgical Processing in the NIST Metallurgy Division. **C. A. Handwerker**, Chief of NIST Metallurgy Division, then gave an overview of the NIST mission. This was followed by slide presentations by **R. J. Schaefer** outlining the NIST Advanced Technology Program (ATP) and **S. J. Dapkunas**, of the NIST Ceramics Division, on the current MSEL Ceramics Coating Program.

Workshop Presentations

Following the introductory slides were presentations of NIST work. **S. D. Ridder** of the NIST Metallurgy Division presented slides to provide an overview of the NIST Metallurgy Division's previous research in intelligent processing, imaging diagnostics, and advanced sensors. **F. S. Biancaniello**, also of the NIST Metallurgy Division presented slides outlining the recent discussions between NIST researchers and the thermal spray industry. These presentations were intended to show the attendees the current status of research in metals processing at NIST and how these recent activities on powder production are relevant to new programs being organized on thermal spray processing.

New research results on non-contact spectrometer-based temperature measurements of particles in flight within a plasma jet were presented by **D. Bonnell**. He discussed correction of the measured spectrum by subtracting emission from the plume. The technique appears to be working well for temperature measurements but showed the puzzling result of temperature increasing with distance of travel. The next speaker, **J. Craig** (Stratonics), showed results from a new imaging pyrometer system based on 2 images, typically at 950 nm and 700 nm, in which the pixels of the two images match precisely. He concluded that temperature decreases with distance of travel. Work on calibration of this new sensor continues through funding provided by a NIST Small Business Innovative Research (SBIR) award.

A. Johnson (NIST Fluid Flow Group) presented slides on techniques for Computational Fluid Dynamics (CFD) modeling of underexpanded gas jets as they apply to a thermal spray plasma jet. This NIST effort on CFD modeling of compressible fluid jets was initiated several years ago to provide a software tool that could be used by engineers to help optimize the design of gas atomizers used for the production of metal powder. This CFD tool has been applied to the design of commercial gas atomizers with significant improvements in production efficiencies. It is likely that similar studies of thermal spray gas jet assemblies could lead to more efficient and/or more controllable thermal spray gun designs.

S. A. Osella (Intelligent Computing Technologies, Inc.) presented slides on a novel technique to develop and implement expert system driven process controllers. The software tool shown in these slides was developed by ICT using funding provided by a NIST SBIR award. The need for this tool was realized during the development of an expert system controller for the NIST gas atomizer. This software can help organize and validate complex process controllers as used for a thermal spray system.

The attendees were brought to the NIST thermal spray facility for a demonstration of the Stratonics sensor measuring in-flight particle temperature and velocity of plasma sprayed zirconia powder. Following this laboratory demonstration several invited speakers presented their views on various aspects of the thermal spray process.

C. Berndt (SUNY Stony Brook) pointed out the need for sensors to be complementary to modeling, and to be related to real sprayers. An abundance of measurements have already been made but standards are needed. One important subject is thermal spray processing of nanoparticles, on which a conference will be held next year. An economic analysis was shown that outlined the current and future projection of the thermal spray market.

C. Moreau (NRC-CNRC) pointed out the need to understand three zones: zone 1, where heat is generated, and voltage fluctuations depending on the surface of the electrode are generated: zone 2, in which the particles are heated and accelerated: and zone 3, in which the coating builds up.

J. Heberlein (U. of Minnesota) described work to characterize the environment that heats the powder. This requires small time-scale resolution monitoring of sound and voltage fluctuations. Using a 100 μ s to 1 ms time-scale resolution could provide useful data concerning the arc characteristics related to cathode and anode erosion that ultimately affect the output flux of torch power.

M. Boulos (U. of Sherbrooke) pointed out that cold particles entrained in the plasma will not be detected by emission techniques, but they can ruin a coating. He described an enthalpy probe which is intrusive but yields good data.

W. Hofmeister (Vanderbilt U.) described NASA-sponsored work on velocity of solidification of undercooled melts, droplet splats with G. Trapaga of MIT, and application of high-speed thermal imaging to the LENS process (a net shape processing technique that consolidates powder with a high-power laser).

DISCUSSION

The discussion was lead by Darryl Crawmer of Praxair. He started the discussion by presenting his own views, as an equipment manufacturer, of industrial needs. The first area he mentioned was SRM's. We already have one for particle size, and Phase II of this is coming out. They need one for X-ray diffraction to show the crystallography of yttria-stabilized zirconia.

The major point of his discussion, however, was the need to bring the thermal spray process under control: at present it is not. If the process were well controlled, post-processing quality control would be a moot point. There is a long way to go before plasma spray can be a 6σ process. Control of the spray process has moved from the old location at the back of the gun (i.e., controlling the applied voltage and current) to control of the energy at the front of the gun (10 years old but still not widely accepted). Still some distance off, in development and acceptance, is control based on particle velocities, temperatures, and trajectories, or characterization of the deposit itself.

Advanced control technology needs to be embedded in such a way that it can be used by real operators, not skilled technicians, and so that it will be available to users beyond the high-tech companies such as Praxair, GE, or Howmet.

In the discussion, it was asked what will inspire people to invest in advanced technology. The response was the opening of new markets which will become available with higher reliability. Most plasma spray is now at 1σ (68%), while high-end shops try to be at 2σ (95%). This is not acceptable when failure of a plasma spray process could shut down a production facility. Another example is coating of a paper roll, which can involve spraying for 24 hours at a time, so there is a need to know if the deposit is uniform.

The drive for these sensors is working from the top down: Praxair, Tafa, GE, P&W, and vendors are developing tools. Interest from the automobile industry is not huge at present, but bore coating could become a driver. Big customers are not currently putting pressure on small suppliers to do more.

Currently, in a \$10 million shop, \$3 million is used to purchase powder, easily half of which is discarded due to various process inefficiencies. The cost of wasted powder (as well as any other costs resulting from poor process control) is simply passed on to the customer, a situation which will change only as the competition increases.

Users want a "magic wand" to stabilize the process - better predictability, reliability, etc. They need better process control, substrate control, and powder control, all parameters that contribute to control of the coating structure. Current practice is to qualify the spray booth at the start of each day, which is not reliable if the gun deteriorates too fast. Current practice by many is reputed to be "if it sticks, ship it," or application of the "hammer test." A sensor for residual stresses would be highly desirable.

Powder supply has huge day-to-day and lot-to-lot variability, and most customers will not pay extra for

more uniform powder. Customers can specify powder characteristics, with GE, Pratt, and RR driving this but the sprayers will pay extra for the powder only if the specifications are tightened. Results can change with time as a result of wear of the electrodes (anode and cathode). Sensors are desired which are fast, cheap, easy, and non-intrusive.

Sensors, in order of importance, are:

- 1) Temperature
- 2) Velocity
- 3) Trajectory
- 4) (others)
- 5) Residual Stress

Temperature, velocity, and trajectory sensors are here but implementation is the problem. A pulsed laser visualization system costs \$80k to \$100k. A few sales might be made of a \$50k system, to high-end users, a system for \$10k to \$20k would sell to every shop. It may be necessary to be more selective in what you need, to cut down on the price.

Benchmarking could be done at NIST to relate product to input and process conditions - a typical NIST activity.

An ASM subcommittee is trying to standardize metallographic techniques to prepare coatings for examination, so that coatings can be more readily compared to each other. The first standard procedures should address zirconia powders and coatings followed by similar procedures for WC. We need standardized powder and standardized evaluation of coatings.

Education, new technologies, and patience are needed.

CONCLUSIONS

Thermal spray technology could attain much more widespread use if one could attain higher levels of reliability, predictability, repeatability, etc., the same characteristics which were identified as needs for numerous surface engineering technologies in the recent ATP-sponsored workshop. High volume markets such as the transportation and consumer electronics industries are reluctant to take advantage of the potential cost savings derived from using thermal spray to replace other processes until they are convinced that the reliability issues are addressed. This generally means that the coatings must be consistent from one production run to the next using feedstock from different sources. There appeared to be a consensus that these characteristics could be achieved by control based on the temperature, velocity, and trajectory of the particulate materials. This would compensate for variability due to differences in powder feed stock and erosion of the plasma gun electrodes. Characterization of gun voltage in the temporal domain with a 100 μ s to 1 ms time-scale should be investigated as a means to quantify erosion of the electrodes.

Currently available sensor/control systems (pulsed laser illuminated) are too expensive (\$80k to \$100k) to be attractive. At \$50k, a few systems might be sold to high technology users, and at \$10k to \$20k the systems would probably become universal. There is some concern among those producing sensors as to the current and future market for the sale of spray equipment. This has a direct effect on the potential market for sensor and control systems. If this total spray processing equipment market is not sufficiently large, then sensor and control system sales will not reach the volume required to realize price reductions. One likely development that will provide increased markets for sensor and control systems is that many of the sensors needed for thermal spray equipment will find use in other processing tools such as atomization, spray forming, rapid prototyping, and welding.

Another technical challenge that needs to be met before substantial improvements can be made to coating reliability is the development of better coating and substrate quality tests. Standard test methods of coating performance such as density, hardness, wear, adhesion, roughness, thermal conductivity, etc. have been developed but most are not well accepted and for most products each company has their own specialized test procedures that they rely on for process quality control. Development of on-line process control sensors that measure coating and substrate properties in real-time will likely lag behind the development and acceptance of off-line standard test methods. A short list of some of the more important test methods and process control sensors existing or needed that were mentioned follows:

Coating quality standard test methods needs

- 1) metallographic specimen preparation methods
- 2) measurement of crystal phase content
- 3) substrate surface preparation and surface roughness measurements
- 4) coating performance or quality measurements (roughness, density, thermal properties, adhesion, etc.)

Reliable, inexpensive rugged sensor needs

- 1) particle temperature, velocity (trajectory)
- 2) substrate roughness
- 3) coating properties (density, thermal properties, etc.)
- 4) anode wear monitor

As techniques for measuring coating and substrate properties are improved the ultimate process potentials will be better known. These measurements will also provide information concerning what sensor and control technologies are needed to realize the higher quality coatings. Further work is needed to assure potential users that the sensors provide valid measurements and that the control systems can use this sensor information to produce reliable, predictable, and repeatable thermal spray coatings. However, even if higher quality coatings are possible, thermal sprayers are unlikely to be interested in new sensor/control systems that will produce these better coatings until their customers start demanding higher quality.

ATTENDANCE LIST**Industry**

Vladimir Belashchenko
TAFE Inc.
146 Pembroke Rd.
Concord, NH 03301
603-223-2188
603-225-4342 (fax)
vlad@tafa.com

Jacques Blain
TECNAR Automation Ltée
3502 First Street
St. Hubert (Quebec)
Canada J3Y 8Y5
450-443-5335
450-443-4880 (fax)
jblain@tecnar-automation.com

Rick Burmeister
Measurement & Control Technologies
810 Greenleaf Ave.
Charlotte, NC 28202
704-334-5878
704-334-1539 (fax)
rburmeister@compuserve.com

J. J. (Sean) Conway
Crucible Compaction Metals
1001 Robb Hill Road
Oakdale, PA 15071
toll free-888-923-2670
412-923-2670
412-788-4240 (fax)
conway@cruciblecompaction.com

James E. Craig
Stratonics, Inc.
23151 Verdugo Drive, Suite 114
Laguna Hills, CA 92653-1340
949-461-7060
949-461-7069 (fax)
info@stratonics.com

Daryl Crawmer
Praxair Thermal Spray Systems
N 670 Communication Drive
Appleton, WI 54915
920-997-6167
920-734-2160 (fax)
dcrawme@appl.psti.praxair.com

Brian A. Hann
Crucible Compaction Metals
1001 Robb Hill Road
Oakdale, PA 15071
toll free-888-923-2670
412-923-2670
412-788-4240 (fax)
hann@cruciblecompaction.com

Y. C. Lau
GE CRD
1 Research Circle
Niskayuna, NY 12309
518-387-6017
518-387-7495 (fax)
Lau@crd.ge.com

David Y. Lee
Stratonics, Inc.
23151 Verdugo Drive, Suite 114
Laguna Hills, CA 92653-1340
949-461-7060
949-461-7069 (fax)

Timothy McKechnie
Plasma Processes
4914 D Moores Mill Rd.
Huntsville, AL 35811
258-851-7653
258-859-4134 (fax)
Tim.McK@plasmapros.com

Stephen A. Osella
ICT, Inc.
6309 John Chisum Ln.
Austin, TX 78749-1839
512-301-2444
intcomtec@aol.com

Tsung-Yu Pan
Ford Research Laboratory
20000 Rotunda Drive
MD 3135, SRL, P.O. Box 2053
Dearborn, MI 48121-2053
313-322-6845
313-323-1129 (fax)
tpan@ford.com

Ron Parker
Stratonics, Inc.
P.O. Box 206
Geneseo, NY 14454
716-346-2447
parker_ron@compuserve.com

Jack Ramsey
Trans-Tech
5520 Adamstown Road
Adamstown, MD 21710
301-874-6453
301-695-7065 (fax)
P.O. Box 69
jramsey@alphaind.com

Jim Ruud
GE Corporate R&D
K-1 MB165
1 Research Circle
Niskayuna, NY 12309
518-387-7052
518-387-5576
rwd@crd.ge.com

Gregory Wuest
Sulzer Metco
Westbury, NY
516-338-2217
516-338-2488 (fax)
gregory.wuest@sulzer.ch

Academia

Christopher C. Berndt
SUNY at Stony Brook
306 Old Engineering
Stony Brook, NY 11794-2275
516-6328507
516-632-8525 (fax)
cberndt@notes.cc.sunysb.edu

Maher Boulos
Universite de Sherbrooke
Centre de Recherche en Technologie des Plasmas
Faculte des Sciences Appliquees
Sherbrooke (Quebec)
Canada J1K 2R1
819-821-7168
819-821-7955 (fax)

Donna Hale
INEEL/Univ. Of Idaho
P.O. Box 1625
MS 3765
Idaho Falls, ID 83415-3765
208-526-1744
208-526-0425 (fax)
lh5@inel.gov

Joachim Heberlein
Univ. Of Minnesota
Dept. Of Mechanical Engineering
111 Church St. S.E.
Minneapolis, MN 55455
612-625-4538
612-624-1398 (fax)
jvrh@me.umn.edu

William H. Hofmeister
Vanderbilt Univ.
Dept. Of Chemical Engineering
P.O. Box 1604
Nashville, TN 37235
615-322-7053
615-343-0466 (fax)
hof@vuse.vanderbilt.edu

National Labs (non NIST)

James R. Fincke
INEEL
Lockheed Martin Idaho Technologies Co.
P.O. Box 1625
MS 2211
Idaho Falls, ID 83415-2211
208-526-2031
208-526-5327 (fax)
jfl@inel.gov

Kendall J. Hollis
Los Alamos National Laboratory
MS G770
Los Alamos, NM 87545
505-665-8223
505-667-5268 (fax)
hollis@mst.lanl.gov

Leslie Kohler
NSWC
9500 MacArthur Blvd.
West Bethesda, MD 20817
Code 612
301-227-5096
301-227-5548 (fax)
KohlerLK@nswccd.navy.mil

Luc Leblanc
National Research Council Canada
75 De Mortagne
Boucherville (Quebec)
Canada J4B 6Y4
450-641-5232
450-641-5106 (fax)
luc.leblanc@nrc.ca

Christian Moreau
National Research Council Canada
75 De Mortagne
Boucherville (Quebec)
Canada J4B 6Y4
450-641-5228
450-641-5106 (fax)
christian.moreau@nrc.ca

John E. Smugeresky
Sandia National Laboratories
MS 9403; Dept. 8712
Livermore, CA 94551-0969
925-294-2910
925-294-3410 (fax)
smug@sandia.gov

NIST

Mail Address for NIST employees:

Name

NAT'L INST STDS & TECH
100 BUREAU DR STOP xxxx
GAITHERSBURG, MD 20899-xxxx

Frank S. Biancaniello
STOP 8556
301-975-6175
301-869-5629 (fax)
frank.biancaniello@nist.gov

William J. Boettinger
STOP 8555
301-975-6160
301-975-4553 (fax)
william.boettinger@nist.gov

David W. Bonnell
STOP 8522
301-975-5755
301-975-5334 (fax)
Bonnell@nist.gov

Paul A. Boyer
STOP 8556
301-975-6970
301-869-5629 (fax)
paul.boyer@nist.gov

Sam R. Coriell
STOP 8555
301-975-6169
301-975-4553 (fax)
sam.coriell@nist.gov

Stanley J. Dapkunas
STOP 8520
301-975-6130
301-990-8729 (fax)
stanley.dapkunas@nist.gov

Albert Davydov
STOP 8555
301-975-4916
301-975-4553 (fax)
albert.davydov@nist.gov

Carol A. Handwerker
STOP 8550
301-975-6158
301-975-4553 (fax)
carol.handwerker@nist.gov

John W. Hastie
STOP 8522
301-975-5754
301-975-5334 (fax)
john.hastie@nist.gov

Rodney D. Jiggetts
STOP 8555
301-975-5122
301-869-5629 (fax)
rodney.jiggetts@nist.gov

Aaron Johnson
STOP 8361
301-975-5954
301-258-9201 (fax)
aaron.johnson@nist.gov

John R. Manning
STOP 8555
301-975-6157
301-975-4553 (fax)
manning@nist.gov

Robert L. Parke
STOP 8556
301-975-6174
301-869-5629 (fax)
robert.parke@nist.gov

Albert J. Paul
STOP 8522
301-975-6004
301-975-5334 (fax)
albert.paul@nist.gov

Patrick Pei
STOP 8520
301-975-3681
301-990-8729 (fax)
patrick.pei@nist.gov

Cary Presser
STOP 8360
301-975-2612
301-869-5924 (fax)
cary.presser@nist.gov

Richard E. Ricker
STOP 8553
301-975-6023
301-975-4553 (fax)
richard.ricker@nist.gov

Stephen D. Ridder
STOP 8556
301-975-6175
301-869-5629 (fax)
stephen.ridder@nist.gov

Robert J. Schaefer
STOP 8555
301-975-5961
301-975-4553 (fax)
robert.schaefer@nist.gov

Jay S. Wallace
STOP 8520
301-975-5984
301-990-8729 (fax)
jay.wallace@nist.gov

PRESENTATION SLIDES*NIST Ceramic Coatings Program*

S. J. Dapkunas (NIST)

NIST CERAMICS COATINGS PROGRAM

**S. J. Dapkunas
Ceramics Division
Materials Science and Engineering Laboratory
National Institute of Standards and Technology**

**Thermal Spray Workshop on Sensors, Modeling and
Control Strategies**

**November 19, 1998
Gaithersburg, MD**

PROGRAM OBJECTIVE

**To develop measurement, characterization and modeling
methods which support improvement of process control and
property/performance prediction**

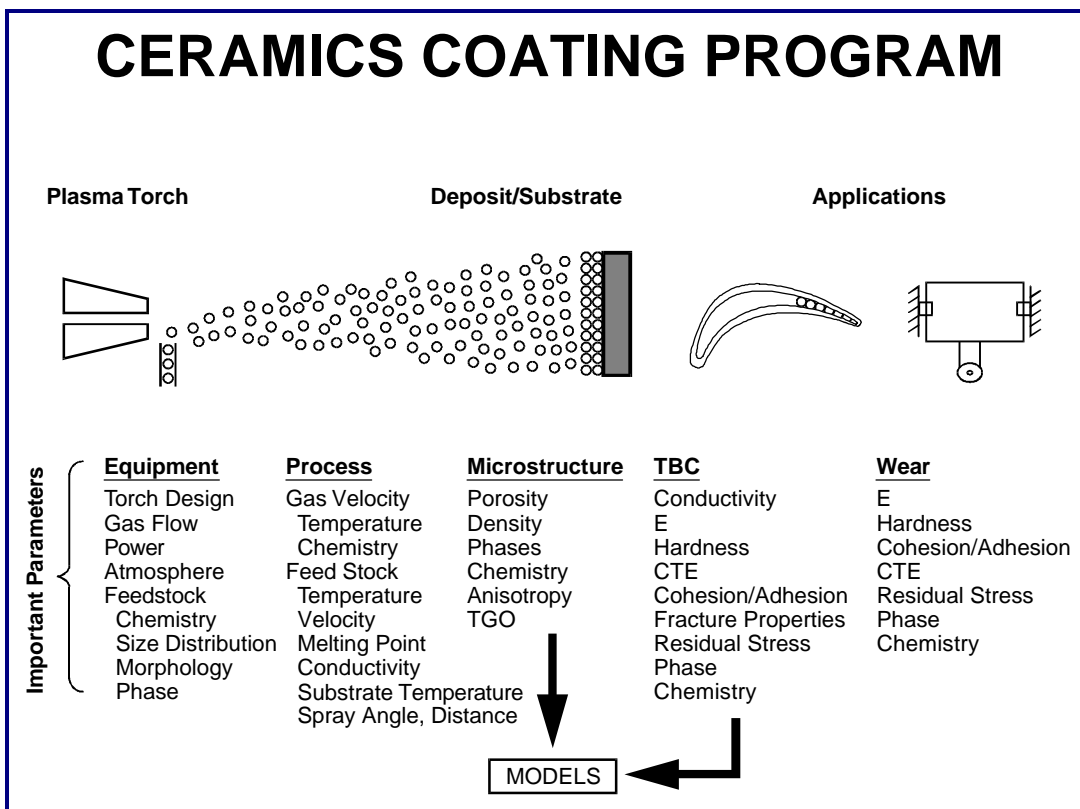
PROGRAM STRATEGY

- *Current Emphasis*
 - Thermal Barrier Coatings
 - Plasma Spray Deposition
- *Future Emphasis*
 - Wear and Erosion Resistant Coatings
 - Additional Processing Types
 - Functionally Graded Materials
- Utilize NIST analytical capability with academic and industrial processing capability.
- Cooperatively set goals with partners, focus on specific issue.
- Focus NIST research efforts on the same materials/samples to intensify effect.
- Transfer results through direct collaboration.
- Implement measurement methods through codified standards, SRMs, data, models.

NIST Ceramic Coatings Program (cont.)

S. J. Dapkunas (NIST)

- COLLABORATIONS**
- Powder Producers
 - Equipment Manufacturers
 - OEMs
 - Instrument Manufacturers
 - Oak Ridge National Laboratory
 - Sandia National Laboratory
 - SUNY/Stony Brook
 - Mechanical Engineering Laboratory/Tskuba
 - National Aerospace Laboratory/Kakuda
 - BAM, Berlin
 - DLR, Cologne
 - IPP, Prague



NIST Ceramic Coatings Program (cont.)

S. J. Dapkunas (NIST)

PROGRAM STRUCTURE**Processing**

Develop characterization and measurement methods for feedstock powder and relate to deposition behavior and microstructural features

Coating Characterization

Develop methods to examine microstructure and properties of coatings to provide input to property model development and relate to processing parameters

Modeling

Develop microstructural models to describe microstructural effects on properties/performance

SRM 1982- Zirconia Thermal Spray Powder- Particle Size Distribution**METHODS INCLUDED IN CERTIFICATION**

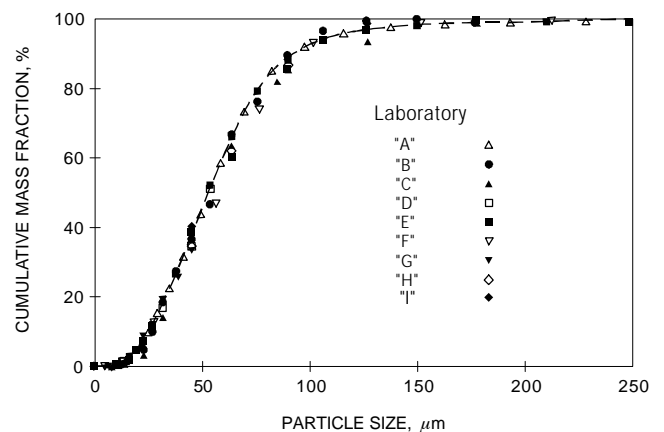
Certified Values- SEM

*Reference Values- Laser Light Scattering
Sieving*

*Additional Information- Chemistry, Specific Gravity, Tap Density,
Hall Apparent Density, Hall Flow Rate,
Specific Surface Area*

PARTICIPATING ORGANIZATIONS

*Leeds & Northrup, Alloys International, Hoeganaes, Sulzer Metco,
Zircoa, Stellite Coatings, Metallurgical Technologies,
Pratt & Whitney, Praxair Surface Technologies, Horiba Instruments,
Coulter Scientific Instruments, Amherst Process Instruments,
Caterpillar, H. C. Starck*

PSD OF ZIRCONIA BY DIFFERENT LABORATORIES USING DIFFERENT MODELS OF MICROTRAC

NIST Ceramic Coatings Program (cont.)

S. J. Dapkunas (NIST)

COLLABORATION WITH SANDIA

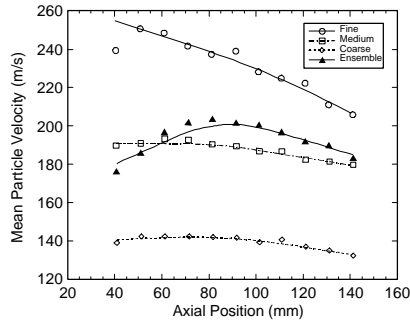


Fig. 5 - Mean particle velocity vs. axial position.

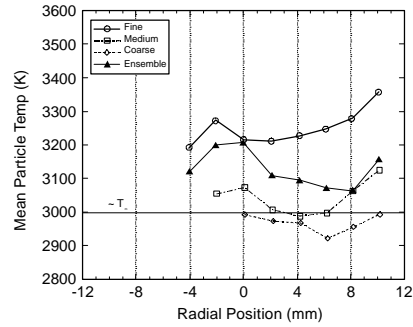


Fig. 7 - Mean particle temperature vs. radial position.

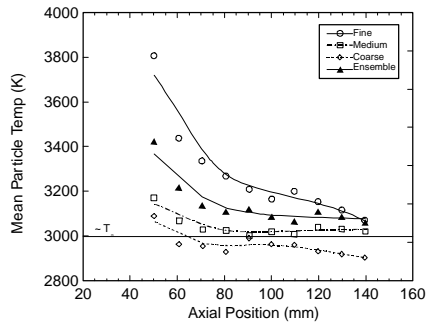


Fig. 6 - Mean particle temperature vs. axial position.

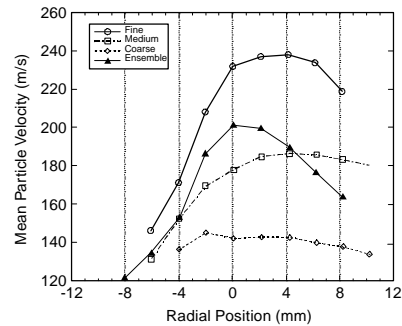


Fig. 8 - Mean particle velocity vs. radial position.

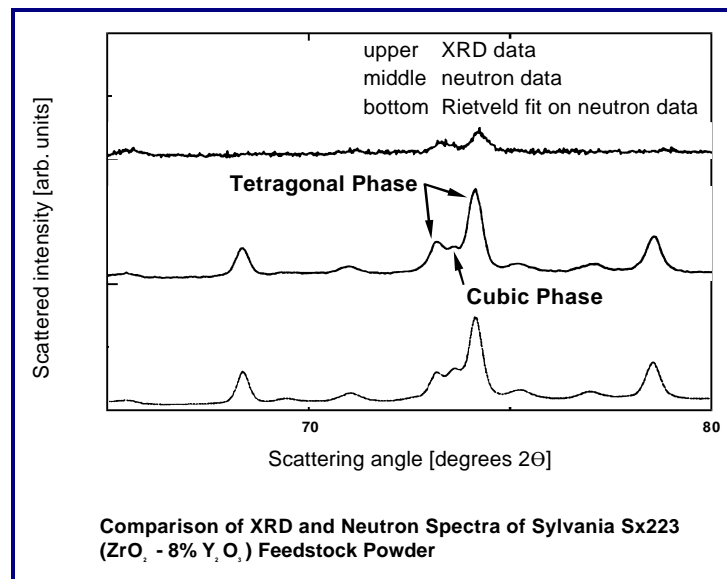
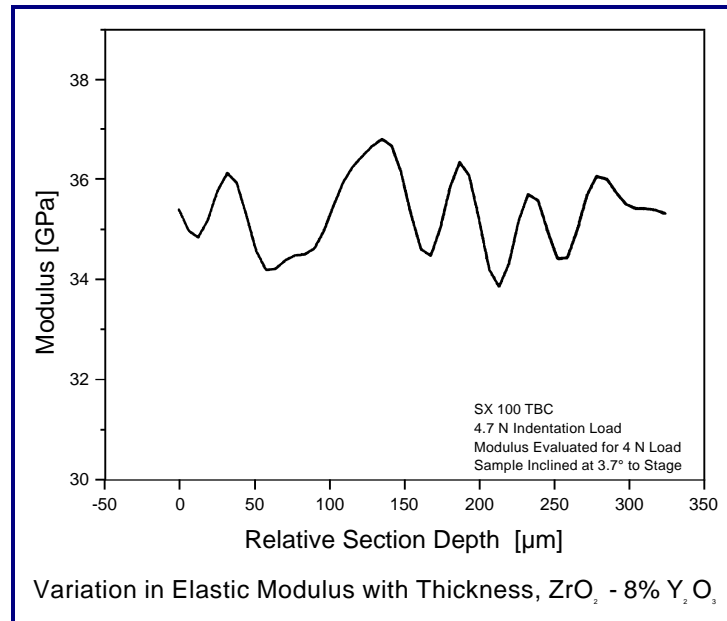
“An Investigation of Particle Trajectories and Melting in an AIR Plasma Sprayed Zirconia”, R. A. Neiser and T. J. Roemer, 1996

SRM 1984- WC/Co Thermal Spray Powder Particle Size Distribution

- *SRM 1984 I - Sintered and Crushed, 1 to 40 um*
- *SRM 1984 II- Agglomerated and Sintered, 10 to 50 um*
- *Round Robin Participants*
 - *Powder Manufacturers- METCO, METECH, H. C. Starck, Osram/Sylvania*
 - *Coaters- TAFA, Stellite, Spray Tech*
 - *Instrument Manufacturers- Leeds and Northrup, Horiba, Coulter*
 - *Other- Sandia, Japan Thermal Spray Society*

NIST Ceramic Coatings Program (cont.)

S. J. Dapkunas (NIST)



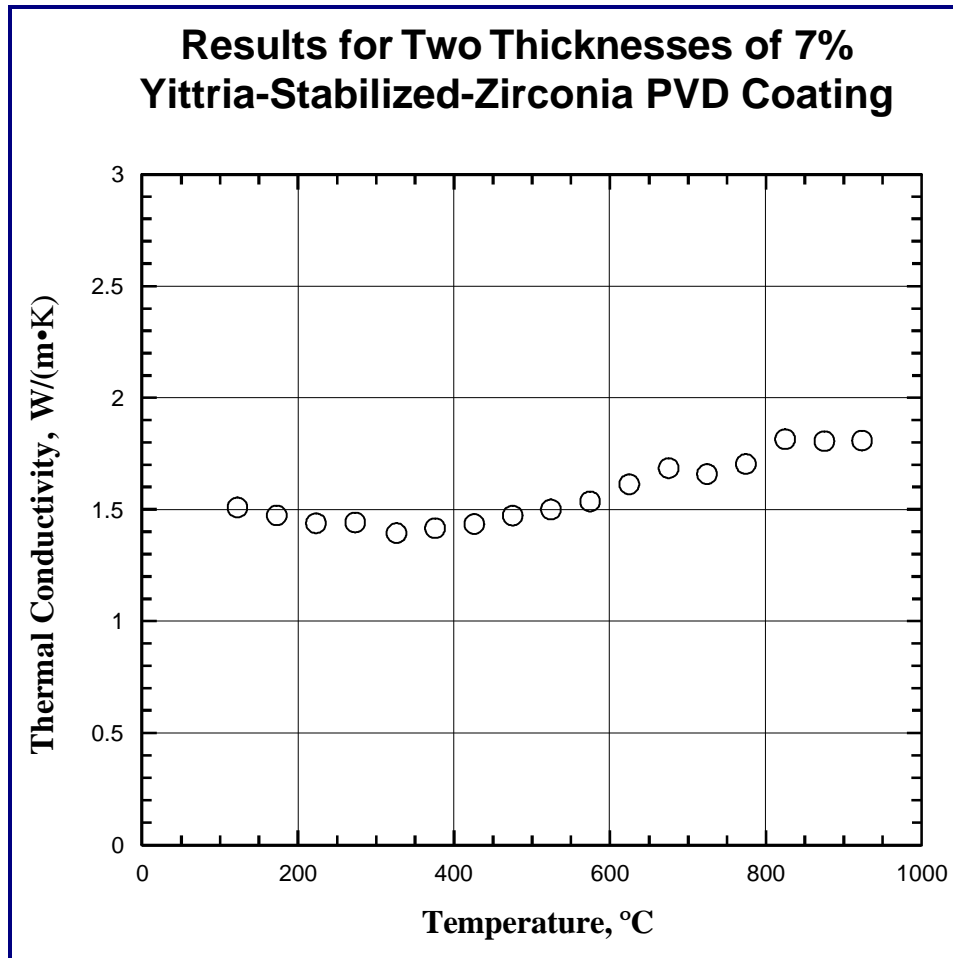
COATINGS CHARACTERIZATION

Thermal properties of coatings

- Guarded hot plate adapted to measurement of coating thermal conductivity.
- Correlation with laser flash method in progress.
- Standard Reference Material for thermal conductivity to be

NIST Ceramic Coatings Program (cont.)

S. J. Dapkunas (NIST)



COATINGS CHARACTERIZATION

Instrumented Indentation Measurements

- Development of technique for measurement of elastic modulus
 - Micro-indentation for thick TBCs
 - Variation of E through thickness determined
 - Data used in microstructural modeling
 - Nano-indentation for thin coatings
 - BAM collaboration
 - VAMAS Round Robin
 - Praxair - ATP

Workshop on Indentaion Measurements and Standards planned to identify issues and approaches.

NIST Ceramic Coatings Program (cont.)

S. J. Dapkunas (NIST)

MODELING

- Object Oriented finite Element (OOF) model developed to provide guidance on role of thermal sprayed microstructure on properties.
 - Predicted E compared with measured E (Instrumented indentation).
 - Models available on WWW
<http://www.ctcms.nist.gov/~wcraig/oof.html>
 - PPMZOOOF - Tool to take an image to an element based representation with constitutive properties specified by a user.
 - OOF - Tool to perform physical tests and obtain microstructural behavior.

Physics Based Finite Element TBC model - SBIR/Optimal Corp.

Design of the Ceramics Coatings Database

The database is divided into four components:

1. Bibliography

Because the information is more or less uniform from one source to the next, a fixed field structure is useful and effective. Separate fields are used for authors' names, title of journal or book, title of paper, volume, issue, page numbers, year, publisher, editor

2. Material Identification

Because processing methods and the kinds and extent of information reported vary greatly from one paper to the next, material identification is provided using a small set of fixed field variables to record generic classification information (such as chemical class is oxide, chemical family is Al-O, formula is Al₂O₃, informal name is alumina, etc.) plus a text field in which the description of the processing method can be entered as fully as information is available.

3. Measurement Methods

Because measurement methods and the procedures followed can vary greatly from one paper to the next and the procedures can be adapted *ad infinitum* for special purposes, measurement methods are described using only one fixed field variable (to record the generic name of the test method) and one text field in which the description of the measurement method can be entered as fully as information is available.

4. Property Tables

Property data are contained in tables with a configuration that is partially predefined. Each table consists of five columns. The names and unit of the property column (such as Hardness in GPa) are preassigned. The names and units of the remaining four columns are defined (if used) at the time of data entry. (This design has been found to be sufficiently flexible to accommodate nearly all of the studies encountered in the development of the databases for bulk structural ceramics and for high temperature superconductors.) The layout of a typical data table might look like:

		Mass Fraction of Y ₂ O ₃	Indentation Load	Hardness
		%	N	GPa

NIST Ceramic Coatings Program (cont.)

S. J. Dapkunas (NIST)

Variables and Properties for a Ceramic Coatings Property Database

The tables on the following pages contain lists of variables and properties that were used, reported, or discussed in a sampling of the literature on ceramic coatings. The sampling consisted of 57 papers drawn from 23 journals.

Journals	# of Papers
ACerS Bul.	1
Adv. Matl. Proc.	1
Colloque de Phys	1
J.Alloy.Comps.	1
J.Am.Cer.Soc.	3
J.Cer.Soc.Jpn.	1
J.Chem.Soc.Jpn.	1
J.de Phys.	1
J.Engr.Gas Turb.Powr.	2
J.Eur.Cer.Soc.	1
J.Mat.Sci.	2
J.Mat.Sci.Let.	2
J.Sol.St.Chem.	3
J.Th.Spray Tech.	11
J.Thermophys. Ht.Trans.	1
J.Tribol.	1
Mat. Char.	1
Mat.Sci.Engr. A	3
Nuc.Instru.Meth.Phys.Res. B	1
Plasma Chem.Plas.Proc.	1
STLE Trib.Trans.	1
Surf.Coat.Tech.	16
Surf.Interface Analysis	1

Variables and Properties for a Ceramic Coatings Property Database, R. G. Munro, NIST, 7/30/98, Page 1 of 4

Processing Variables

Variable	Type	Variable	Type
Process name	text	Powder injection point	numeric
Carrier gas	text	Powder wheel speed	numeric
Carrier gas flow rate	numeric	Primary gas	text
Cooling rate	numeric	Primary gas flow rate	numeric
Deposition efficiency	numeric	Primary gas mass flow rate	numeric
Deposition method	text	Raw material feed rate	numeric
Flow rate	numeric	Relative surface travel rate	numeric
Fuel gas	text	Reynolds number	numeric
Fuel gas flow rate	numeric	Rotation speed	numeric
Nozzle diameter	numeric	Secondary gas	text
Nozzle length	numeric	Secondary gas mass flow rate	numeric
Oxyfuel ratio	numeric	Spray standoff distance	numeric
Particle flow pattern	image	Spray impingement angle	numeric
Particle velocity	numeric	Spray gun input power	numeric
Plasma gas	text	Substrate temperature	numeric
Plasma gas flow rate	numeric	Torch rotation speed	numeric
Plasma gas pressure	numeric	Torch translation velocity	numeric
Plasma spray power level	numeric	Torch traversing speed	numeric
Powder feed rate	numeric	Total gas flow rate	numeric

Variables and Properties for a Ceramic Coatings Property Database, R. G. Munro, NIST, 7/30/98, Page 2 of 4

NIST Ceramic Coatings Program (cont.)

S. J. Dapkunas (NIST)

Powder Variables		Specimen Variables	
Variable	Type	Variable	Type
Name	text	Binder	text
Density	numeric	Binder, Amount of	numeric
Hall flow rate	numeric	Bond coat	text
Melting point	numeric	Bond coat, Amount of	numeric
Particle size	numeric	Element	text
Particle size aspect ratio	numeric	Element, Amount of	numeric
Particle distribution	numeric	Phase	text
Particle shape	text	Phase, Amount of	numeric
Thermal conductivity	numeric	Substrate	text
Thermal expansion (CTE)	numeric	Top coat	text
		Top coat, Amount of	numeric

Test Variables	
Variable	Type
Test name	text
Corrodent species	text
Environment	text
Heating rate	numeric
Load	numeric
Loading rate	numeric
Lubricant	text
Number of cycles	numeric
Penetration depth (of indenter)	numeric
Sliding speed	numeric
Temperature (of coating)	numeric
Temperature (of substrate)	numeric

Variables and Properties for a Ceramic Coatings Property Database, R. G. Munro, NIST, 7/30/98, Page 3 of 4

Properties			
Property	Type	Property	Type
Absorption band	numeric	Oxidation, Scale thickness	numeric
Absorption coefficient	numeric	Oxidation, Weight gain	numeric
Coating thickness	numeric	Poisson's ratio	numeric
Corrosion rate	numeric	Pore size	numeric
Creep rate	numeric	Porosity	numeric
Creep stress exponent	numeric	Refractive index	numeric
Density	numeric	Scratch adhesion critical load	numeric
Elastic (Young's) modulus	numeric	Sound velocity	numeric
Electrical resistance	numeric	Spalling onset time	numeric
Erosion resistance	numeric	Specific heat	numeric
Fracture toughness	numeric	Spectral reflectivity	numeric
Friction coefficient	numeric	Strength, Adhesion	numeric
Grain size	numeric	Strength, Bond	numeric
Grain size, Aspect ratio	numeric	Strength, Cohesion	numeric
Grain size, Distribution	numeric	Strength, Compressive	numeric
Hardness	numeric	Strength, Creep	numeric
Heat transfer coefficient	numeric	Strength, Flexural	numeric
Infrared spectra	numeric	Strength, Shear	numeric
Interfacial toughness	numeric	Strength, Tensile	numeric
Lattice parameters	numeric	Strength, Tensile bond	numeric
Lifetime, Coating	numeric	Stress relaxation exponent	numeric
Lifetime, Fatigue	numeric	Surface roughness	numeric
Lifetime, Thermal cycling	numeric	Texture coefficient	numeric
Lifetime, Thermal fatigue	numeric	Thermal conductance	numeric
Lifetime, Thermomechanical fatigue	numeric	Thermal conductivity	numeric
Mean free path	numeric	Thermal diffusivity	numeric
Melting point	numeric	Thermal expansion	numeric
Micrograph	image	Thermal shock resistance	numeric
Oxidation, Activation energy	numeric	Wear coefficient	numeric
Oxidation, Products	text	Wear rate	numeric
Oxidation, Rate	numeric	Weibull modulus	numeric
Oxidation, Resistance	numeric	XPS spectra	numeric

Variables and Properties for a Ceramic Coatings Property Database, R. G. Munro, NIST, 7/30/98, Page 4 of 4

Process Diagnostics

S. D. Ridder (NIST)

Process Diagnostics**S. D. Ridder and F. S. Biancaniello**

*Thermal Spray Coatings Workshop
National Institute of Standards and Technology
Gaithersburg, MD 20899
November 19, 1998*

Past work at NIST in spray processing was focused on metal powder production via gas atomization. Several imaging techniques were developed to provide information to help understand the disruption process and to provide data for process models. Many of these techniques are suitable for use in diagnostics of thermal spray systems.

Diagnostic and Control Sensors for Spray Systems

1. Fraunhofer diffraction
 - size of particles/droplets in flight
 - rapid response (>2 Hz) control sensor
2. Schlieren/Shadow photography
 - diagnostics of gas and plasma jets
 - non-intrusive
 - used to validate fluid flow models
3. Double pulse xenon flash illuminated video
 - 30 fps double exposure
 - DIV (Digital Image Velocimetry) of particles/droplets
 - size and shape of particles/droplets in flight
 - potential for control sensor
4. High-speed video (50-100 ns exposure time)
 - 30 fps multiple exposure
 - will be optimized for harsh plasma spray environment
5. 10,000 fps cinema
 - 20-30 ns exposure high intensity diffuse illumination
 - surface details of particles/droplets
 - particle entrainment in the plasma jet
 - trajectory of particles/droplets in flight
 - particle/droplet impact with substrate
6. Holography (3D image of particles/droplets in flight)
 - hologram provides infinite depth of field
 - multiple exposures (20 ns pulse duration)
 - DIV of particles/droplets

Process Diagnostics (cont.)

S. D. Ridder (NIST)

10,000 fps cinema is used to capture dynamic flow phenomena.

10,000 fps Cinema

diagnostics of dynamic particulate plumes that preserves sequential events (temporal resolution=100 μ s)

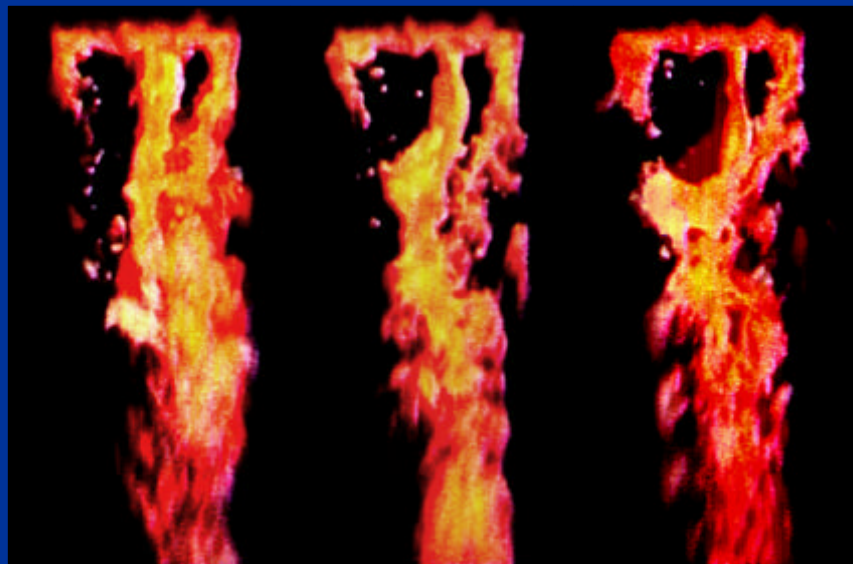
images can be formed from thermal incandescence or by triggered laser light pulses

dynamic breakup events and high speed particles can be "frozen" with short , 20 ns, laser pulses

highly luminous spray processes are imaged with coherent light through narrow band filters

This slide shows a three frame sequence from a 10,000 fps movie imaged with the incandescent light of the atomization plume. These movies show several interesting phenomena associated with the liquid delivery and disruption in a close-coupled gas atomizer. The liquid is drawn into the gas flow from a recirculating "base flow" region in the vicinity of the metal pour tube tip. The pour tube tip is at the top of each frame but does not show in these images. The liquid metal is seen to recirculate with little gas mixing in the upper half of each frame. It then rapidly accelerates (blurs) and moves away as it mixes with the gas flow in the bottom half of each image.

frame sequence from high speed cinema

 $\Delta t = 100 \mu s$

Inconel alloy 625

Ar atomizing gas

Process Diagnostics (cont.)

S. D. Ridder (NIST)

The NIST holocamera can produce holograms of highly dynamic phenomena such as gas atomization or thermal spray. Each hologram can be recorded with from one to several (two or three) separate 20 ns laser exposures. Multiple exposures can provide velocity and time resolved disruption data. Droplets or particles as small as 20 μm can be resolved and each hologram has “infinite” depth-of-field. This is a common characteristic of holographic images. The hologram itself is a record of the light phase information present in the object beam over the time of exposure.

Holography of droplets and particles

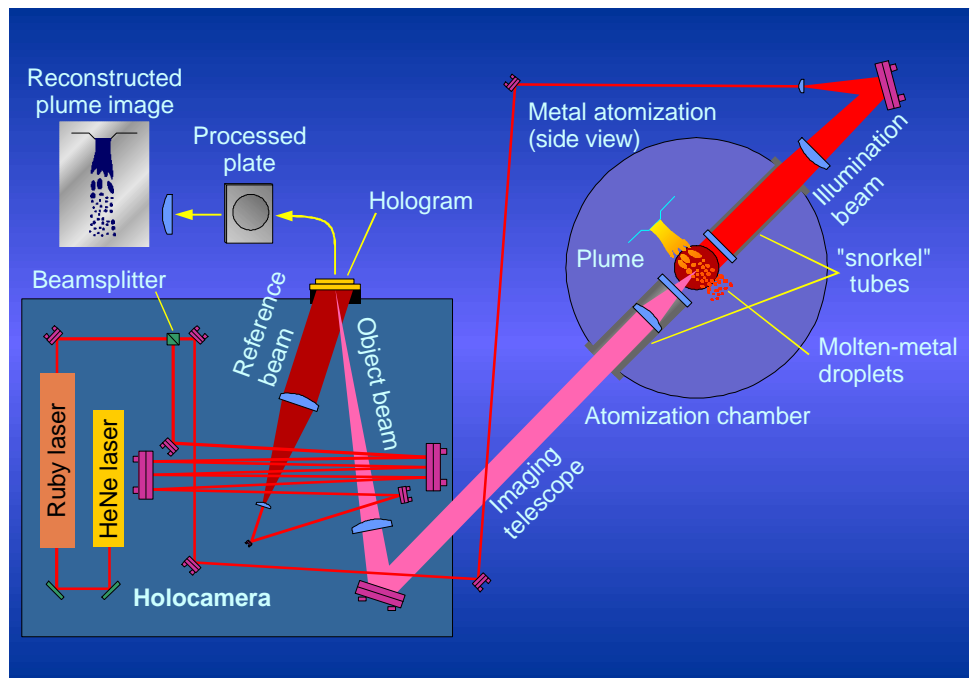
coherent optical technique for recording high resolution images of dynamic 3-D particulate plumes

resolution of 10 μm possible throughout spatial volumes of several cubic centimeters

dynamic breakup events and high speed particles are “frozen” with short, 20 ns, laser pulses

highly luminous spray processes are viewed with coherent light through narrow band filters

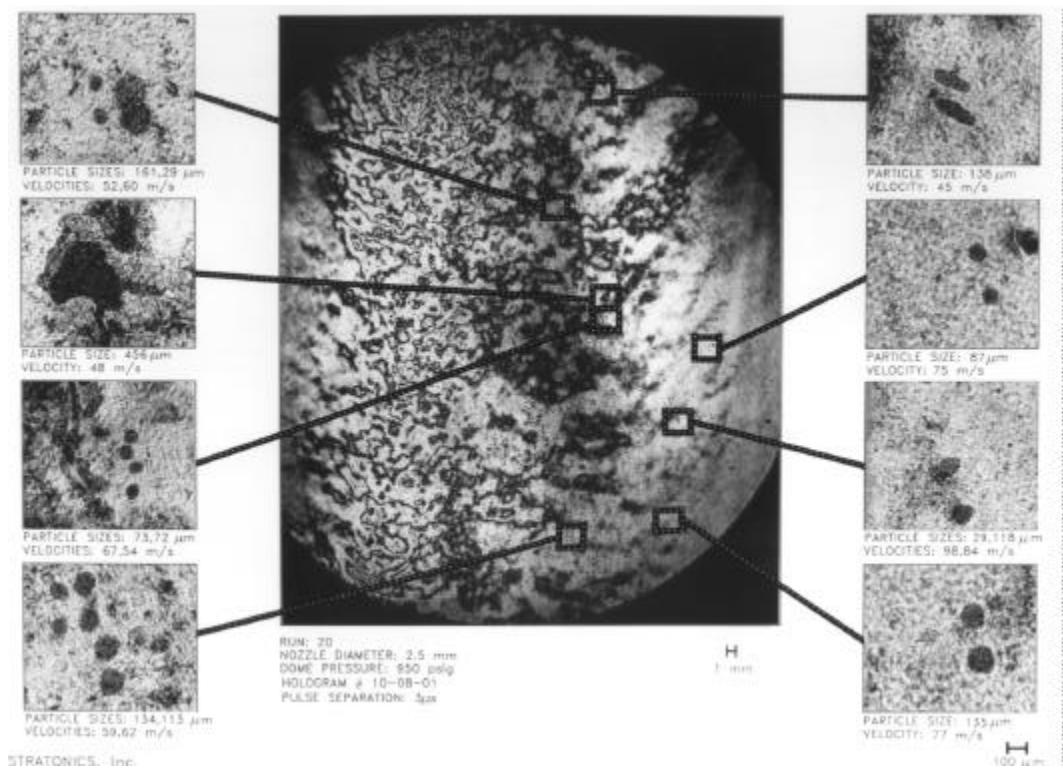
In the NIST holocamera setup the atomization plume passes through the object beam between the “snorkel” tube viewports. The holograms are analyzed by placing them back in an optical setup that duplicates the reference beam configuration used during exposure. A reconstructed image is formed in space that faithfully represents the light phase information present during exposure. Standard photography equipment can be used to view the reconstructed image focusing anywhere within the three-dimensional space defined by the object beam and the two “snorkel” tube viewports.



Process Diagnostics (cont.)

S. D. Ridder (NIST)

This slide shows a typical two-dimensional image taken from a double exposure hologram of the plume of a gas atomizer (SIGMA). In this hologram the object beam was directed to pass through the plume downstream from the region shown previously in the 3 frame high-speed movie sequence. Two 20 ns laser pulses were used with 3 μ s delay between each exposure. On either side of the central low magnification image are several higher magnification views from selected regions. These double exposure holograms reveal both the motion of stable spherical droplets, and disruption dynamics in larger unstable liquid metal shapes.



Rational for NIST program aimed at developing sensors and control systems for thermal spray.

Need for Diagnostics, Sensors and Modeling in Thermal Spray

Thermal spray coatings have not been sufficiently reproducible to satisfy most industrial requirements

- *improved process design and processing control needed*
- *automated "intelligent" processing needed*
- *need improved reliability in coatings so that industry does not need to inspect every part before installation (inspection is very costly)*

Diagnostics, sensors, and modeling will lead to:

- *development of process simulators to test effect of varying process conditions. Use computer simulations rather than expensive production tests.*
- *automated feedback and control to provide reproducibility and reliability in thermal spray coatings*

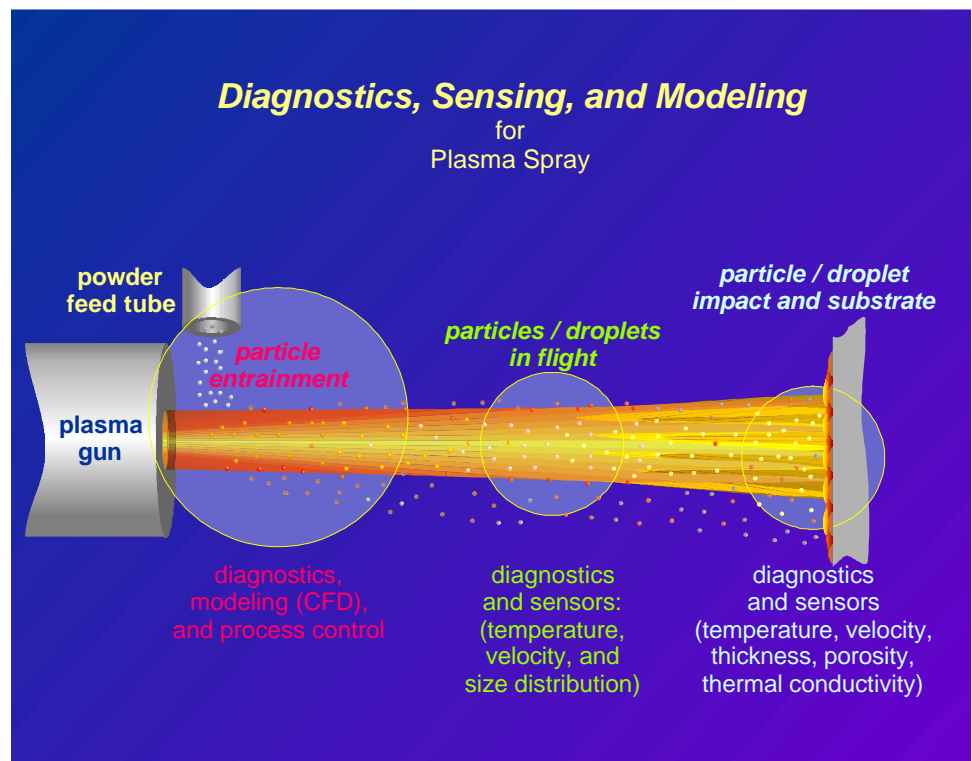
Process Diagnostics
(cont.)

S. D. Ridder (NIST)

Industry Needs to be fulfilled:

- a) *Several US industry representatives: (GE, GM, Ford, Caterpillar / Solar Turbine, Miller Thermal / Praxair) have expressed the need to implement **automated control and design improvements** in commercial spray systems, primarily aimed at moving from the current practice based on "operator art" to an **"Intelligent Processing" control technique** using **advanced sensors***
- b) *This project is aimed at addressing the **diagnostic, sensing, modeling, and control** issues as applied to Thermal Spray Processing in general and Plasma Spray Coatings in particular*
- c) *Specific measurement needs to be addressed include: in-flight measurements of particle size, speed, and temperature
spray deposit temperature, thickness, texture, and porosity
as functions of processing conditions*
- d) *DOD/DOE are de-emphasizing non-military technology transfer, thus making NIST involvement in the development of these technologies more important*

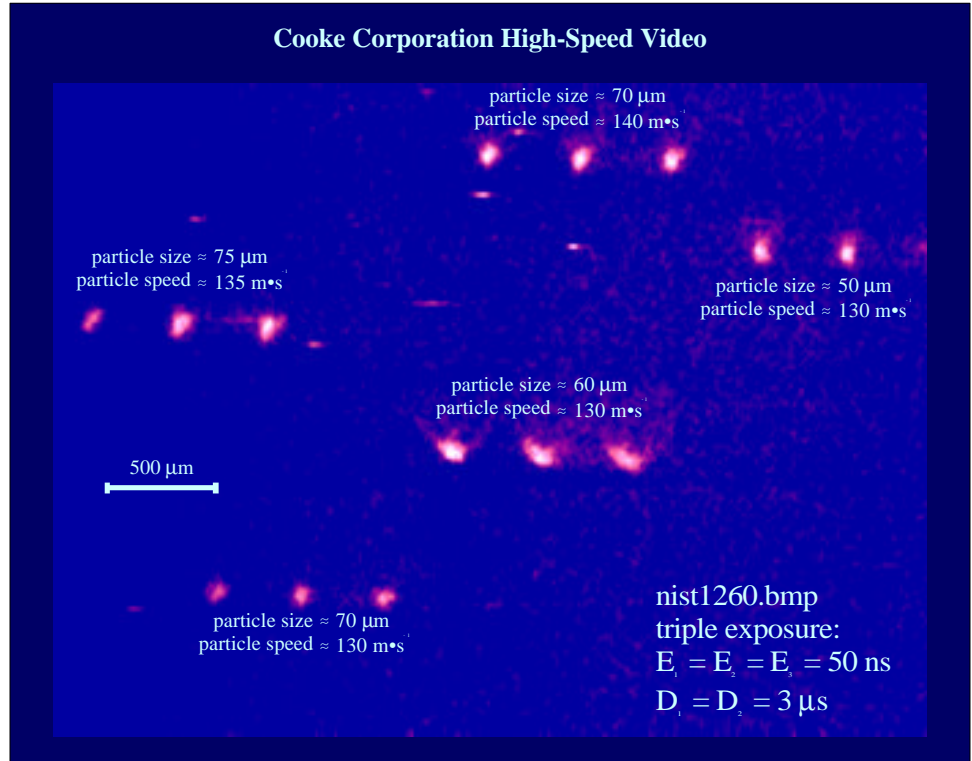
Schematic showing plasma spray process and where NIST research will focus.



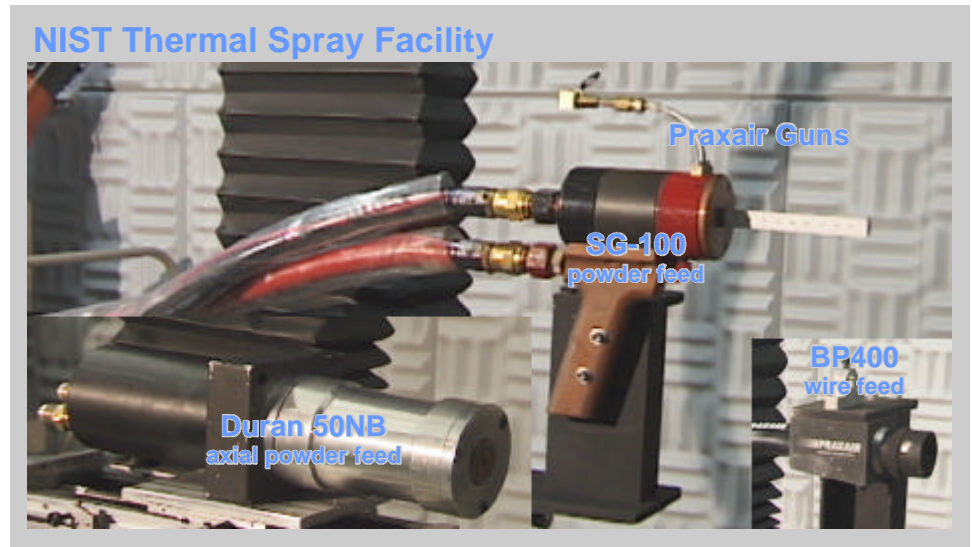
Process Diagnostics (cont.)

S. D. Ridder (NIST)

This slide, of thermal spray particles in flight, is an example of one of the imaging systems being developed at NIST for spray processing diagnostics. This image was made using a new high speed video camera with a peltier cooled CCD. Developed in response to a NIST funded SBIR solicitation, this camera can superimpose up to 10 images per frame with exposures as short as 50 ns. Framing rates are determined by CPU and data bus speed. 30 fps are possible using a 300 MHz CPU with a 100 MHz data bus.



Some of the spray guns available in the NIST Thermal Spray Facility.



Spectroscopy Measurements (Summary)

Spectroscopy of Thermal Spray Plumes

P.K. Schenck, *D.W. Bonnell*, J.W. Hastie,
(presented at the *Thermal Spray Coatings Workshop*, NIST, 11/19/1998)

Background: NIST is in the latter stages of an SBIR development program (Stratonics) aimed at implementing two-color pyrometry of particulates in thermal spray plasmas. High speed CCD camera technology is being used to both time- and spatially-resolve the particulates and to derive their temperature. However, the effect of discrete spectral emissions on the measurements needs to be established. Also, an independent method of temperature measurement is desirable to validate the pyrometric approach. Both of these needs can be accomplished through simultaneous detailed spectroscopic measurements on plasma spray plumes. A tandem spectroscopic-pyrometric study was initiated jointly with the Metallurgical Processing Group (MPG) and Stratonics, using the MPG's research spray facility at NIST. The spectroscopic approach and preliminary results are outlined here. This collaboration utilizes expertise in spectroscopy, high temperature processes, and temperature measurement, and the availability of a highly portable fiber-optic-coupled visible/near-IR spectrometer. Of particular interest was the question of contributions to the emission from the arc, including possible interferences from constituent line spectra, both from plasma gases and vaporized material.

Experimental: The spectrometer used was an integrated Ocean Optics* mini-crossed Czerny-Turner spectrometer/CCD detector system (see figure below), with a fixed range of approximately 380-926 nm and approximately 1 nm resolution. The spectrometer's fiber-optic coupling had a fixed 25 μm slit assembly (1000 μm high) to assure that the fiber position from one setup to the next did not affect the system calibration. For this work, spectra were taken at 50, 20 and 10 kHz digitizer rates, averaging 4 scans, for effective collection times of 81, 204, or 409 ms. End points are normally discarded before data processing as not being fully illuminated by the grating, to give a final range of 384-895 nm.

The optical fiber used was supplied by the Metallurgical Processing Group, and was a polymer-clad single-strand quartz fiber 1.0 mm effective diameter with standard SMA couplings at each end. This fiber showed a single flaw (evidenced by light leakage through the sheath), but the output image of a distributed light source showed no obvious patterning that might be indicative of a seriously damaged fiber. The fiber was approximately 7-1/2 m long and was installed in the experimental facility through a long pipe, allowing the spectrometer and data system to be located outside the spray area. Most of the fiber length was shielded from stray light.

Initial survey spectra (see Bare Fiber figures, below) were taken at two positions using just the fiber tip as a collector, indicating that plasma light was a serious background contaminant, and that careful shielding and a collimating optical element was needed. The collection optic prepared consisted of a 12.7 mm f/1 quartz lens mounted in a housing specially constructed to allow the fiber to be adjusted at the rear focal point. A blackened lenshood extending approximately 3.5 cm beyond the face of the lens ($l/d \sim 3$) was added to further reduce off-axis light. The fiber was fine-adjusted to the focal point by projecting light through the fiber and moving the fiber to produce the most uniformly illuminated projected spot. This spot had a diameter of 2.5 cm at a distance of 25 cm, the nominal working distance. This corresponds to an acceptance angle (full-cone angle) of less than 6 degrees (~ 0.1 rad). Off-axis light acceptance appeared to be minimal.

Our optical system was aimed at the pyrometer input lens using projected light (see Schematic of experimental layout, below) At the lens of the pyrometer, the projected light circle from the fiber's optical system was completely within the pyrometer's front lens element. Still, we found that including a simple lenshood on the pyrometer as a scattered light trap significantly reduced background light.

A set of measurements were taken under actual spray conditions, with particles of nearly monosized Inconel 625., beginning 30 cm downstream ("Far"), and at 5 cm intervals moving upstream to the 15 cm location ("Near"). The vertical location of the particulate stream was adjusted based on the pyrometric image, and did not necessarily peak the spectrometer signal. Integration intervals chosen to give maximum signals of at least 1/2 full scale. Neither blank nor particulate free spectra were taken except after the final 15 cm data collection for this series. Analysis with, and without blank subtraction at this point indicated were nearly identical, indicating that the background plasma interference had been effectively eliminated. The plasma operating parameters (gas flow/composition) were altered slightly toward the end of this set because of low supply gas pressure.

*Mention of specific companies or products is solely for identification. NIST makes no claim that these companies or products are particularly more appropriate for the applications mentioned than other similar items.

Spectrometer wavelength calibration was accomplished by taking a spectrum of a standard Hg calibration lamp, and deriving a polynomial correction expression that corrected all observed line centroid channel (pixel) positions to the known line positions. Wavelength error after calibration was negligible with respect to the wavelength span of individual pixels.

Spectrometer sensitivity calibration was accomplished by taking a spectrum of a calibrated standard radiance source (Optronics Labs, Inc. - a broad-filament incandescent source) with the entire spectrometer assembly, including the fiber optic and lens assembly attached just as used for experiments, aimed at the lamp. It was necessary to use an aperture to restrict the field of view to just the calibration point on the lamp. Calibration without the restriction aperture affected final temperatures determined by approximately 8 K (resulting in lower derived T's). This difference is probably the largest calibration error effect. The standard lamp was supplied with a series of absolute radiance calibration points at selected wavelengths. These data were fitted piecewise with Planck functions to interpolate to the exact wavelengths for each channel (pixel) of the spectrometer. Each point of the observed calibration spectrum was then divided into the resulting calibration table to obtain a new set of factors that could then be used to correct each observed spectrum, pixel by pixel, for the complete system sensitivity.

To process each data spectrum, dark subtractions were done before sensitivity corrections. It should be noted that, while Ar lines were still discernable in the particulate-bearing plumes at 15 cm, the contributions were relatively small, and became much smaller at longer distances. We consider this good evidence that stray light is controlled, but additional tests are needed to verify that conclusion. When the particle-free plume spectra were subtracted, all line-spectral features essentially vanished, except perhaps slight distortions at the locations of the lines. For some of the data, it was not practical to take comparable particle-free spectra. Those data sets were treated without that correction, and the effect was minimal. After background subtractions and sensitivity corrections were made, the resulting spectra were fitted to a Planck function with amplitude and temperature as the fitting variables.

$$I(\lambda, T) = \frac{A}{\lambda^5 (\exp^{c_2/\lambda T} - 1)}$$

where A and T were non-linear fitting parameters; A was a scale factor that included factors in viewing and particle geometry and T was the derived blackbody/graybody temperature. λ are the measured wavelengths and $c_2 = 1.438786E7$ [nm·K] is the second radiation constant.

Results and Discussion: The included figure shows final corrected I vs λ data for the last measurement position in the spray (at ~15 cm downstream), where all experimental setup corrections were finalized and there was an opportunity to obtain a particle-free background spectrum. The best-fit Planck-law curve gives a derived temperature of 2557 ± 2 K, where the statistical uncertainty is the standard deviation of the parameter. The curve data appear to arise from a very good blackbody, with only minor deviations between 850 and 900 nm, which have no significant effect on the result. We implicitly assume that particle emissivity is essentially independent of wavelength (the “gray-body” assumption). Since the fit includes an amplitude parameter, only the wavelength dependence of the emissivity is not accounted for. We did notice that, using an initial sensitivity calibration series from our standard radiance lam, no Planck curve fit all the data. That initial calibration was taken without an aperture to restrict FOV, and thus included light from filament locations at significantly different temperatures from the calibration point. We thus note that the fitting process does not yield this good a fit over the entire span of the thermal spray data unless the data are Planckian (i.e., represent a region with a defined average T).

We feel that we have resolved most of the data analysis issues, and that there are only small systematic errors remaining in the data analysis. Clearly, It is more difficult to assess the accuracy with the data currently available and with the uncertainties inherent in making ensemble-average measurements of an inherently dynamic process. We were able to analyze other data sets by assuming that blanks were similar, and ignoring the particle-free background subtraction. For the replicate point at 15 cm, the resulting derived temperature was 2549 ± 3 K (after recalibration), indicating that the statistical and replicate uncertainties are comparable. An earlier data set, from a separate start/run of the torch (but at the same conditions) before the final scattered light changes were made to the experimental setup yielded a value of 2536 ± 2 K. Thus, the replicate error could be of the order of 20-25 K. We examined fitting subsets of the data, with the expected result that the uncertainty in derived T was greater. The single-data-set fit figure below also includes equivalent Planck curves, matched to the data at the average corrected intensity, with values of T 100 K more and less than the fitted value. It is clear that differences in T of that magnitude would result in very different curve shapes than we observed. Thus, our true sensitivity is much better than ± 100 K. The replicate error value of 25 K noted above seems to be a reasonably conservative estimate of our run-to-run uncertainty.

Other sources of error include the possibility that the particles are not good gray bodies (*i.e.*, the emissivity variation with wavelength, $\epsilon(\lambda) \neq \text{constant}$), or that different-sized particles have different effective emissivities. We reanalyzed the data, assuming 1 percent and 5 percent linear variations in emissivity over the span of the spectra. These different assumptions resulted in changing the derived temperatures by about 5 K and 22/24 K, respectively. Decreasing $\epsilon(\lambda)$ increases T, and vice versa. This order of variation is certainly not unrealistic. When we applied a reference $\epsilon(\lambda)$ curve for W as a model to our data, the derived T decreased by 90 K. Thus, $\epsilon(\lambda)$ uncertainties could be a significant source of error, even for two-color-type pyrometry or for our multispectral determinations.

Another possible source of experimental error for the spectroscopic measurements is the acceptance angle of the current optical train. We are clearly sampling over the entire width of the particulate stream at all distances, and physical differences in the plume at different distances could affect the averaging process. In particular, the absolute total intensities were greater at greater distance, indicating that the wider plume at longer distances was still within the field of view. Less likely is the possibility that we are still accepting significant amounts of stray light, or that reflected light from the plasma is a major contributor. Other possible sources of error include the possibility that particles are obscured by vaporizing material or that there are dynamic changes in average T on the timescale of our data collection. Our observation of Cr emission in the wide area early scans clearly indicates that some metal vapor is present and excited by the plasma. Simple calculations of vaporization rate indicate that the vapor pressure of Cr can be more than one bar, and that several percent of the Cr could be vaporized during the particle flight time. All these errors, it should be noted can affect the individual particle pyrometry, as well.

It should be noted that the averaging process of the spectrometric data tends to be essentially exponentially weighted toward the higher temperature contributors. Thus, differential cooling processes (*i.e.*, cooling of some particles by entrained air or radiant emission, as opposed to others remaining shielded by hot gas) might not be well averaged without a more restricted view of the plume. There is clearly sufficient emission to allow additional restriction of the field of view.

Analysis of the points taken from 30 cm to 15 cm as discussed above all fall within ± 11 K, and are thus only statistically different from the other measurements. The slight upwards trend shown in the Temperature vs Position figure may easily be due as much to changes in experimental conditions (perhaps due to the increased visual area presented by the downstream plume with respect to its spatial extent upstream, or to the likelihood that hotter particles will move further, changing the temperature distribution of the plume, *etc.*) as to actual trends in the plume. As noted, there are several possible physicochemical effects (including the possibility of reaction heating of plume particles by atmospheric oxygen, changes in size and emitting surface due to vaporization, vaporization obscuring the upstream particle emission more than downstream, axial particle energy distribution effects, and others still to be considered) that could explain such a trend, but we do not currently consider our replicate precision to be sufficient to assert that the apparent data trend is significant.

Comparison of our data with the results of the particle-imaging pyrometer were treated in Stratonics' presentation. In comparing measurements, it needs to be recognized that there is likely a distribution of temperatures among the particles at any point in the plume stream. The integration time of our spectrometer is sufficiently long, and the current field of view sufficiently broad, that we are averaging over an ensemble of the particles passing our sampling region. That we see what amounts to a well equilibrated blackbody simply means that all the major emission sources in view have a blackbody-like visible emission profile (*i.e.*, Planckian) and the sum over all particles is again Planckian. Thus, to compare the two types of measurements, the pyrometric analysis needs to assess the effective distribution of particles (both number and by area), and apply a suitable averaging function. It would be desirable to use the temperature and size distribution data from the imaging pyrometer to generate a simulated DC or average brightness of the spray for comparison with our data.

Conclusions: We have demonstrated a spectroscopic technique to obtain a high-quality ensemble average temperature of the particulate stream in a plasma spray apparatus. We still need to consider questions regarding the radial temperature distribution, and the "best" way to arrange the spectrometry apparatus to provide a comparable viewpoint to that of the particle-imaging pyrometer. It would also be useful to extend our wavelength range to more closely match that of the pyrometric filters in use, in order to identify just where emission interferences may become important in the pyrometer's band pass regions. Other effects, such as particle size, size distribution, and plasma emission interferences at closer points in the spray plume still need to be investigated.

Spectroscopy Measurements (Vuegraphs)

D. W. Bonnell (NIST)

Multichannel Spectroscopy of plume/particles**Purpose:**

- thermal vs non-thermal emission
- interferences for purpose-built pyrometer
- Planck Law temperature probe - test of “temperature”
- insight into transport - hot or what?

Approach:

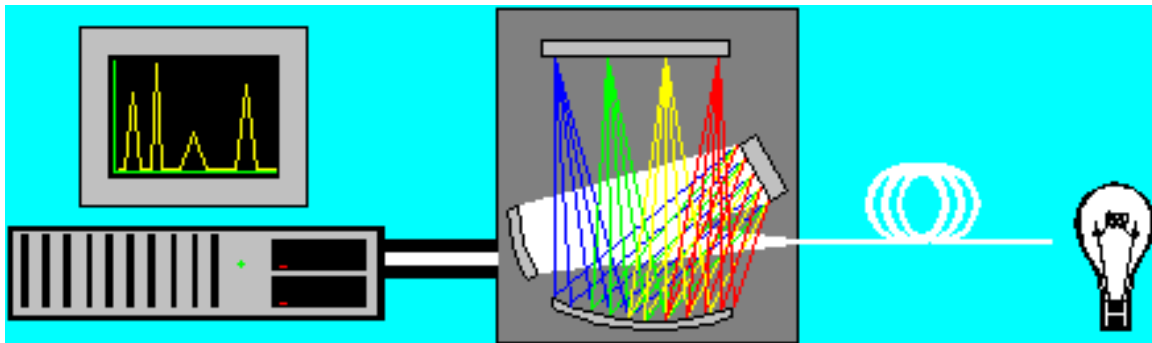
- commercial broad multispectral spectrometer
- silica fiber-optic coupled
- control of imaging area - only moderate time/space resolution
- Blank & particle-free backgrounds subtracted
- calibrate relative spectrometer response, correct spectra
- fit Planck fn, ~375—900 nm

Problems:

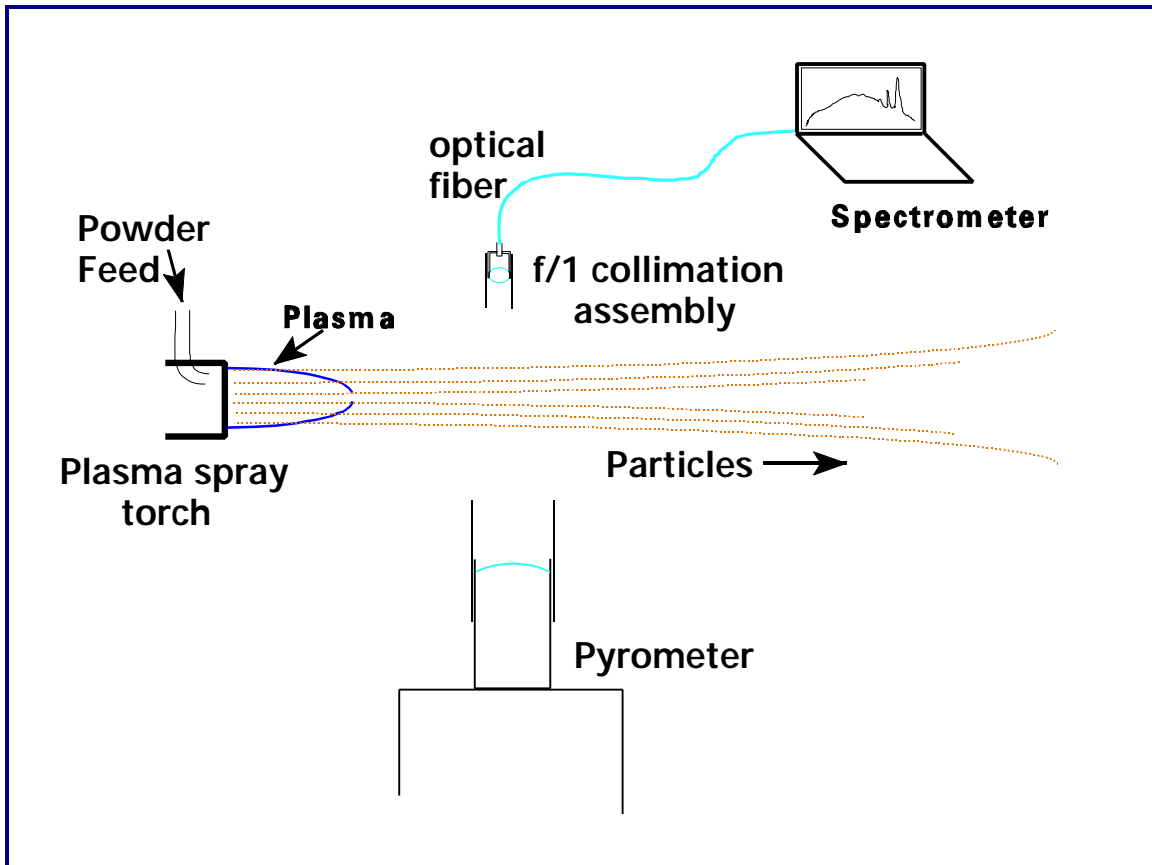
- Temperature/energy distribution in plume
- Light acceptance
- Scattered light control - from particles (PIs), walls, apparatus
- Plume axis vs PI axis and torch axis
- PI visual density - optically thick or semitransparent?
- 2-color pyrometry vs 1000+-color spectrometry
- PI-by-PI imaging vs “ensemble averaging”
- Strong surface curvature of small PIs
- Gas effects!
 - torch gas(es)
 - vaporized from PIs - obscuration?
 - turbulence, segregation, expansion cooling...
- Sensitivity, resolution of T
- What do we mean by “temperature”

Spectroscopy Measurements (Viewgraphs, cont.)

D. W. Bonnell (NIST)



Schematic of fiber-coupled spectrometer - Courtesy OceanOptics, Inc.

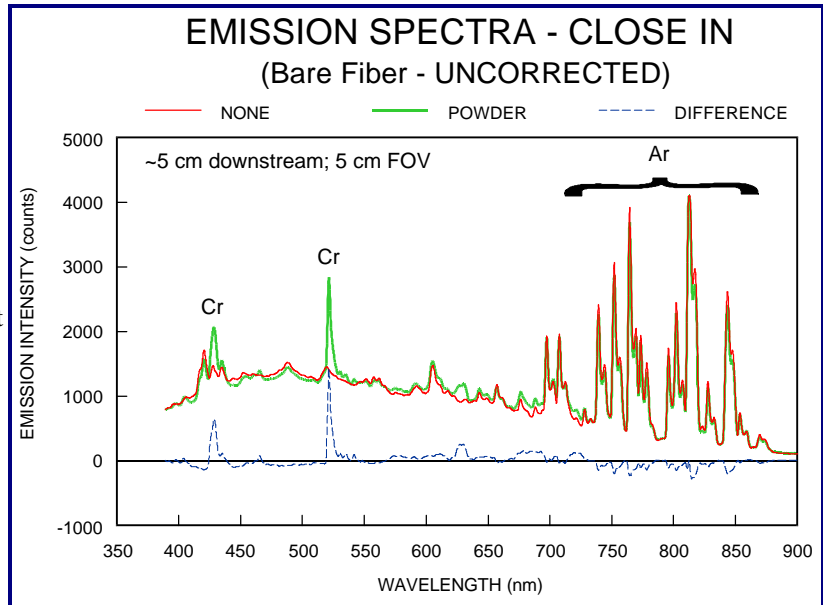


Schematic of experimental layout for simultaneous measurements with ThermoViz® imaging pyrometer and fiber optic-coupled spectrometer.

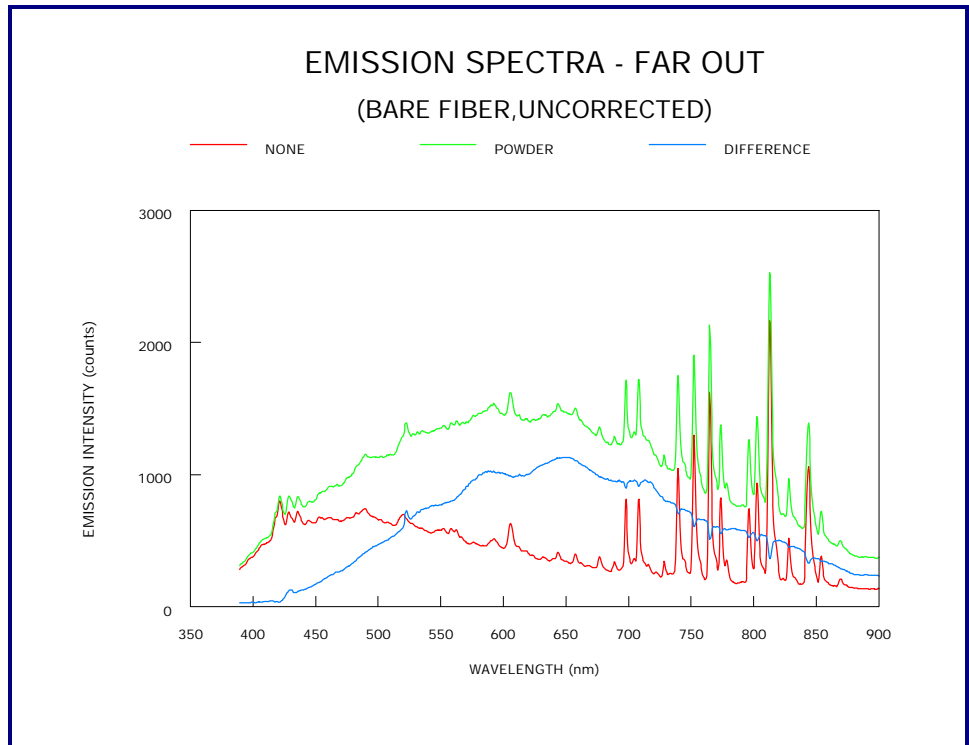
Spectroscopy Measurements (Vuegraphs, cont.)

D. W. Bonnell (NIST)

Spectra taken with bare fiber probe, ~5 cm downstream, ~5 cm FOV. The discrete line cluster at ~440 nm, and at ~530 nm are from Cr; the lines above ~700 nm are Ar plasma lines. Note that almost none of the plasma light comes from the powder (difference spectrum).



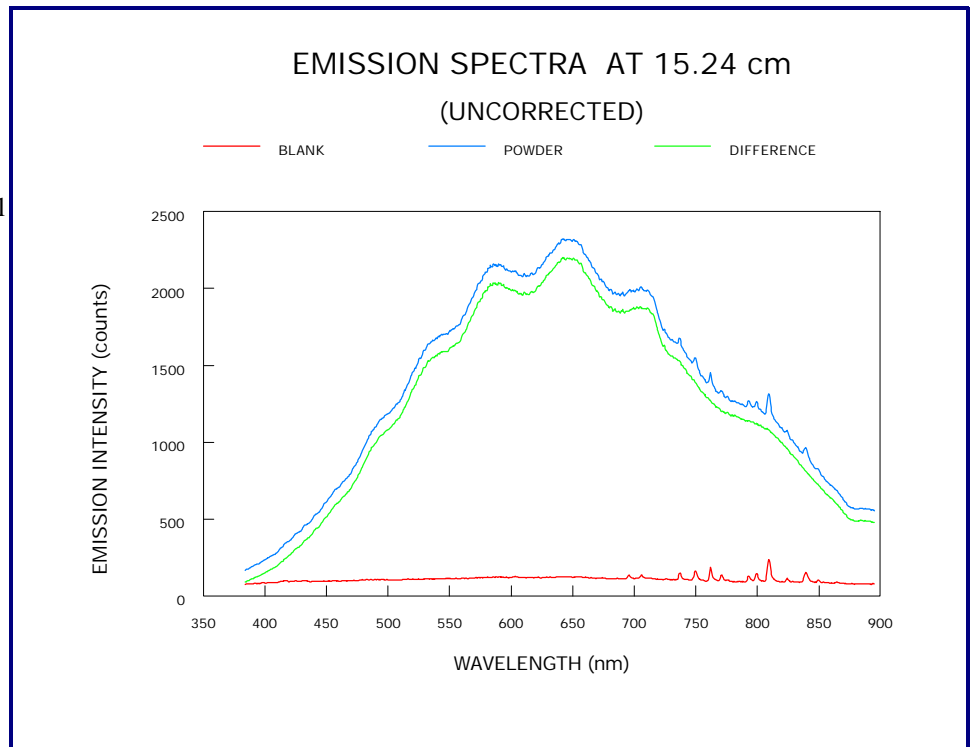
Spectra taken with bare fiber probe, ~15 cm downstream, ~5 cm FOV. The lines above ~700 nm are, as before, Ar plasma lines, and are essentially all plasma light.



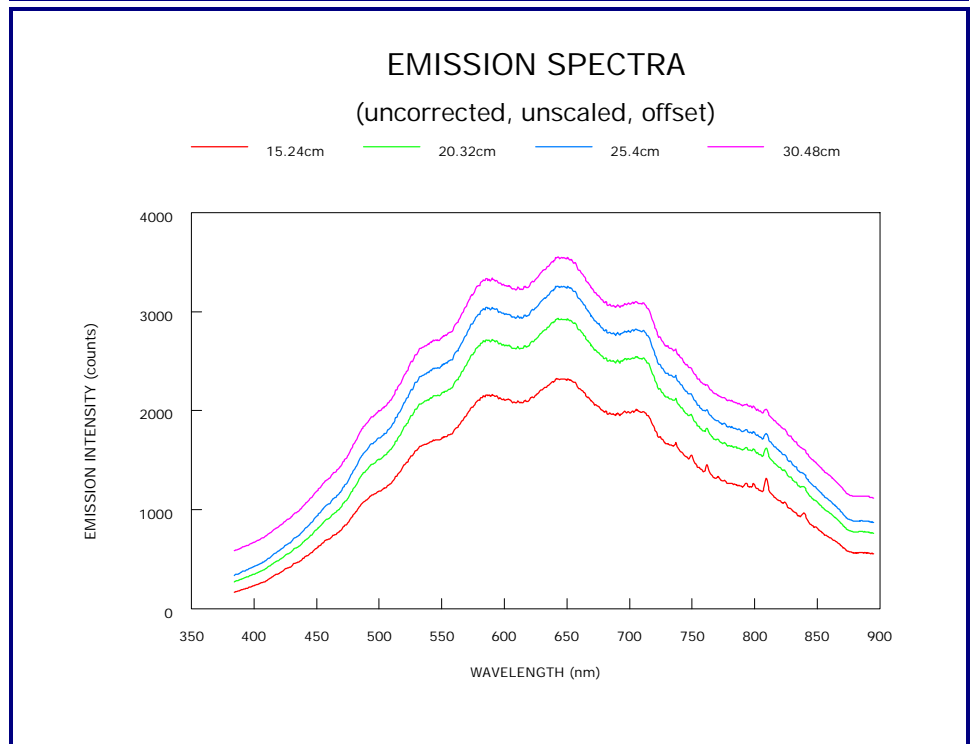
Spectroscopy Measurements (Vuegraphs cont.)

D. W. Bonnell (NIST)

Uncorrected (for sensitivity) emission spectra with F/1 lens, and lens-hood assembly; FOV ~ 2.5 cm. The material sprayed was 446 Ferritic SS powder, - 63 +23 micron size.



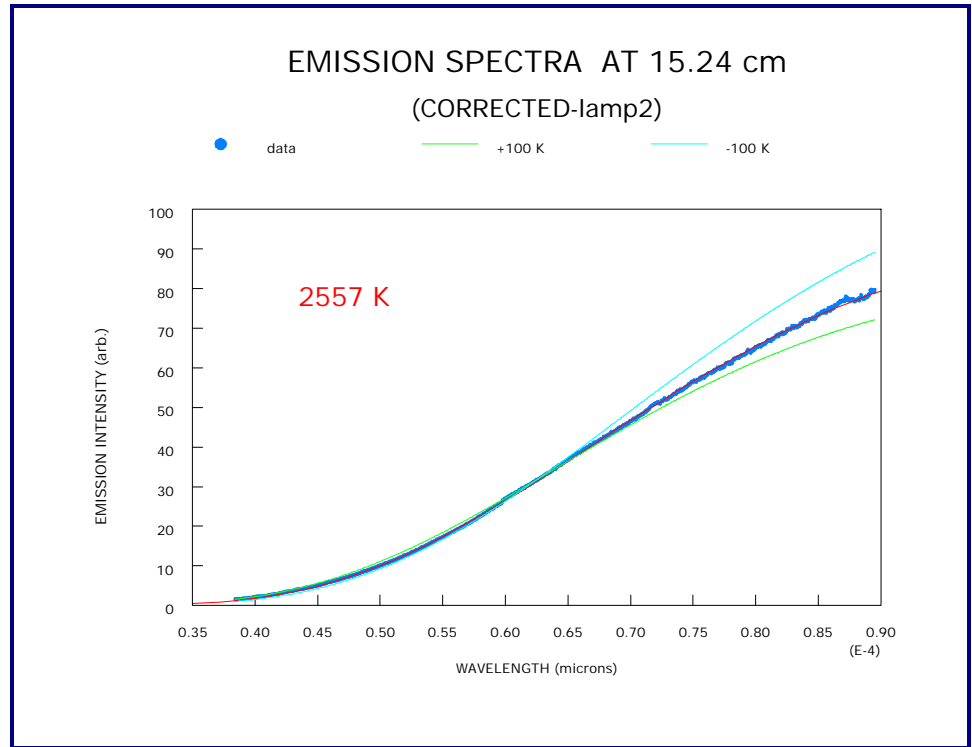
A sequence of spectra, as above, at various distances downstream. Note that the actual raw intensities are comparable, and have been offset here for visibility.



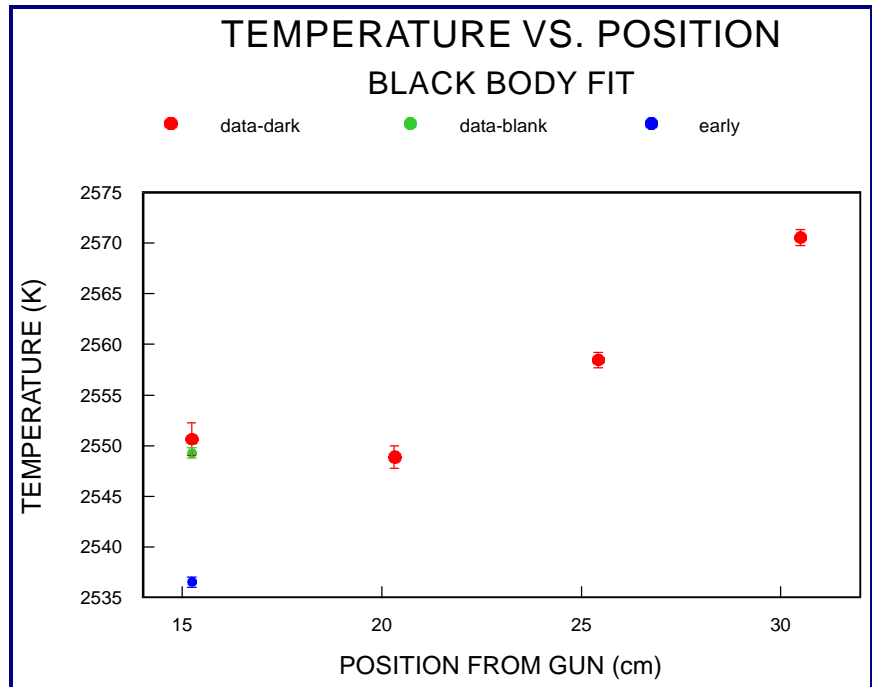
Spectroscopy Measurements (Vuegraphs cont.)

D. W. Bonnell (NIST)

Spectrum as above, after intensity correction against standard radiance source- the vertical axis is relative to the standard. The red curve is a fitted Planck function, for the temperature shown. The two dashed curves represent Planck curves for temperatures 100 K higher, and lower. Estimated error from all sources is <50 K, excluding non-gray body emissivity effects.



Resulting Temperature vs position downstream in torch spray. The trend is not considered significant. The constant temperature behavior probably reflects a combination of reaction heating and particle surface oxidation.



Spectroscopy Measurements (Vuegraphs cont.)

D. W. Bonnell (NIST)

Conclusions/Summary

- **Downstream dominated by PI thermal radiation**
 - but still some line emission
 - various absorption mechanisms seem small
 - Planck radiation behavior looks really good
- Apparent agreement between image and spectroscopy
 - far field interferences either small, or similar at both scales
 - depends on averaging methods
 - other problems noted can be made small
 - T nearly constant in far field (25-50 cm downstream)
 - T is quite high
 - Vapor pressure question
- Measurement/analysis problems grow near the torch
- Calibration effects can be serious error sources
- Similar questions for measurement geometry?!
- Both spectroscopy and imaging have robust advantages
- Simple pyrometry likely to have serious problems
- What data do transport models need?
 - reactive effects
 - vaporization
 - composition changes?
 - T distributions


Thermal Imaging

J. E. Craig (Stratronics)

An imaging pyrometer was developed to measure surface temperature of hot metal objects and particle temperature, velocity and size in thermal spray, spray-forming and atomization processes.

Two-wavelength imaging provides true, high-resolution temperature measurement, even with emissivity variation caused by roughness or oxidation. The system, having a field of view that spans the entire particle stream in thermal spray devices, provides continuous measurement of the entire particle stream. The software locates particle streaks in acquired thermal images, determines the intensity ratio and dimensions of each streak, and calculates the particle temperature, velocity and size. Measurements in the NIST thermal spray facility are described.


A broad range of material processes require a temperature imaging solution that provides accuracy on objects whose temperature or emissivity varies across the surface. Temperature imaging provides measurements at thousands of points, as opposed to the single spatially averaged result from spot pyrometers. Although infrared imaging cameras provide spatial resolution, they utilize a single waveband and form a temperature image from the intensity image by assuming a single value for the emissivity in the entire scene. This proves problematic when the emissivity varies across the object. Also, infrared imaging cameras are only available at high cost, thereby limiting their widespread application to industrial use.



A Two-Wavelength Imaging Pyrometer for Measuring Particle Temperature, Velocity and Size in Thermal Spray Processes

J.E. Craig, R.A. Parker, D.Y. Lee
Stratronics, Incorporated

Thermal Spray Coatings Workshop
 NIST, Gaithersburg, MD
 November 18, 1998



Introduction

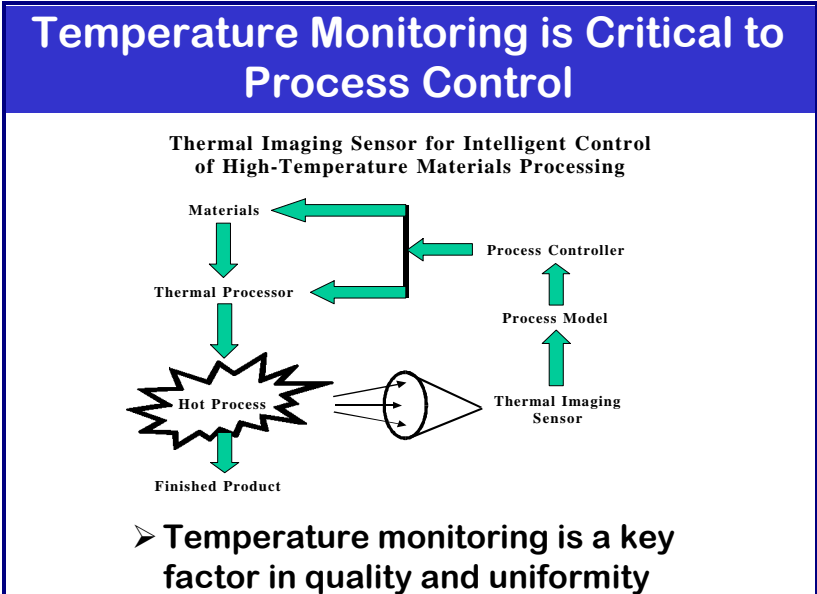
- **Two-wavelength imaging pyrometer for metal processing applications is developed**
- **Imaging pyrometer applied to hot metal objects**
- **Application to furnace using borescope technology**
- **Particle temperature monitoring for thermal spray**

Thermal Imaging (cont.)

J. E. Craig (Stratronics)

Recently, multiple wavelengths have been incorporated into instruments in an effort to deal with the variation in emissivity of the object. The issue of emissivity variation is particularly problematic for high temperature materials processes. A common theme to all this work is that each sensor was developed to monitor a particular process, albeit, steel, semiconductor wafers or pulverized coal combustion. While Meriaudeau, (Meriaudeau, 1996) described an imaging device for monitoring steel, which used only a single wavelength; it was concluded that a two-wavelength approach would be much more robust against effects of emissivity variation. For some materials, such as silicon wafers, this problem is overwhelming without using many wavelengths (Kaplinsky, 1998).

The key design feature in the imaging pyrometers used for this study is a filter pairing of the brightness of the long and short wavelength at each point on the heated surface or particle. Surface temperatures are imaged with a standard charge coupled device (CCD) video camera while particle streak imaging is achieved by incorporating a special short-exposure CCD camera (Morris, Karmali, 1997). This special camera features a high-resolution (640 by 480 pixels) array which is cooled and read out with 12 bit dynamic range. Another unique imaging feature of this camera is its electronic shutter. This feature provides from 1 to 10 exposures per video frame with each exposure duration adjustable from 50 ns to 1.0 ms. The frame rate for each video camera is 30 Hz. Single exposures of (1 to 10) μ s are typically used to obtain particle streak images with appropriate lengths. The streak length, adjusted with the exposure duration, is set in the range of 10 to 30 pixels. The signal to noise ratio of the streak intensity and the velocity resolution is improved by forming longer streaks. However, care was required in setting the streak length to avoid overlapping streaks and to insure that each streak begins and ends within the FOV.



Why Two-Wavelength Imaging Measurements

- Provides true, high-resolution temperature measurement
- Insensitive to emissivity variation across surface
- High-resolution temperature images result from two-wavelength design
- Precision optical design provides matched magnification, differential focus and registration to sub pixel resolution*

* Patent Pending

Specifications Imaging Pyrometers	
Surface	Particle
Temperature Range 600-2300°C (3-10°C)	Temperature Range 1200-2700°C (60°C)
Resolution Standard: 300 H x 480 V Across FOV, 20 μ m Optional: 500 or 1000 lines w/cooled chip & 12 or 16 bit A/D	Velocity: 10-900 m/s, (5%) Size: 30-300 μ m (30 μ m/pixel)
Electronic Shutter Speed: 7 exposure times from 16 ms to 130 μ s	Field of View: 1/2 inch format: 6.4 x 18.6mm 2/3 inch format: 8.8 x 25.8mm Electronic Shutter: 0.1 μ s to 10 ms

Thermal Imaging (cont.)

J. E. Craig (Stratronics)

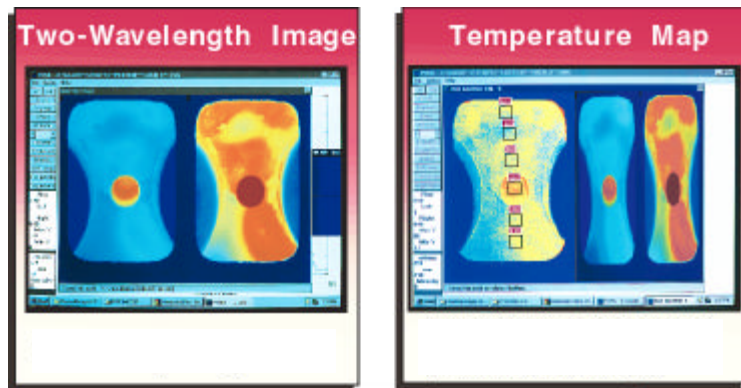
A demonstration of the SIP was performed in the Material Processing lab at the University of California at Santa Barbara. A round steel disk with an internal heating element and thermocouple was used as the thermal source of known temperature. The pyrometer was designed for maximum accuracy in the relatively low temperature range of 1200 K to 1400 K. Therefore, filters were selected in the longer wavelength region of the camera response. A video lens was selected having a FOV of 50 mm by 100 mm at a distance of 500 mm.

The image acquired with the steel block at its highest temperature is shown. The left image is from the short wavelength filter and the right image is from the long wavelength filter. A wire was placed on the steel block surface to provide a focusing aid for the surface pyrometer.

In another sequence of images, recorded as a movie, the temperature of the steel block was slowly raised by 3 K. The temperature measurement of the SIP, relative to the thermocouple measurement, is in excellent agreement throughout the movie. The best linear fit to the data shows that the temperature varied 3.3 K degrees, while the thermocouple measurement indicates slightly less than 3 K, again indicating the good agreement between the imaging pyrometer and the thermocouple measurements. However, there is local fluctuation of a few degrees in the SIP measurement and an absolute difference of 4 K.

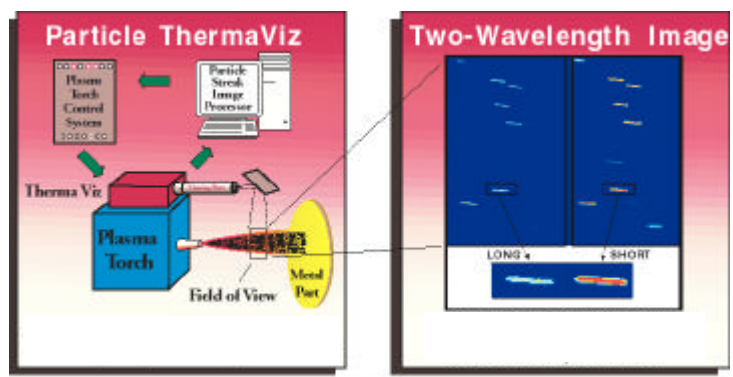
The PIP was installed in the NIST Thermal Spray Facility to measure particle temperature, velocity, and size. The two-wavelength imagery captures particle streaks in fast exposures, shown by the long and short wavelength images (right and left respectively) of nickel-based superalloy particles within the spray plume of a DC plasma torch using a mixture of argon and helium gases. Several particle streaks are observed in the image, which spans a FOV, 5 mm by 15 mm. A single particle streak image has been magnified. Particle measurements are currently performed in a post-processing step. Since the FOV spans the particle stream, the particle measurements can be averaged into several spatial regions spanning the particle stream. Thus, every image provides up-dates to particle temperature, velocity, and size profiles across the stream.

SURFACE Imaging Pyrometer System



- System provides simultaneous, high-resolution images of short and long wavelengths
- Software analyzes the brightness ratio to measure true-temperatures of surfaces with varying emissivity

PARTICLE Imaging Pyrometer System



- System provides continuous monitoring throughout entire particle stream
- System captures simultaneous images, locates streaks and analyzes data

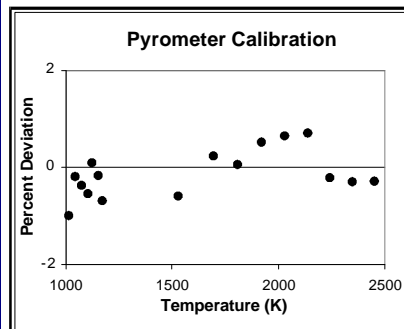
Thermal Imaging (cont.)

J. E. Craig (Stratronics)

The pyrometer was configured with a filter pair with pass-bands centered at 800 nm and 900 nm and the short-exposure CCD camera fitted with a front lens having a demagnification of 1/3. The pyrometer was then focused on the tungsten filament lamp described in the previous section. The intensity was measured in the long and short wavelength regions for filament current values between 12 A and 40 A. The intensity ratios (long over short wavelength) were determined and associated with the known temperatures of the tungsten filament. A single constant is used in the calibration of the pyrometer to achieve the best fit with the known filament temperature. The constant is determined using radiometric model of the pyrometer response to gray-body radiation. The uncertainty of the measured temperature was below 8 K over this range of calibration.

The radiometric model derived calibration constant incorporates three important components of the two-wavelength, imaging pyrometer response function: the two band-pass filter transmission characteristics, the relative spectral response of the CCD camera and the spectral curves for a Planck radiator. The deviation of the calibration constant from its ideal value of unity, which is typically $\pm 10\%$, is a measurement of the validity and accuracy of the radiometric model.

Pyrometer Calibration, 1000-2500 K

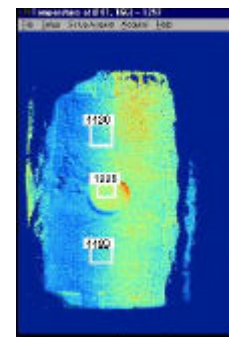


- Tungsten filament lamp used for higher temperature range (1000 - 2500K)
- A gray-body source used for low temperature range
- Standard deviation, 7.66 K

Heat Treating Application of Surface Pyrometer



- Cooled borescope is used as interface to furnace
- Pyrometer optics compatible
- Temperature images achieved

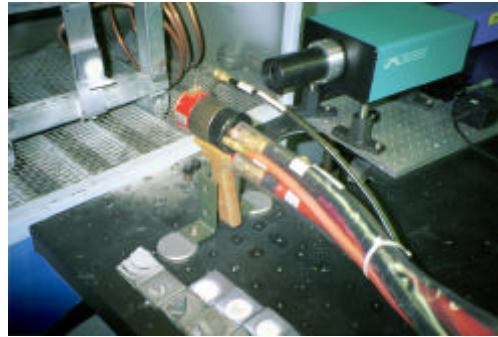


Temperature Map

Thermal Imaging (cont.)

J. E. Craig (Stratronics)

Thermal Spray Application of Particle Pyrometer at NIST

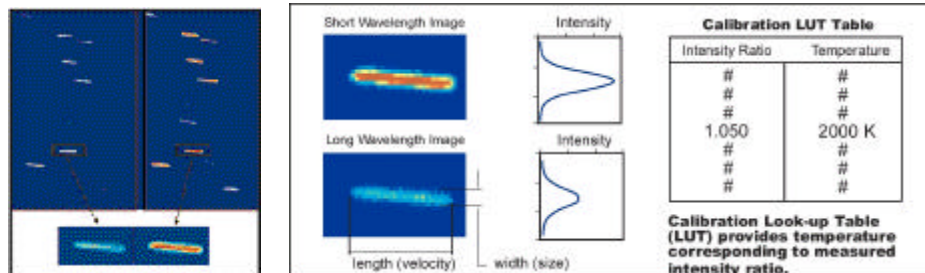


- DC plasma torch, argon/helium gases
- Nickel-based super alloy particles

B99-07

Movies with 135 frames were recorded in 4 seconds with the pyrometer focused at three points along the particle stream, 15 cm, 20 cm and 25 cm. The number of particle streaks were measured across the particle stream. About 800 to 1000 particles were included in each number profile. The FOV was adjusted at each distance to re-center on the particle stream, which drops a few millimeters between 15 cm and 25 cm. The relative vertical position of the three FOV's were not recorded, but were of the order of a few millimeters. The profiles indicate that the particle stream was spreading with distance. The particle count histogram at the 15 cm position indicated that the peak occurred at the 150 pixel column position (3.75 mm at 25 $\mu\text{m}/\text{pixel}$). The center of the FOV was at 300 pixels, or 7.5 mm.

Particle Measurements

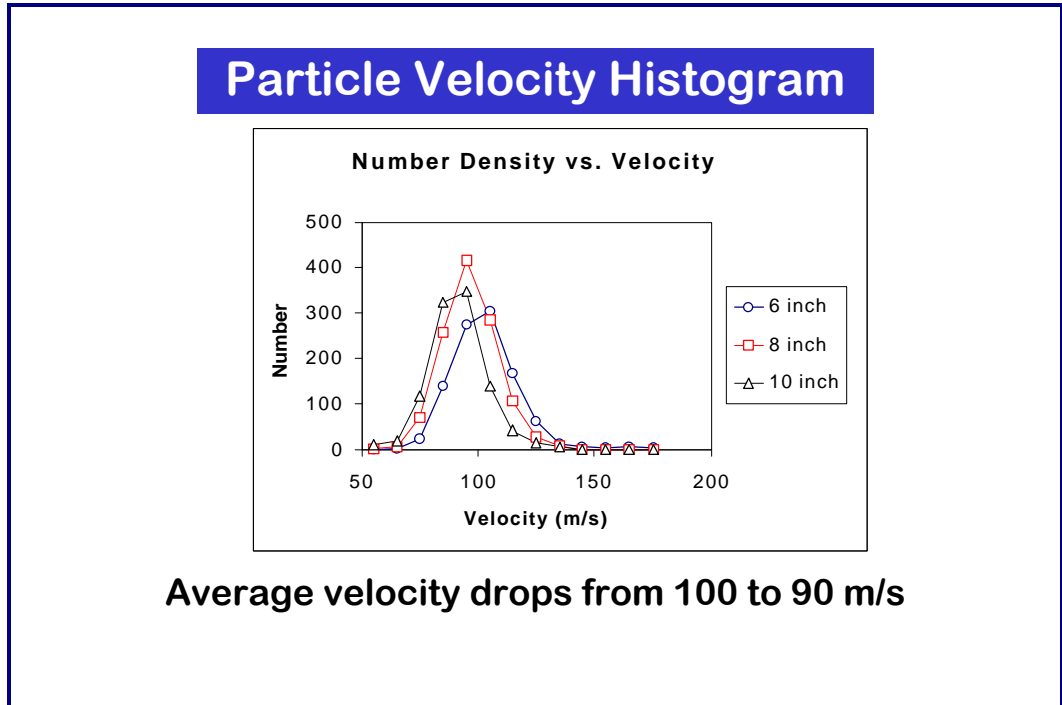


- Short-exposure (5 μs) particle streak images
- Measures temperature, velocity and size

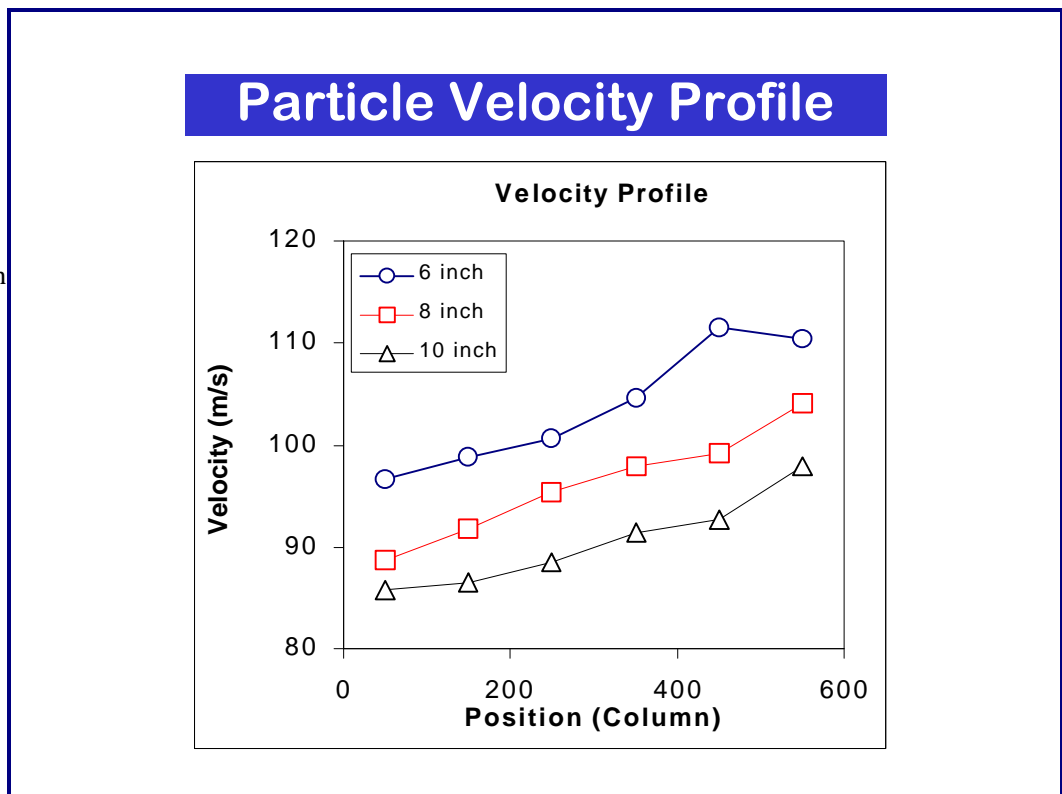
Thermal Imaging (cont.)

J. E. Craig (Stratronics)

The velocity histogram was constructed for data recorded at all three locations. Most of the velocity measurements fall between 75 m/s and 125 m/s. The mean velocity drops from 100 m/s to 90 m/s as position changes from 15 cm to 25 cm.



The velocity profile is shown in this slide for the data at all three locations. Again, it is clear that the mean velocity drops about 10 m/s as position changes from the 15 cm to the 25 cm locations. The highest velocity particles are on the top of the particle stream (high column number) but there are very few of these events.

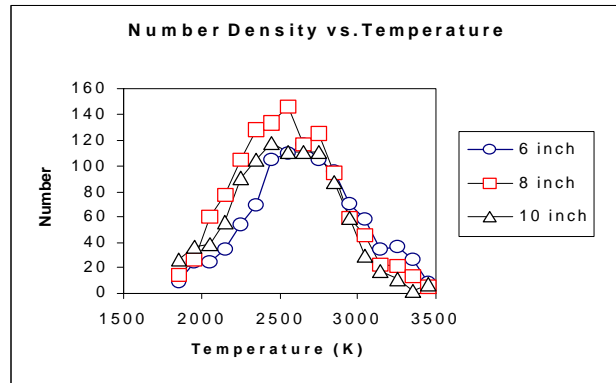


Thermal Imaging (cont.)

J. E. Craig (Stratronics)

Most temperature measurements fall between 2000 K and 3000 K.

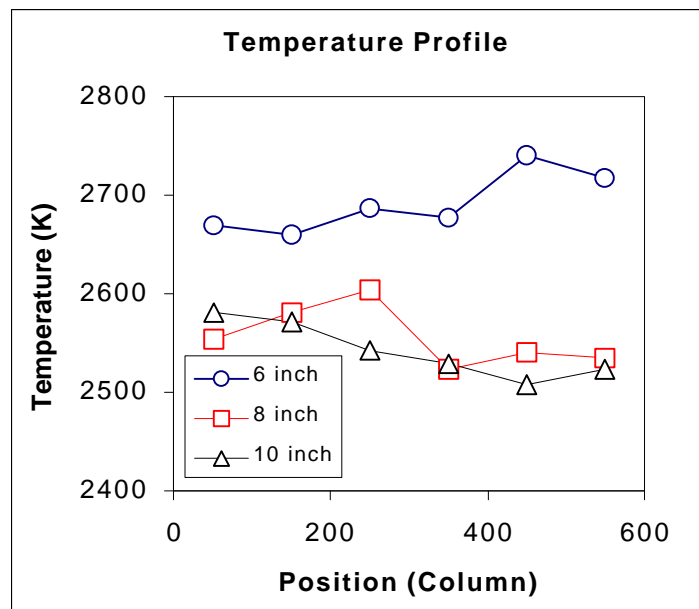
Particle Temperature Histogram



Average temperature drops from 2675 to 2520K

The temperature profiles at all three locations are nearly constant across the entire FOV.

Particle Temperature Profile



Thermal Imaging (cont.)

J. E. Craig (Stratronics)

Conclusions: A surface imaging pyrometer (SIP) and a particle imaging pyrometer (PIP) have been developed to measure either the surface temperature of hot metal objects or to measure particle temperature, velocity and size in thermal spray, spray-forming and atomization processes, PIP.

The resolution of the temperature image is 300 by 480 pixels across the FOV, which can range from a few millimeters in a highly magnified configuration to a full meter in a de-magnified configuration. The pyrometer output is standard video signal with a frame rate of 30 Hz. The pyrometer has been calibrated across a wide range of temperature, i.e. from (873 to 2700) K, to an uncertainty of 8 K. The major feature of the technology is the simultaneous imaging at two-wavelengths and the resulting ability to

measure true-surface temperature of high temperature objects with variable emissivity. The variation can occur across the surface of the object, or it can occur in time, for example as an object reaches a temperature, where oxidation begins. The feature is also important for process environments, in which the surface is being coated or formed, by droplets or powder. In that case, the result is a randomly rough texture or one with a significant variation in emissivity. The sensor is designed for adaptation and integration into process control systems by virtue of its software system. This technology has the potential to provide a significant improvement in modern, thermal process control systems.

The SIP instrument with analysis software has been developed to measure true surface temperature distributions with high resolution and accuracy for materials that are graybody radiators, i.e. a body whose emissivity is constant with wavelength. For materials that deviate from graybody behavior, an apparent ratio temperature will be inferred. The error will depend upon how much the emissivity varies with wavelength in the range between the short and long wavelengths. Future research has been proposed to study and model the error in the apparent ratio temperature inferred from the ratio of spectral radiances for target materials having unequal emissivities at the two wavelengths, thus permitting more accurate measurement on a broader range of materials. The technology shows considerable potential to monitor process uniformity, improve quality and reduce cost in advanced high-temperature, materials processing.


The PIP has a FOV that spans the entire particle stream in typical, thermal spray devices, and provides continuous measurement of the entire particle stream. Software was developed to determine temperature, velocity and size of each particle from the intensity ratios and dimensions of the particle streaks. Measurements of plasma-sprayed nickel-based particles have been obtained over a range of distances from the plasma torch showing the decay of temperature and velocity and the spreading of the particle stream associated with increasing distance from the torch. The particle temperature measurements were confirmed with a second measurement with a spectrometer. The comparisons between the two temperature measurements showed agreement to within 60 K. The particle velocity measurements will be validated in a future effort.

References

M. Kaplinsky, et al, "Recent Advances in the Development of a Multi-wavelength Imaging Pyrometer", *Opt. Eng.*, 36(11) Nov. (1998), p. 3176-3187.

F. Meriaudeau, et al, "Temperature Imaging and Image Processing in the Steel Industry", *Opt. Eng.*, 35(12), (1996), p. 3470-3481.

J. Morris and M. Karmali, "CCD Camera Helps Analyze Print Head Problems", *Photonics*, Aug. 1997.



Conclusions

- **Innovative two-wavelength imaging pyrometer measures surface and particle temperature with high resolution and accuracy**
- **Surface temperature accuracy varies from 3-8K over 200 K range and 2000K range respectively**
- **Particle temperature measurements accurate to 60K**
- **Sensor is designed for integration into process control systems by virtue of its powerful software capabilities**

*Numerical
Simulation of
Underexpanded
Jets*

A. Johnson (NIST)

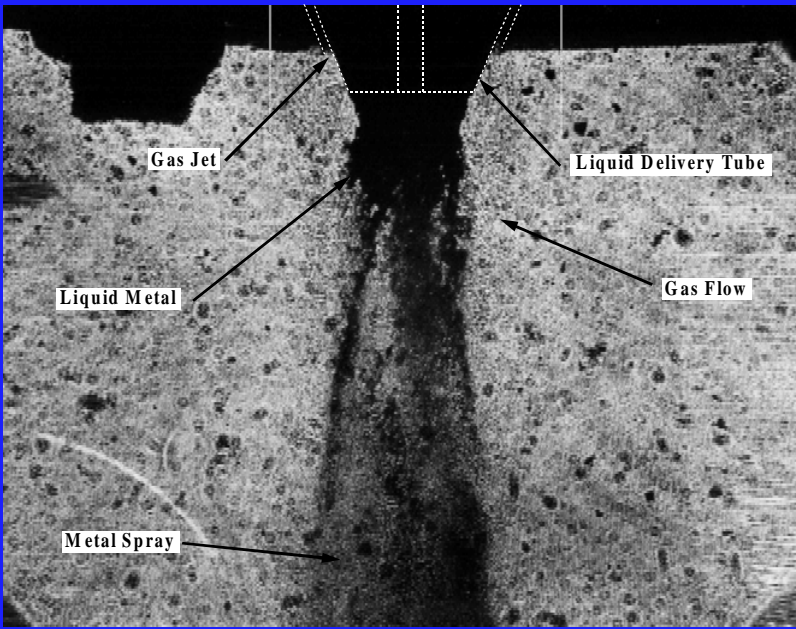
NIST

*Numerical Simulation of
Underexpanded Jets*

Aaron Johnson and Pedro I. Espina

*Thermal Spray Coatings Workshop
National Institute of Standards and Technology
Gaithersburg, MD 20899
November 19, 1998*

NIST



The micrograph shows a cross-section of a spray gun nozzle. A central channel is labeled 'Liquid Metal'. To its left, a 'Gas Jet' is shown. To its right, a 'Liquid Delivery Tube' is visible. Below the nozzle, a 'Gas Flow' is indicated. At the bottom, a 'Metal Spray' is shown. Dotted lines indicate the nozzle's geometry.

Gas Jet

Liquid Metal

Metal Spray

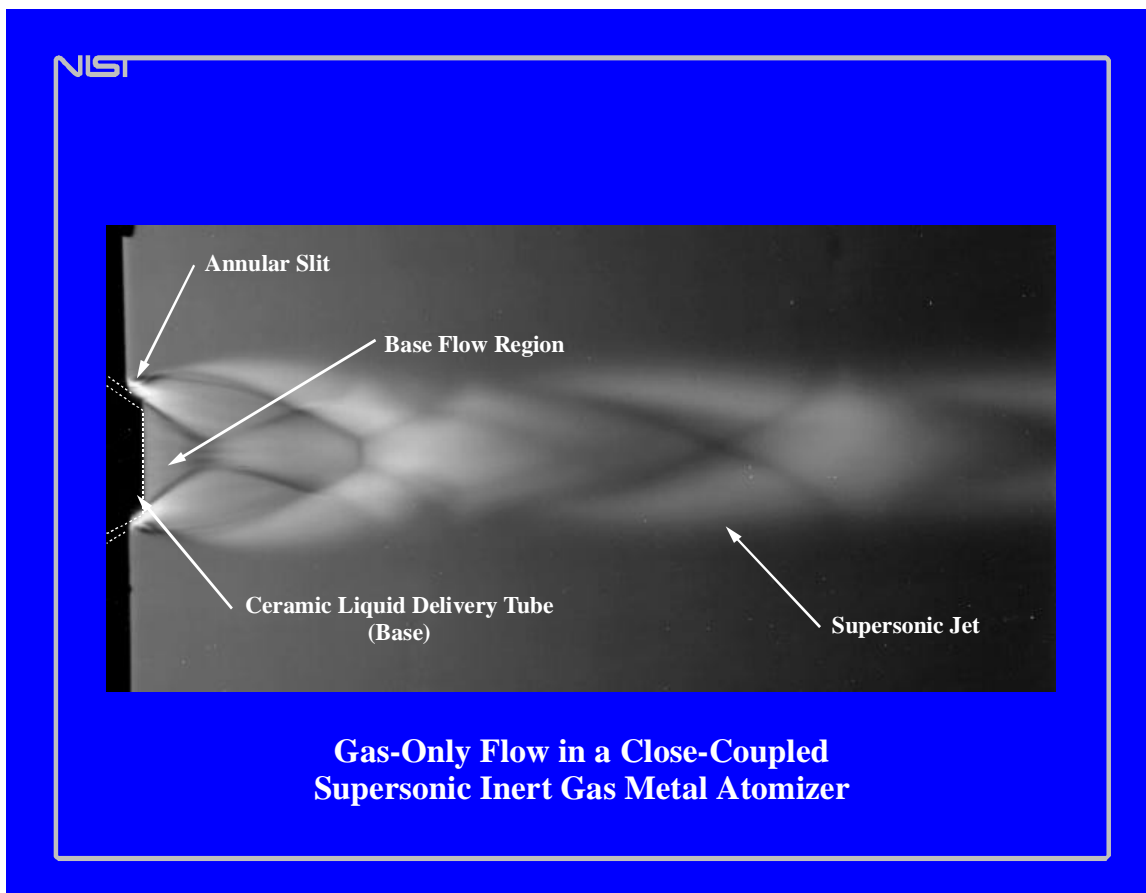
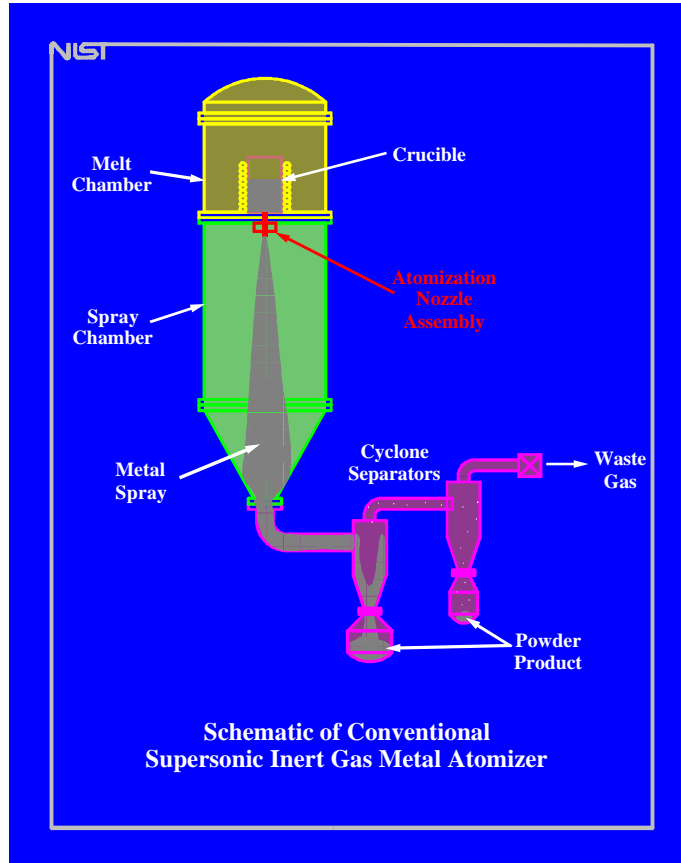
Liquid Delivery Tube

Gas Flow

Gas-Metal Atomization

Numerical Simulation of Underexpanded Jets
(cont.)

A. Johnson (NIST)



*Numerical
Simulation of
Underexpanded
Jets (cont.)*

A. Johnson (NIST)

NIST

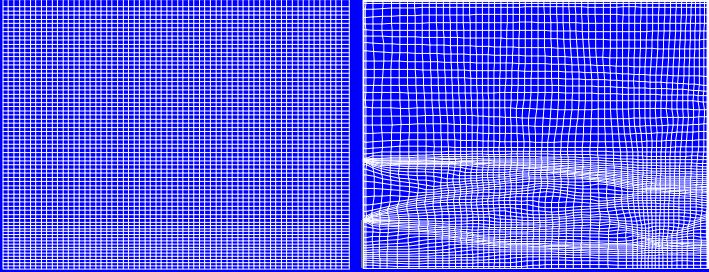
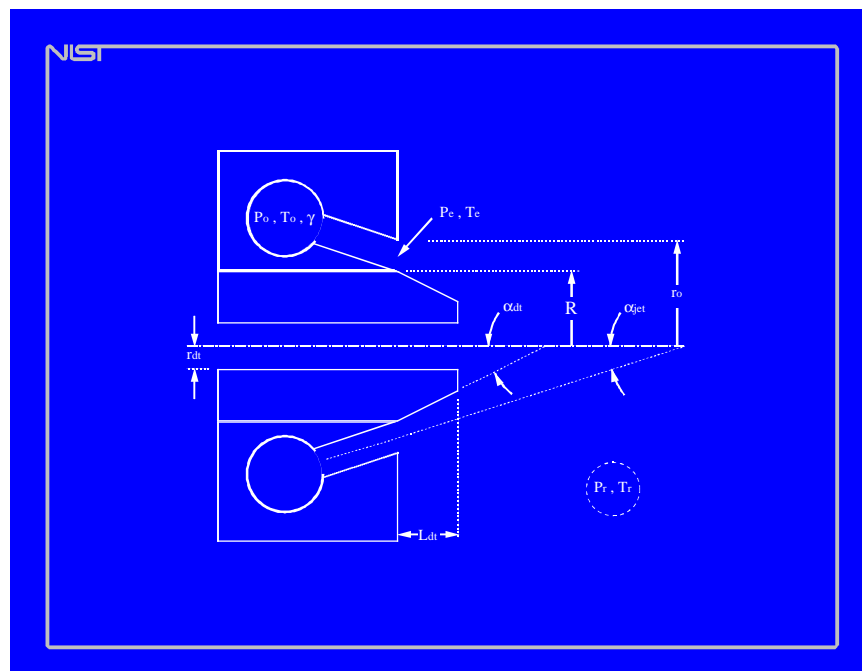
Numerical Method

Compressible Navier-Stokes Solver (NPARC 2.1)

- *Descendant of the NASA ARC2D and ARC3D codes*
- *Beam and Warming Approximate factorization algorithm*
- *2nd order central-differencing*
- *Equations formulated in strong conservation form for a curvilinear system*
- *Diagonalized implicit matrices*
- *Euler backward time differencing*
- *Implicit 2nd and 4th order Jameson-style artificial dissipation*

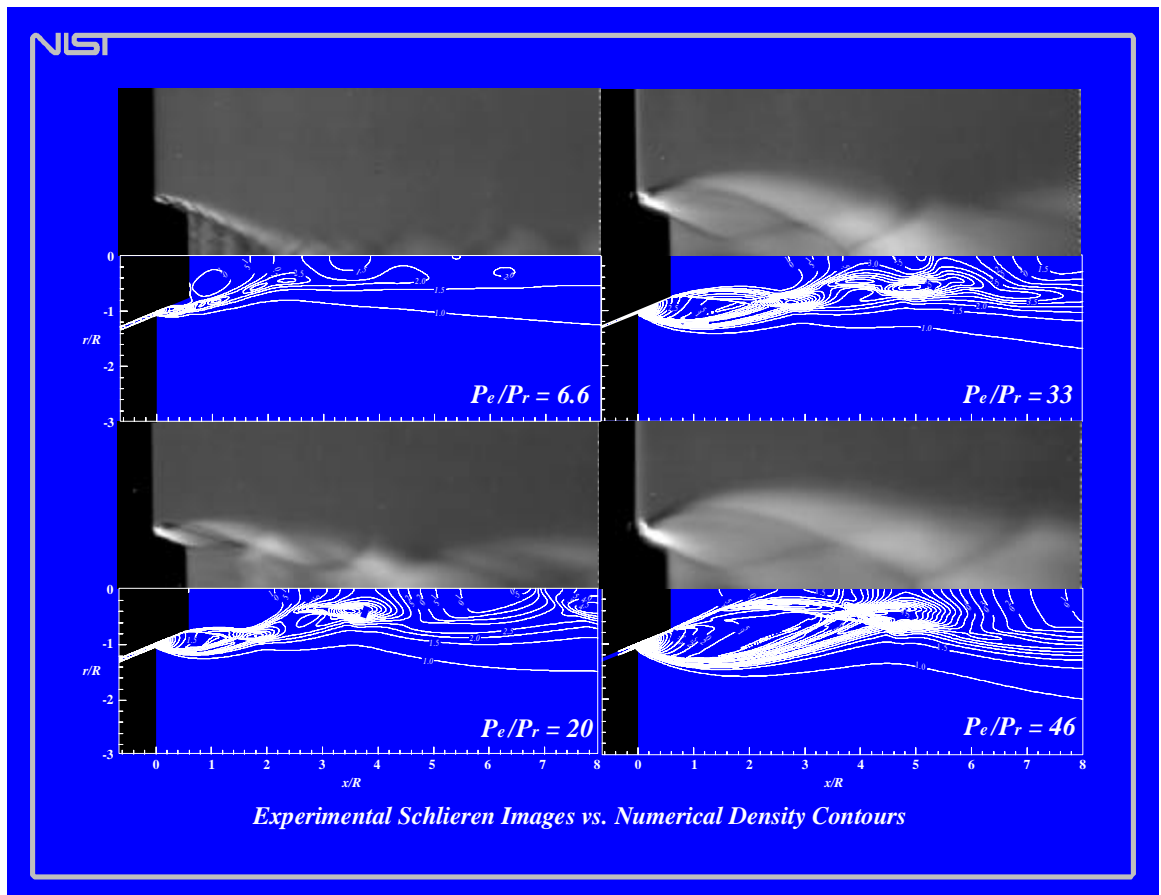
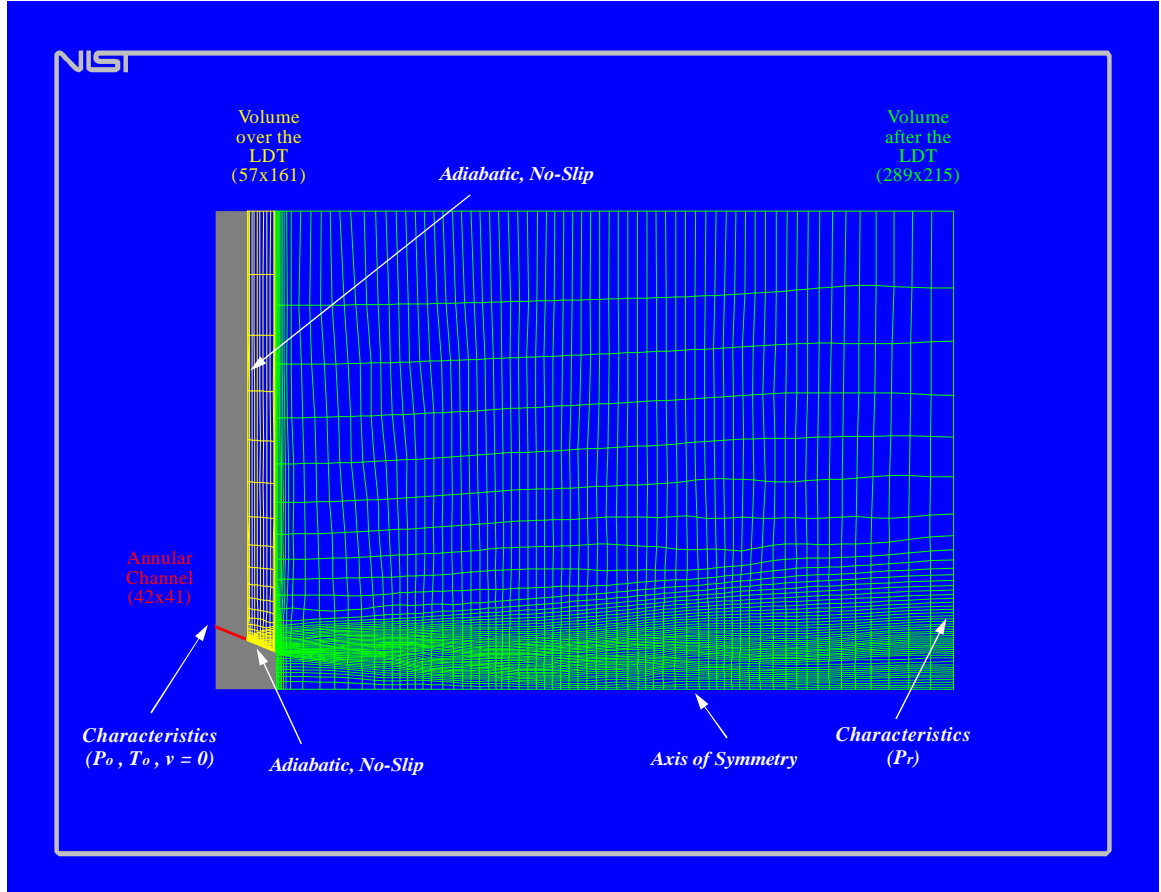
Grid Adaptation Program (SAGE)

- *Parabolic formulation*

Numerical Simulation of Underexpanded Jets (cont.)

A. Johnson (NIST)



Numerical Simulation of Underexpanded Jets (cont.)

A. Johnson (NIST)

NIST

Conclusions

1. Results have shown these Pressure Ratio effects.

- *Numerical results in good agreement with schlieren images.*
- *Aspiration behavior appears to be correlated with the structure of the separation region.*
- *Low pressure ratios, or long LDT, lead to flow separation increasing the chances of freeze-off.*
- *Atomizers should be easier to operate at high pressure ratios.*

2. Limitations of Research

- *The numerical method can not be used to make quantitative predictions of the aspiration pressure nor of flow separation.*
- *Predictions of the aspiration and separation need validation.*
- *Liquid is expected to have an influence on the structure of the gas flow.*
- *Future work should study the effects of particle loading on the structure of the gas flow.*

Process Control

S. A. Osella (ICT)

ICT

MEL

Process Control

Stephen A. Osella, Ph.D.
Intelligent Computing Technologies, Inc.
intcomtec@aol.com
512-301-2444

November 19, 1998

ICT

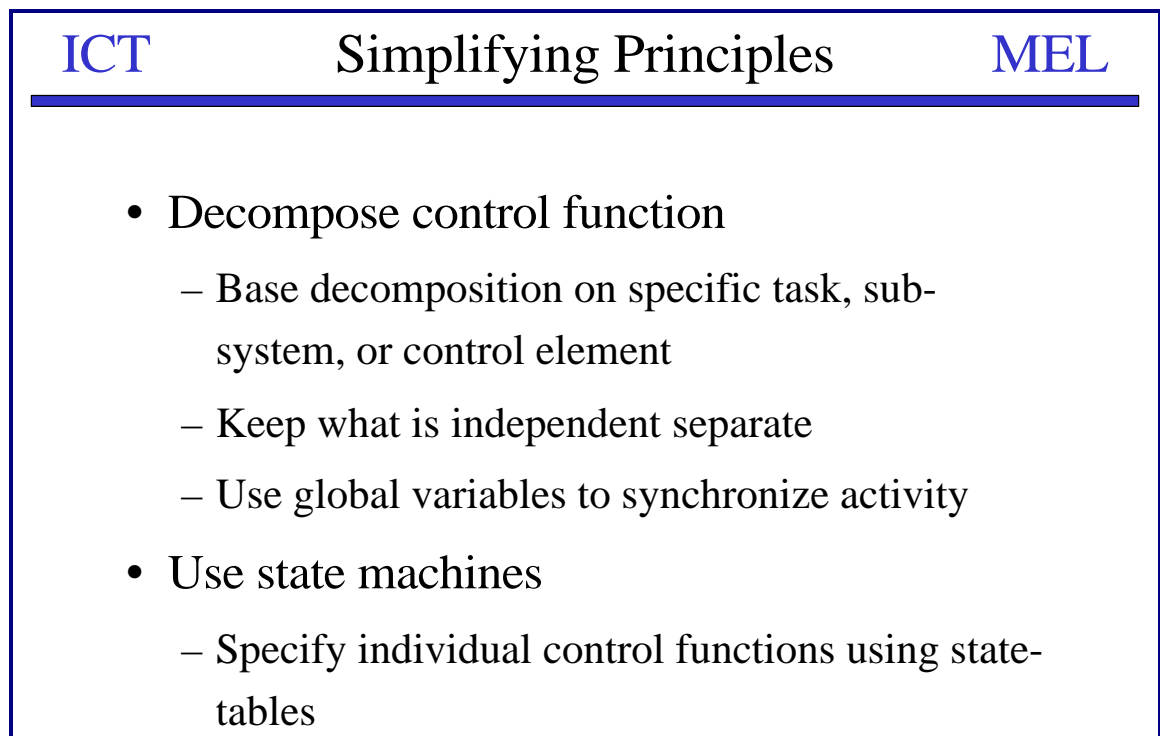
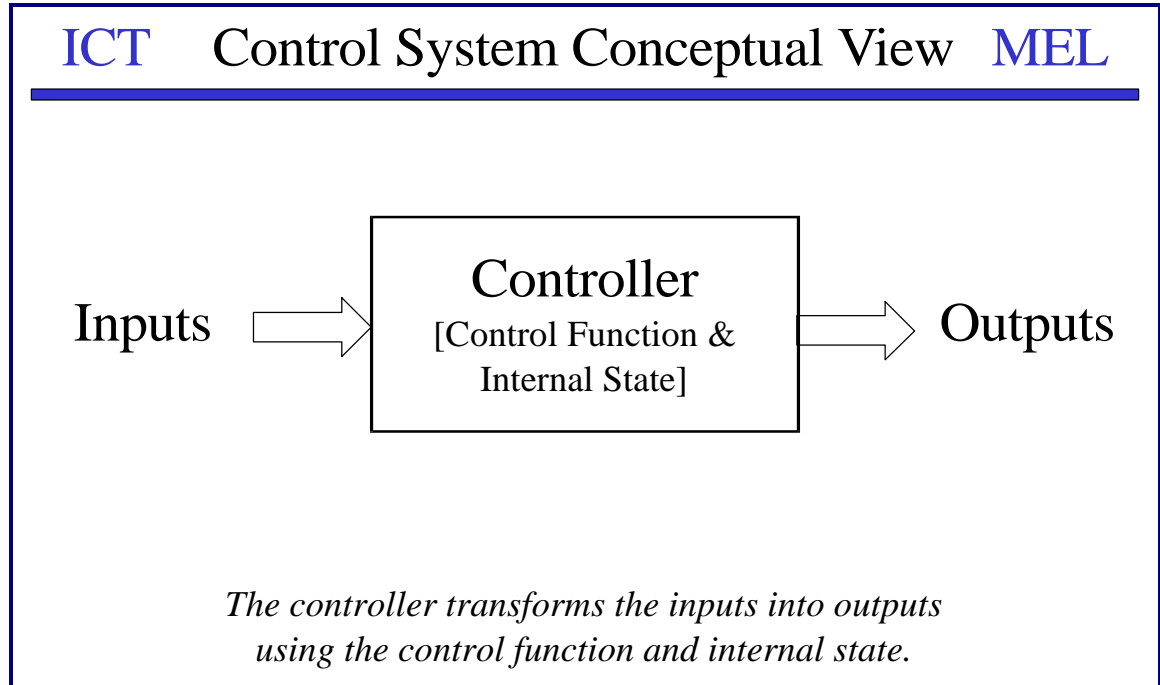
Process Control Basics

MEL

- Modern process control systems are very complex involving:
 - many instruments measuring pressure, temperature, flow, level, etc.
 - control elements such as valves, pumps, heaters, etc.
- Output control is either:
 - Manual : operator effects control
 - Automatic : hardware or software machine
- Control elements are either:
 - On-Off : ex. Valve
 - Continuous : ex. Motor RPM

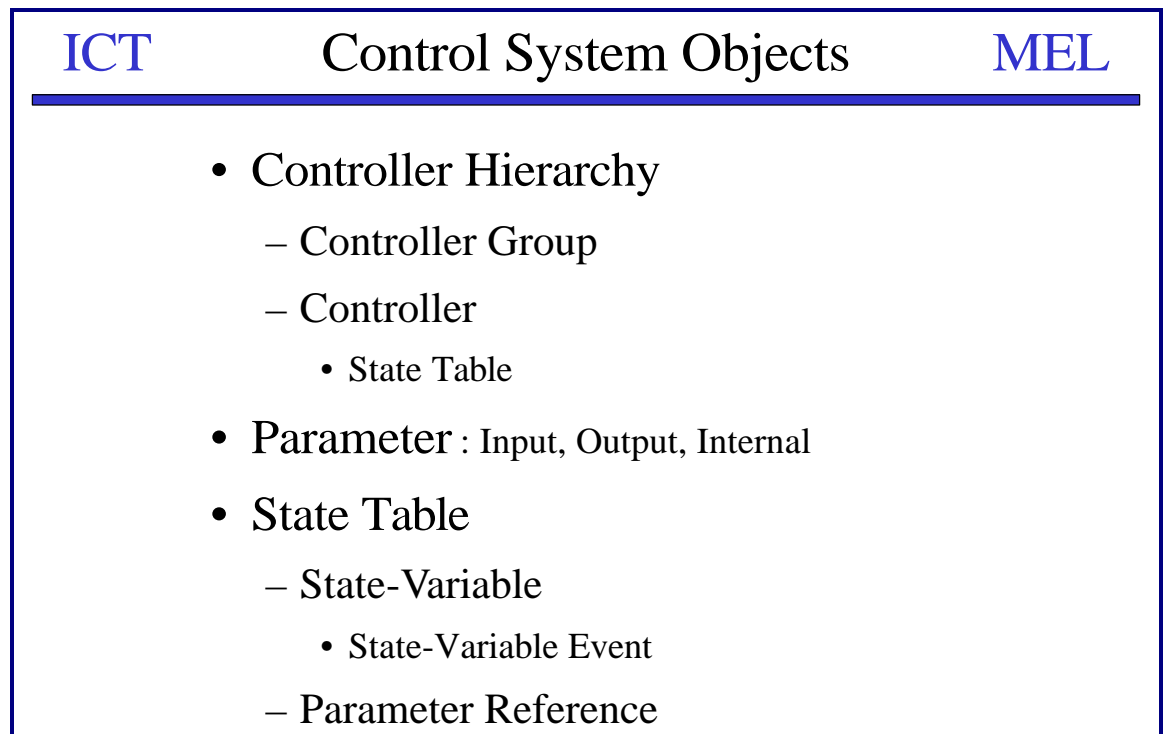
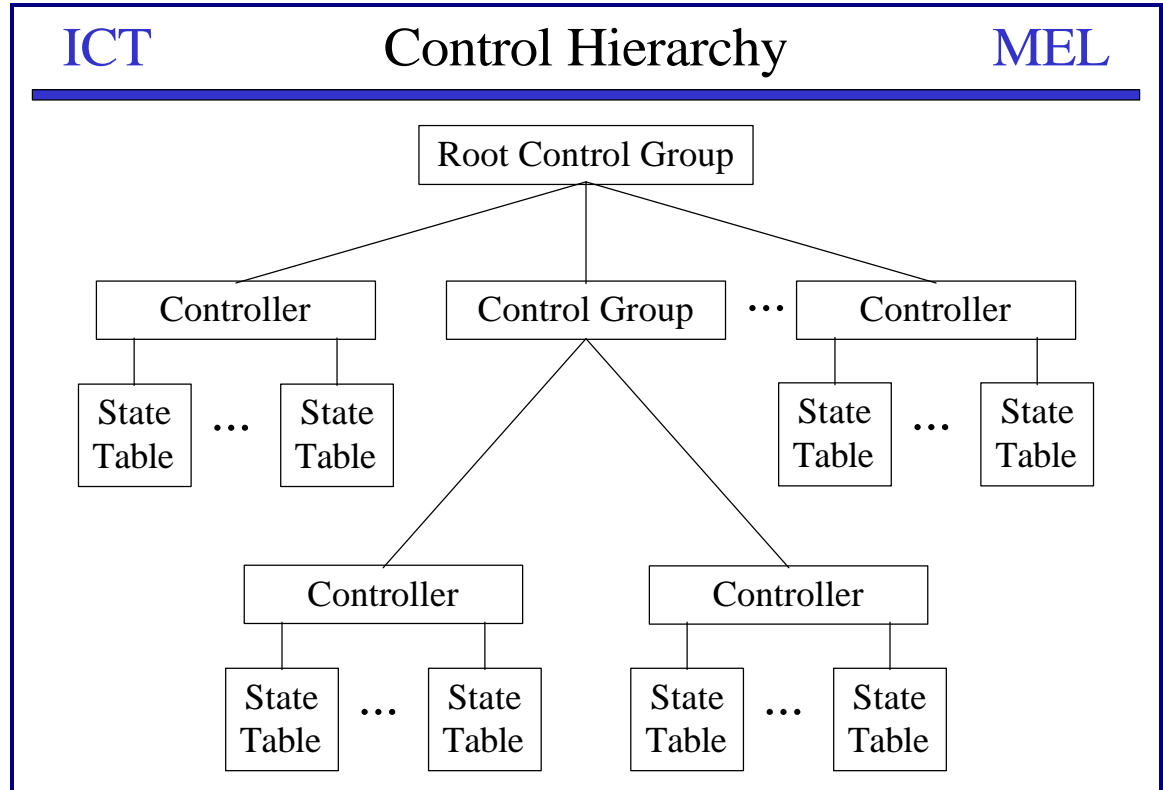
Process Control
(cont.)

S. A. Osella (ICT)



Process Control
(cont.)

S. A. Osella (ICT)



Process Control (cont.)

S. A. Osella (ICT)

ICT

Control System Workbench

MEL

Parameters	Type	Mode	Index	Setting	Balance	Index
Exhaust_Temperature	OBL	Input/Output	0	Constant	-	-
External_Die_Temperature	OBL	Input/Output	1	Constant	-	-
Die_Plenum_Temperature	OBL	Input/Output	2	Constant	-	-
Tundish_Temperature	OBL	Input/Output	3	Constant	-	-
Melt_Chamber_Temperature	OBL	Input/Output	4	Constant	-	-
Melt_Chamber_Pressure	OBL	Input/Output	5	Constant	-	-
Atomizing_Chamber_Pressure	OBL	Input/Output	6	Constant	-	-
Die_Plenum_Pressure	OBL	Input/Output	7	Constant	-	-
Supply_Pressure	OBL	Input/Output	8	Constant	-	-
Line_Pressure	OBL	Input/Output	9	Constant	-	-
Intrinsic_OI_Gamma	OBL	Input/Output	10	Constant	-	-
Pressure_Ratio	OBL	Output Only	11	Standalone	Yes	1
Gas_Metal_Ratio	OBL	Output Only	12	Standalone	Yes	2
Cyclone_Arm_LED	TF	Input/Output	13	Constant	-	-
Stopper_Rod_LED	TF	Input/Output	14	Constant	-	-
Die_Gas_Valve_LED	TF	Input/Output	15	Constant	-	-
Cyclone_LED	TF	Input/Output	16	Constant	-	-
Separation_Valve_LED	TF	Input/Output	17	Constant	-	-
MC_Fill_Valve_LED	TF	Input/Output	18	Constant	-	-
MC_Vent_Valve_LED	TF	Input/Output	19	Constant	-	-
Pouffing_Valve_LED	TF	Input/Output	20	Constant	-	-
Safety_Valve_LED	TF	Input/Output	21	Constant	-	-
Actual_Number_Of_Motors	I32	Input/Output	22	Constant	-	-
Alarm	TF	Input/Output	23	State Table	-	-
Backfill_Done	TF	Internal	-	State Table	-	-
Enable_Backfill	TF	Internal	-	State Table	-	-
Enable_Motors_On	TF	Internal	-	State Table	-	-
TimeOut	U32	Internal	-	State Table	-	-
Separation_Valve	TF	Output Only	24	State Table	-	-
Log_Data	TF	Output Only	25	State Table	-	-
Cyclones	TF	Output Only	26	State Table	-	-
Stopper_Rod	TF	Output Only	27	State Table	-	-
Die_Gas_Valve	TF	Output Only	28	State Table	-	-
Enable_Control	TF	Internal	-	State Table	-	-
Backfill	TF	Input/Output	29	State Table	-	-

ICT

Control System Workbench

MEL

	Enable_Backfill_SV	Backfill_SV	Pme_It_Pdb	MC_Fill_SV	In_Dead_Band	Active_Table	Backfill_Done	MC_Fill	Backfill
0	true	true	true	true	true				
1	true	true	true	true	false			TRUE	
2	true	true	true	false	true			TRUE	
3	true	true	true	false	false			FALSE	
4	true	true	false	true	true			FALSE	
5	true	true	false	true	false			FALSE	
6	true	true	false	false	true	Done	TRUE		
7	true	true	false	false	false			FALSE	
8	true	false	true	true	true	Idle		FALSE	
9	true	false	true	true	false	Idle		FALSE	
10	true	false	true	false	true	Idle			
11	true	false	true	false	false	Idle			
12	true	false	false	true	true	Idle		FALSE	
13	true	false	false	true	false	Idle		FALSE	
14	true	false	false	false	true	Idle			
15	true	false	false	false	false	Idle			
16	false	true	true	true	true	Idle		FALSE	FALSE
17	false	true	true	true	false	Idle		FALSE	FALSE
18	false	true	true	false	true	Idle		FALSE	FALSE
19	false	true	true	false	false	Idle		FALSE	FALSE
20	false	true	false	true	true	Idle		FALSE	FALSE
21	false	true	false	true	false	Idle		FALSE	FALSE
22	false	true	false	false	true	Idle		FALSE	FALSE
23	false	true	false	false	false	Idle		FALSE	FALSE
24	false	false	true	true	true	Idle		FALSE	FALSE
25	false	false	true	true	false	Idle		FALSE	FALSE
26	false	false	true	false	true	Idle			
27	false	false	true	false	false	Idle			
28	false	false	false	true	true	Idle		FALSE	FALSE
29	false	false	false	true	false	Idle		FALSE	FALSE
30	false	false	false	false	true	Idle			

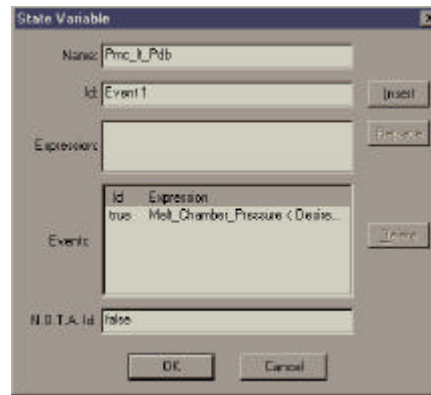
Process Control
(cont.)

S. A. Osella (ICT)

ICT

Control System Workbench

MEL



- Each state-variable is defined by a number of events
- Each event is a logical expression
- Event expressions are evaluated in order until one is TRUE
- If none is TRUE, the “None Of The Above” event is triggered
- A State is a combination of state-variable events (State Table row)

ICT

Control System Workbench

MEL

- **Controller Verification**
 - Controller logic is “syntactically” verified
 - Semantic verification is planned
-
- **Automatic Code Generation**
 - C-language code
 - LabVIEW Code Interface Node resource

*Sensors and
Controls for
Thermal Spray:
Is there a need?*

C. C. Berndt
(SUNY Stony Brook)

1

Sensors and Controls for Thermal Spray: Is there a need?

Christopher C. Berndt

SUNY at Stony Brook

cberndt@notes.cc.sunysb.edu

* NIST presentation 1998

C. C. Berndt



The Thermal Spray Market in 1990

2

	Annual Sales (\$M)	
	US	World
Coating applicators & Job Shops	410	900
OEMs	160	280
Military	45	60
Other	15	20
Total	630	1260
Suppliers of equipment, systems & materials	275	430

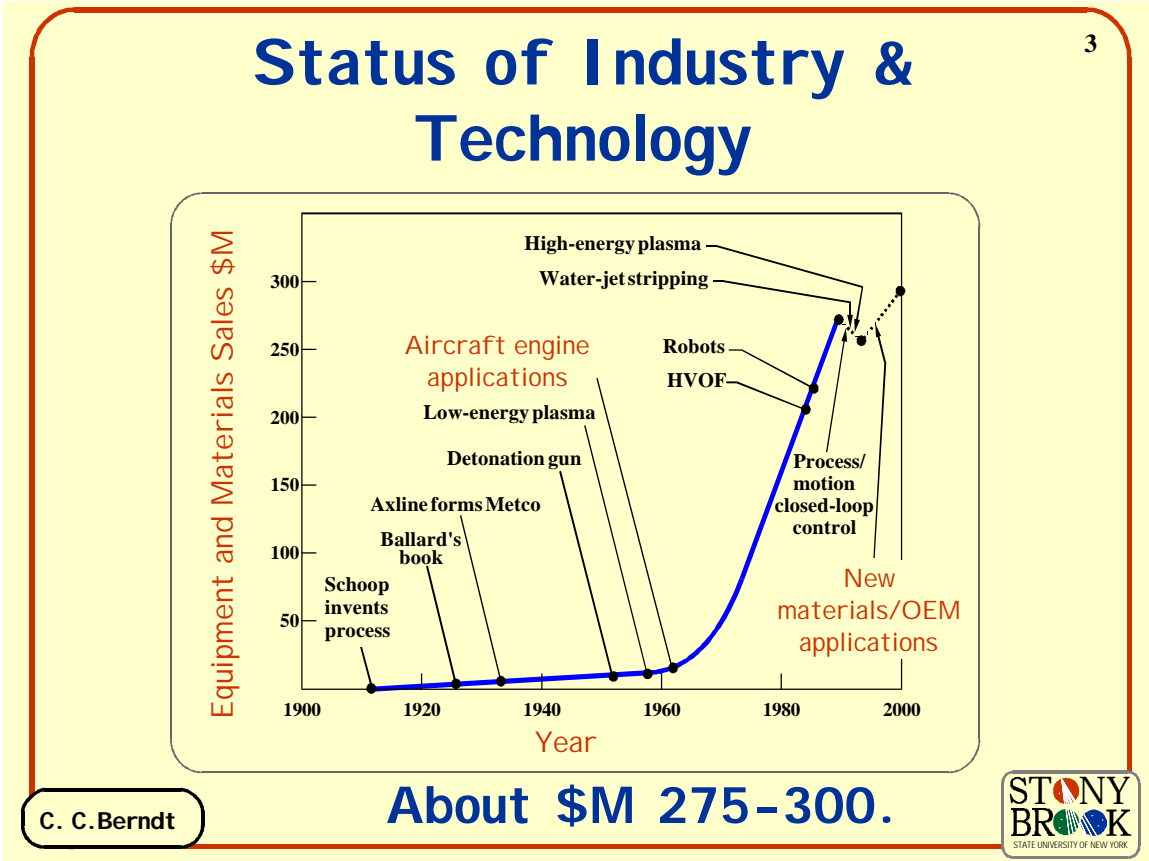
Is this an accurate measurement of the TS Market?

C. C. Berndt



Sensors and Controls for Thermal Spray: Is there a need? (cont.)

C. C. Berndt (SUNY Stony Brook)



C. C. Berndt

The Commercial Future of Thermal Spray 4

(November, 1998)

	1997		2002		AAGR
Type	\$M	%	\$M	%	%
Thermal Spray	380	53.5	510	51.7	6.1
CVD	151	21.3	218	22.1	7.6
PVD	141	19.8	186	18.8	5.7
Other	38	5.4	73	7.4	14.0
Total	710	100.0	987	100.0	6.8

- Source: Business Communications, Norwalk, CT
- AAGR = Average annual growth rate.
- Other = dipping, spraying, sol-gel, laser-assisted.

Note: Only North America

C. C. Berndt

Sensors and Controls for Thermal Spray: Is there a need? (cont.)


C. C. Berndt
(SUNY Stony Brook)

5

Questions & Comments

- Thermal spray is being commingled with the other techniques; e.g., sol-gel, laser.
- “High technology” is creeping into thermal spray. What will people be willing to pay for it?
- The more important question (which has not been addressed) is “How many guns / systems are there in the marketplace?” , 500 or 5,000 units?
- Does control improve the economics of thermal spray industry?

C. C. Berndt




6

Is there Money in “Control/ Sensors”?

Total \$'s = \$M510

Percent \$'s on Equipment	\$M	Percent \$'s on Equipment	\$M	Total %
10	51	10	5.1	1
10	51	20	10.2	2
10	51	30	15.3	3
20	102	10	10.2	2
20	102	20	20.4	4
20	102	30	30.6	6
30	153	10	15.3	3
30	153	20	30.6	6
30	153	30	45.9	9

C. C. Berndt



*Sensors and
Controls for
Thermal Spray:
Is there a need?
(cont.)*

C. C. Berndt
(SUNY Stony Brook)

7

Processes and Markets

Year	Plasma	Arc Wire	Combustion Wire	Combustion Flame	HVOF
1960	15	15	35	35	
1980	56	6	11	28	
2000	48	15	4	8	25

- “High tech / advanced” methods are taking a larger market share.

C. C. Berndt



8

Control Tools Currently Available

- There are some general commercial control systems that are available and that have been proven for thermal spray.
 - In-Flight Particle Pyrometer.
 - Tecnar DP2000 for measuring temperature.
 - Control Vision.
- Who is using these tools - other than research Institutions?

C. C. Berndt



*Sensors and
Controls for
Thermal Spray:
Is there a need?
(cont.)*

C. C. Berndt
(SUNY Stony Brook)

9

Other Control Tools in the Research Phase.

- **Acoustic Emission** to measure torch performance & erosion; hence implying life and microstructure.
- **Laser thickness gages.**
- **Laser non-destructive methods.**

C. C. Berndt



10

Practicality?

- **Who will pay for control tools / sensors?**
- **Is tool development a terminal SBIR activity?**
- **Are such tools robust?**
- **What will these devices enable?**
 - Higher productivity?
 - Better microstructures?
 - Processes that would not be available otherwise?
- **Does the work force need an advanced degree to use **such equipment?****

C. C. Berndt



*Sensors and
Controls for
Thermal Spray:
Is there a need?
(cont.)*

C. C. Berndt
(SUNY Stony Brook)

11

Sensors / Controls that are Important

- Impact properties (temperature, velocity, size).
- Residual stress / strain, Elastic modulus.
- Real time thickness.
- Deposition efficiency.
- Surface roughness.
- A “direct microstructure” sensor.
E.g., porosity

The vital factor is to have these available in a user-friendly and economical mode.

C. C. Berndt



12

Conclusions

Remember the question:

**“Sensors and Controls for Thermal Spray: Is there a need?”
and**

“Will such devices be accepted by the thermal spray constituency?”

The answer is “YES!”

C. C. Berndt



*Sensors for
Controlling
Thermal Spray
Processes*

C. Moreau (NRC-
CNRC)



National Research Council Canada
Conseil national de recherches Canada

NRC · CNRC

Sensors for Controlling Thermal Spray Processes

***Christian Moreau and Luc Leblanc
Industrial Materials Institute***

***Thermal Spray Workshop,
NIST, Gaithersburg, MD
18 November 1998***



Canada

Outline

- Introduction
- Sensing Techniques (Processes and Materials)
 - zone 1: Heat Generation
 - zone 2: Particle Heating and Acceleration
 - zone 3: Coating Built-up
- Control Strategies
- Conclusions

NRC · CNRC

*Sensors for
Controlling
Thermal Spray
Processes (cont.)*

C. Moreau (NRC-
CNRC)

Aerial View of IMI



NRC · CNRC

IMI Mission

Promote the growth and competitiveness of Canadian industry, through research and development activities related to *materials processing technologies*

NRC · CNRC

*Sensors for
Controlling
Thermal Spray
Processes (cont.)*

C. Moreau (NRC-
CNRC)

IMI - Overview

Created 1978

Moved to Boucherville 1983

Staff 150

of which: Scientific/Eng 75

Technical 50

Budget 17M\$

NRC · CNRC

Core Competencies

Materials Behavior

- Development and improvement of processes optimizing microstructure to obtain higher performance materials
- Development and experimental validation of process modeling software
- Development and use of optical and ultrasonic sensors for process and quality control

NRC · CNRC

*Sensors for
Controlling
Thermal Spray
Processes (cont.)*

C. Moreau (NRC-
CNRC)

Process Instrumentation - Expertise

Nondestructive characterization

Optical inspection

Ultrasonic techniques

NRC · CNRC

Optimum Process Control

- The key physical process variables and key characteristics of the coating for the application it is dedicated to must be identified and controlled.
- Elements required to control the process:
 - the optimum value of these process and coating key variables must be known
 - the sensors to monitor these characteristics must be available
 - the controller must be able to modify the input spray variables to compensate for any deviations identified

NRC · CNRC

*Sensors for
Controlling
Thermal Spray
Processes (cont.)*

C. Moreau (NRC-
CNRC)

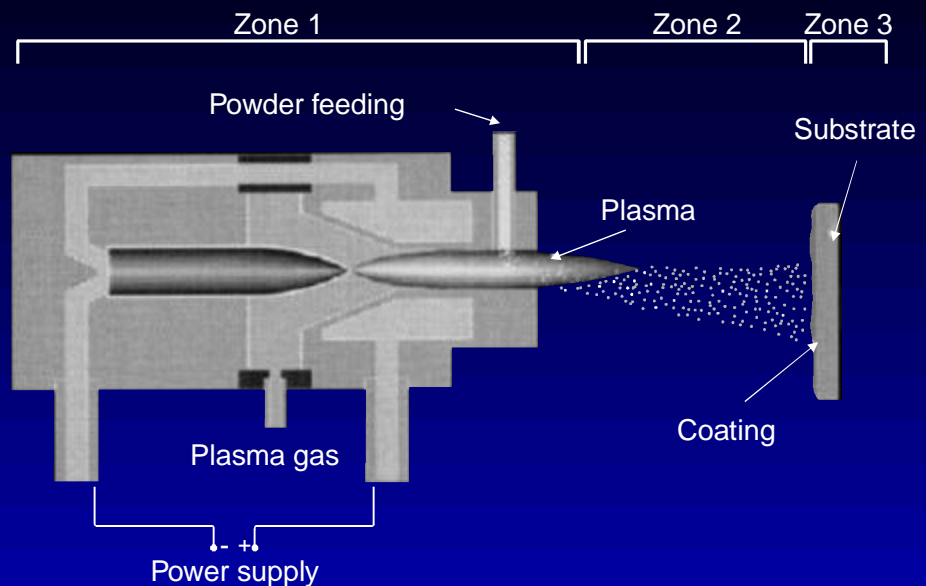
Practical Requirements

In establishing a control strategy, one must take into account:

- costs of the sensors and controllers
- ruggedness of the sensors
- ease to use
- operator training (technical skills)

NRC · CNRC

Diagnostics in Thermal Spray Processes



NRC · CNRC

*Sensors for
Controlling
Thermal Spray
Processes (cont.)*

C. Moreau (NRC-
CNRC)

Sensing Techniques Zone 1: Heat Generation

- Present state-of-the-art technology based on the monitoring and control of input variables in Zone 1:

Spray Processes	Main input variables
DC plasma	arc current arc gas flow rates
HVOF/ flame	fuel flow rate oxygen or air flow rate

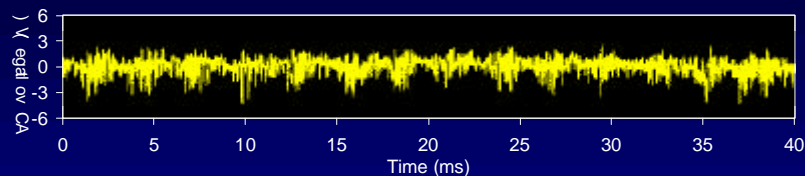
- Input energy or net plasma energy

NRC · CNRC

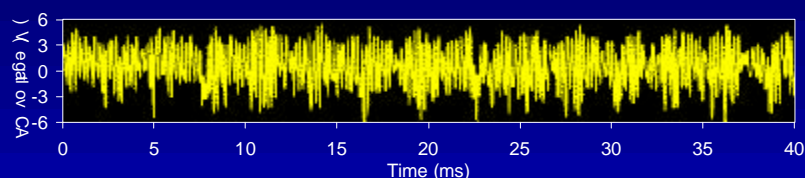
Voltage Fluctuations

Time Evolution

- At the beginning of the wear experiment



- At the end of the wear experiment (40 hours)



NRC · CNRC

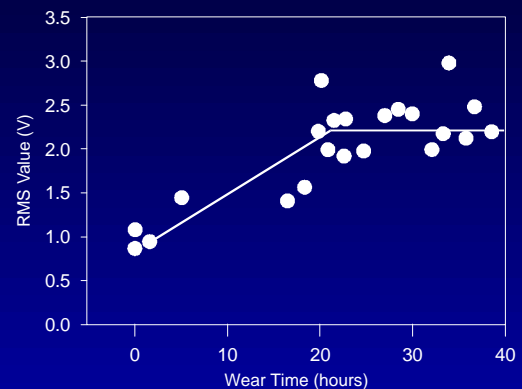
*Sensors for
Controlling
Thermal Spray
Processes (cont.)*

C. Moreau (NRC-
CNRC)

Voltage Fluctuations

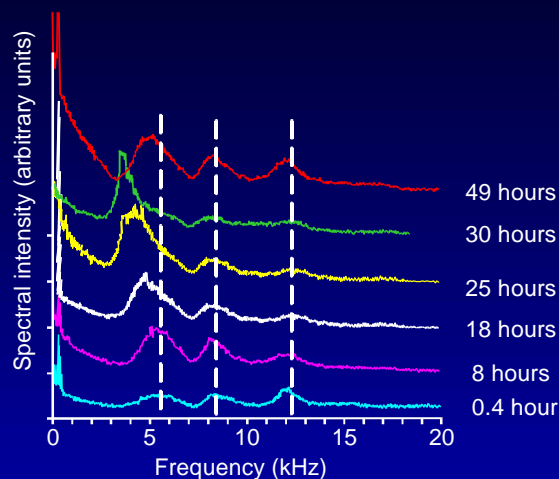
Time Evolution of the Root Mean Square

- Increase of the voltage fluctuation rms value during the first 20 hours of spraying. A plateau was reached for the remainder of the wear experiment.



NRC · CNRC

Voltage Signature Evolution



- Three distinct frequency regions are identified in the voltage signatures.
- During fifty hours of spraying, regions located around 8.3 kHz and 12.3 kHz did not evolve significantly.
- However, region located around 5.0 kHz shifted significantly.

NRC · CNRC

*Sensors for
Controlling
Thermal Spray
Processes (cont.)*

C. Moreau (NRC-
CNRC)

Monitoring of Fluctuations in Plasma Spraying

- Signals correlated to the arc root movement:
 - voltage fluctuations
 - acoustic emission
 - high speed imaging
 - plasma light intensity fluctuations
- Advantages (specially voltage signatures):
 - easy to implement
 - low cost
- Disadvantages:
 - how to react?

NRC · CNRC

Sensing Techniques Zone 1: Heat Generation

- Techniques for monitoring the temperature, velocity and composition of the hot gas jets:
 - emission spectroscopy
 - coherent anti-Stokes spectroscopy (CARS)
 - Rayleigh spectroscopy
 - enthalpy probe
 - oxygen sensors
- Difficult to use in a production environment

NRC · CNRC

*Sensors for
Controlling
Thermal Spray
Processes (cont.)*

C. Moreau (NRC-
CNRC)

Zone 2: Particle Heating and Acceleration

- The structure and properties of the sprayed coatings depend directly on the temperature and velocity of the particles before impact
- Various techniques were developed for particle diagnosis in laboratory:
 - Two-color pyrometry
 - laser Doppler anemometry (phase)
 - laser Two-focus
 - streak camera
- Concerns:
 - complexity, fragility, high technical skill and safety

NRC · CNRC

Particle Diagnosis Techniques: Simplified Approaches

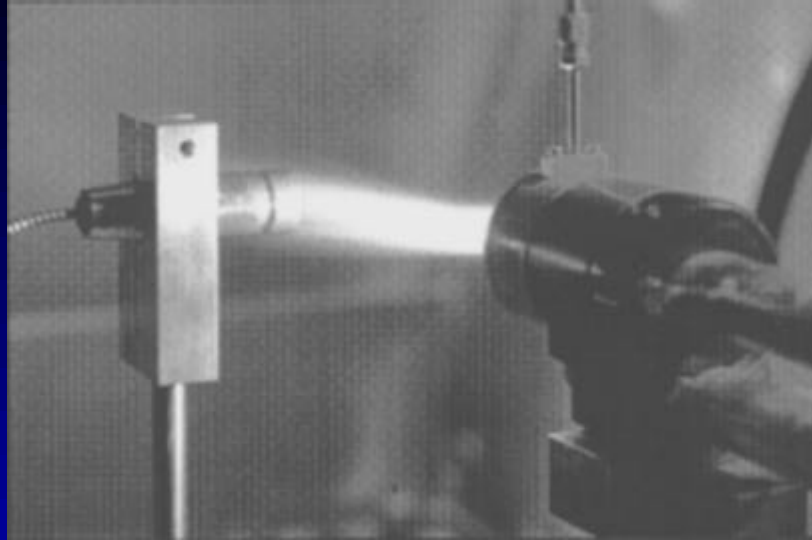
- Use of the thermal radiation emitted by the hot particles
- Linear camera for monitoring the orientation, width and intensity of the particle jet
- Commercial systems for monitoring the particle temperature and velocity

NRC · CNRC

Sensors for Controlling Thermal Spray Processes (cont.)

C. Moreau (NRC-CNRC)

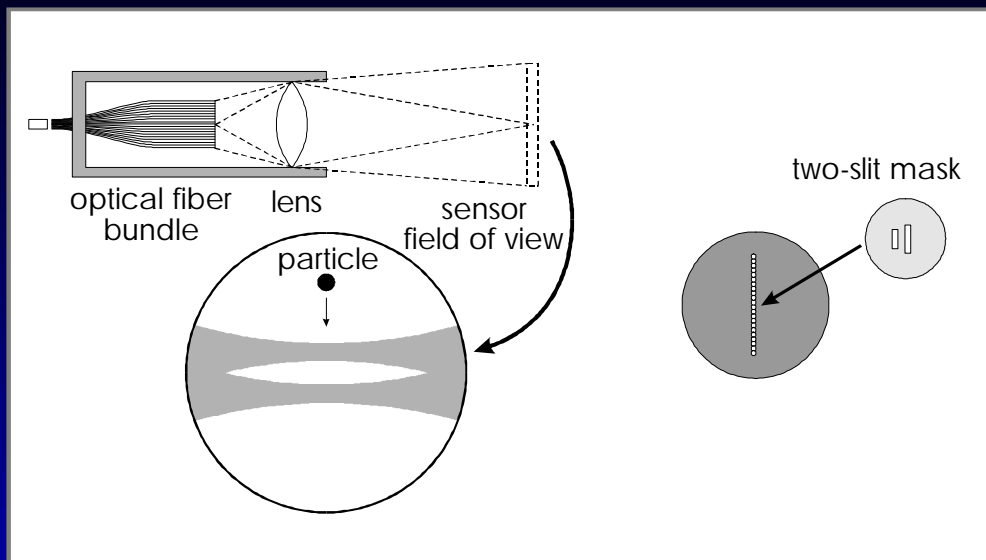
On-line Particle Monitoring During Thermal Spraying



DPV2000 Tecnar Automation Ltee

NRC · CNRC

The Sensor Head



NRC · CNRC

*Sensors for
Controlling
Thermal Spray
Processes (cont.)*

C. Moreau (NRC-
CNRC)

Particle Diagnosis System DPV2000

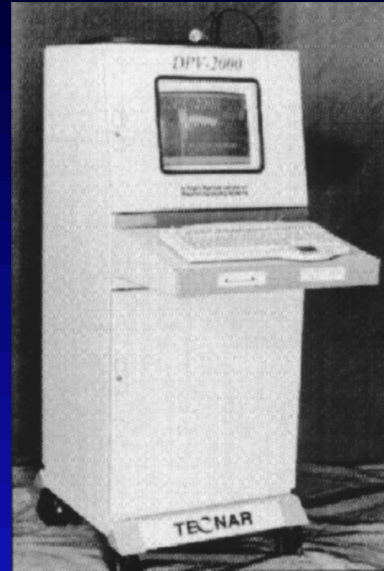
On-line Monitoring:

Particles:

Temperature
Velocity
Diameter

Particle Jet:

Intensity
Orientation
Width

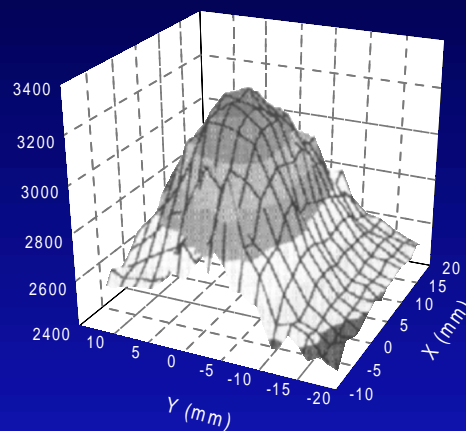


NRC · CNRC

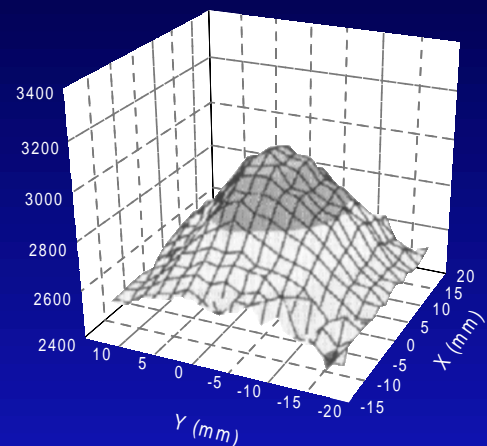
Long Term Stability of the Plasma Spray Process

Particle temperature ($^{\circ}\text{C}$)

1 hour



37 hours

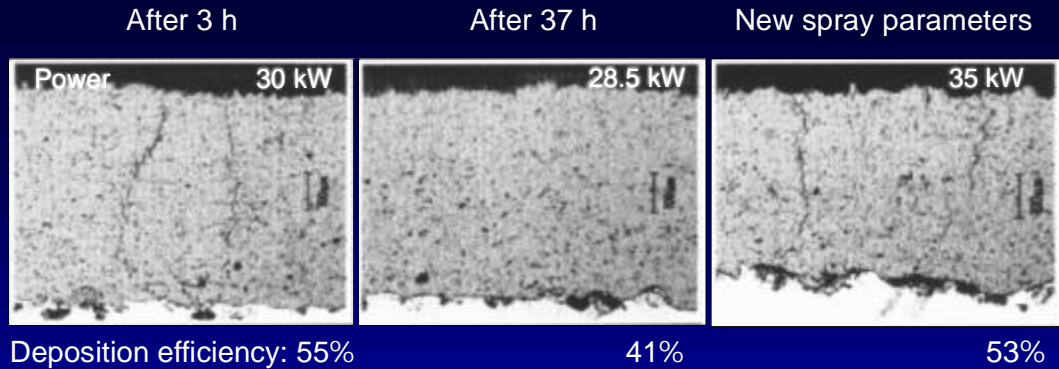


NRC · CNRC

Sensors for Controlling Thermal Spray Processes (cont.)

C. Moreau (NRC-CNRC)

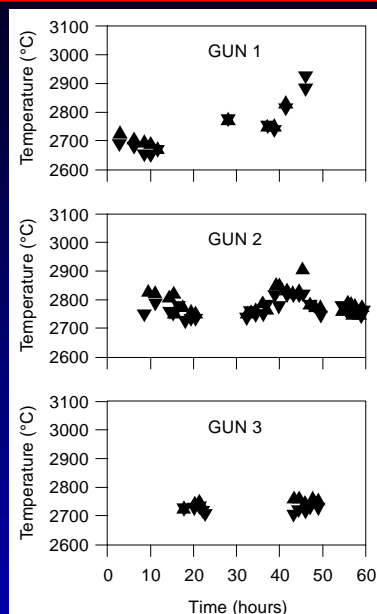
Evolution of Coating Microstructures



- Coatings sprayed after 3 hours and with new spray parameters are very similar (microstructures, deposition efficiencies).

NRC-CNRC

Time Evolution of the Particle Temperature



3 Different Torches

- Yttria-zirconia powders
- Low power plasma (20 kW)
- Radial injection of powders
- Constant power control

NRC-CNRC

*Sensors for
Controlling
Thermal Spray
Processes (cont.)*

C. Moreau (NRC-
CNRC)

Zone 3: Coating Build-up

- Monitoring of the substrate and coating temperature during spraying
- Characterization of the substrate preparation
- Coating characteristics and NDT

NRC · CNRC

Substrate and Coating Temperature

- Influence on:
 - the interface quality between lamellae
 - residual stresses
 - crack formation
 - thermal conductivity
 - elastic modulus, etc.
- Measuring techniques:
 - one- or two-color pyrometry
 - infrared camera

NRC · CNRC

*Sensors for
Controlling
Thermal Spray
Processes (cont.)*

C. Moreau (NRC-
CNRC)

Coating Characteristics and Nondestructive Testing

- Various techniques (with and without contact):
 - high resolution camera
 - triangulation
 - eddy current
 - thermal wave
 - laser-ultrasonics
- Properties to measure:
 - thickness
 - elastic moduli
 - thermal conductivity
 - porosity
 - defects

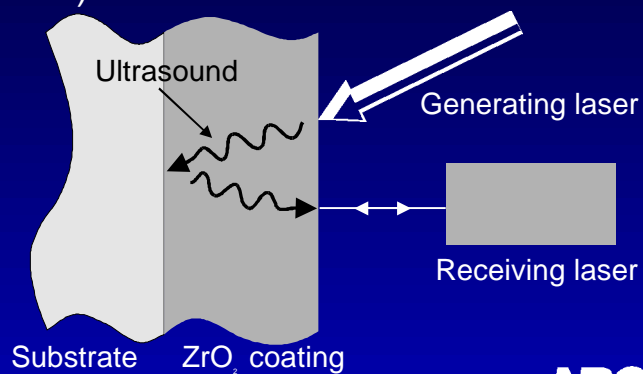
NRC · CNRC

Laser Ultrasonic Principle

CO₂ laser generating 120 ns duration pulses

No coupling medium

Detection using a Nd:YAG laser (50 μs pulse duration)

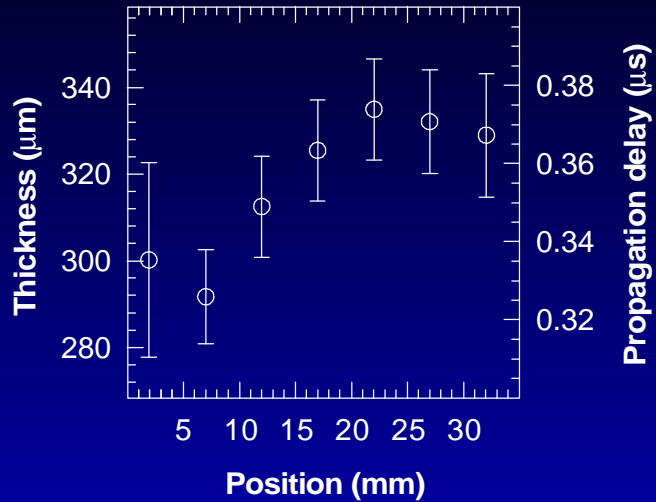


NRC · CNRC

Sensors for Controlling Thermal Spray Processes (cont.)

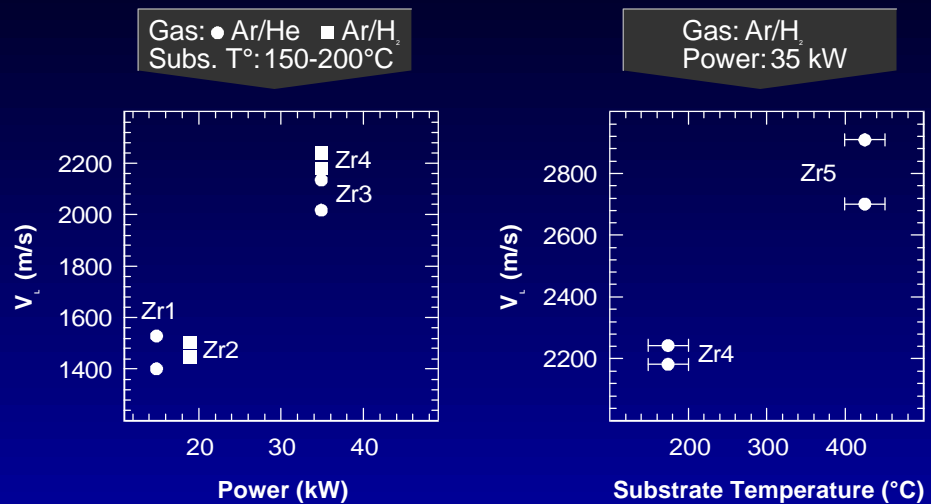
C. Moreau (NRC-CNRC)

Thickness and Propagation Delay Vs Position



NRC · CNRC

Effect of Spray Conditions on Sound Velocity

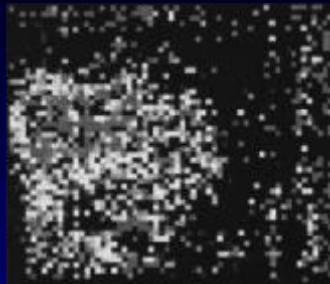


NRC · CNRC

*Sensors for
Controlling
Thermal Spray
Processes (cont.)*

C. Moreau (NRC-
CNRC)

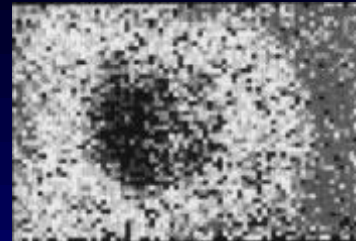
Ultrasonic Imaging of Artificial Defects



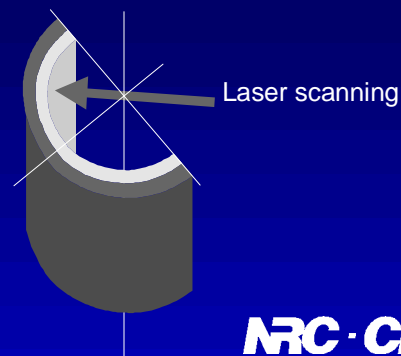
Fingerprint 20mm ϕ (delay)



Silicone 22mm ϕ (amplitude)



Grease 20mm ϕ (delay)



NRC · CNRC

Feedback Strategy

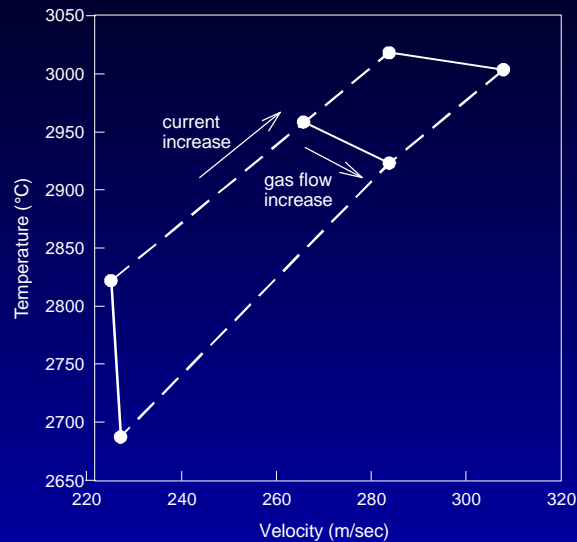
- Complex task because the process involves many parameters influencing the coating properties
- Monitoring spray parameters is important but having a means to react to correct any detected drift is better

NRC · CNRC

*Sensors for
Controlling
Thermal Spray
Processes (cont.)*

C. Moreau (NRC-
CNRC)

Control of Particle Parameters



- Ar- 33% He
- Yttria-stabilized zirconia

NRC · CNRC

Conclusion

- The objective of developing advanced controls is to produce coatings having the same properties day after day or whose properties are within a range of values acceptable for a specific application
- To reach this goal, one needs:
 - reliable spray equipment
 - consistent feed materials
 - adapted sensing and nondestructive evaluation techniques
 - efficient controllers

NRC · CNRC

*Sensors for
Controlling
Thermal Spray
Processes (cont.)*

C. Moreau (NRC-
CNRC)

Conclusion

- Controlling key physical parameters during spraying should make it possible the transport of the spraying parameters from one booth to another (booth equivalency)
- A good understanding of the physical and metallurgical processes involved in thermal spraying is mandatory to implement adequate control strategy

NRC · CNRC

Measurement of DC Plasma Arc Fluctuations

J. Heberlein (U. of Minnesota)

Three different arc operating modes in a DC plasma torch have been identified through arc voltage measurements, the restrike mode, the takeover mode and the steady mode. These operating modes strongly influence plasma processes such as plasma spraying. The occurrence of the arc operating modes depends on the torch operating parameters, arc current, plasma gas composition and plasma gas flow rate. The end-zone images of the arc inside the anode-nozzle have been captured by a CCD video system with a high shutter speed. The end-zone images suggest that the thickness of the cold gas boundary layer between the arc column and the anode surface is the most important variable influencing the arc mode occurrence and transition.

Effects of The Cold Gas Boundary Layer on Arc Fluctuations

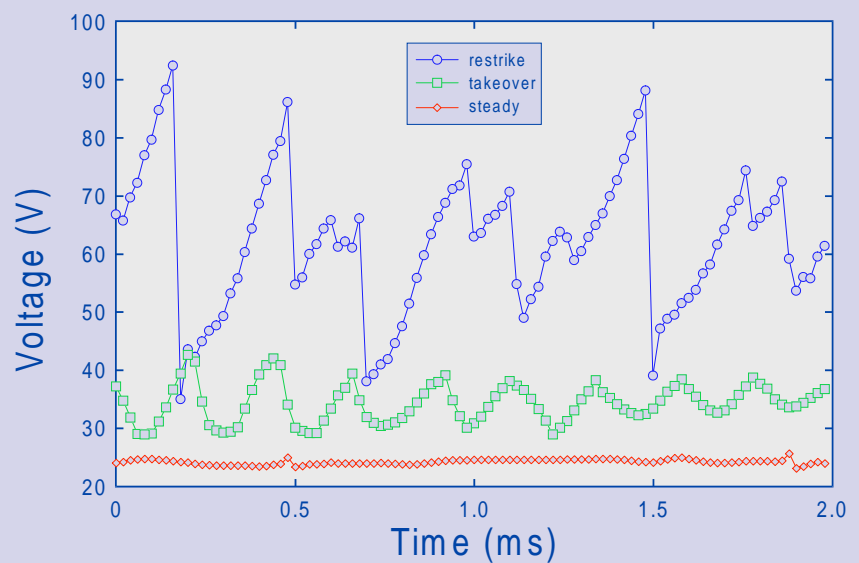
Z. Duan¹, K. Wittmann¹, J. F. Coudert²,
J. Heberlein¹, and P. Fauchais²

¹ University of Minnesota
111 Church St. SE
Minneapolis, MN 55455
USA

² University of Limoges
123, Avenue Albert-Thomas
Limoges 87060
France

Thermal Spray Coatings Workshop
National Institute of Standards and Technology
Gaithersburg, MD 20899
November 19, 1998

From the characteristics of the voltage waveforms, we can define three basic arc operating modes as shown in this slide. The first one is called the "restrike" mode, which is represented with a saw-tooth shape waveform and a large fluctuating amplitude. The second one is the "takeover" mode, which has an approximately sinusoidal or triangle shape waveform with a relative low fluctuating amplitude. With the same torch configuration and arc gas mixtures, the restrike mode is related to a high mean voltage and the takeover mode is related to a low mean voltage. The last basic mode is the "steady" mode, which is identified with a nearly flat profile and mostly a very low mean voltage.

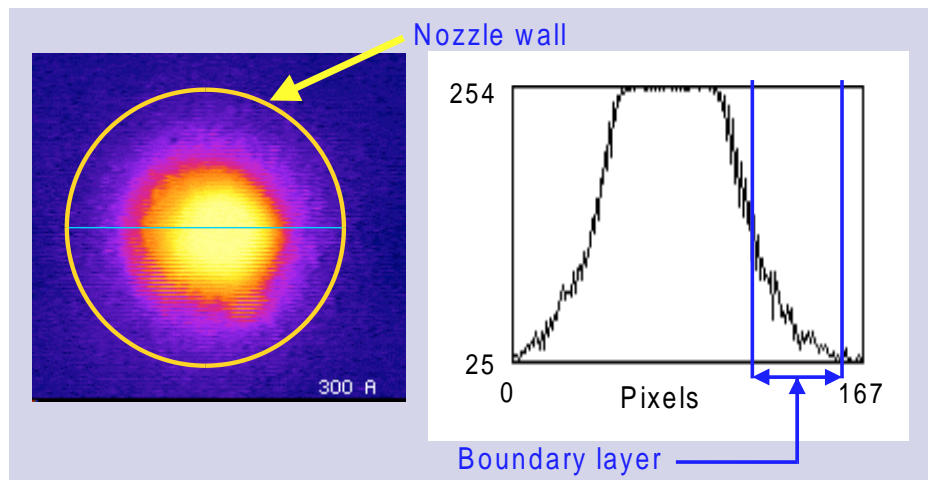
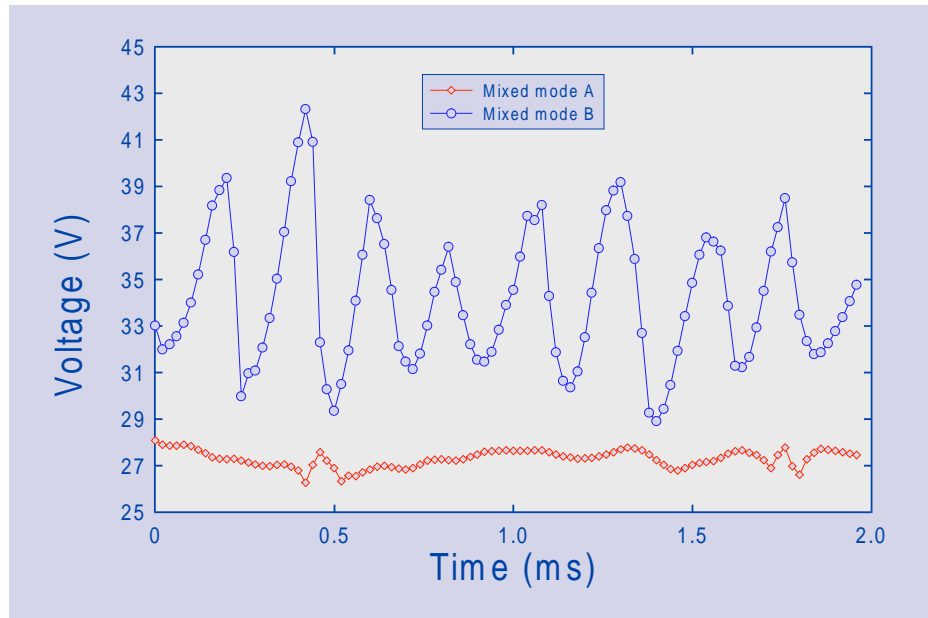


Measurement of DC Plasma Arc Fluctuations (cont.)

J. Heberlein (U. of Minnesota)

The voltage traces obtained over an extensive space of operating parameters show the arc, in the most cases, not in a perfectly distinct mode but with a mixed characteristic. The mixed characteristics could be a combination of the restrike and the takeover modes or a combination of the takeover and the steady modes, as shown in this slide. In order to present results easily and clearly, the arc instability characteristic is assigned a numerical value (referring to "mode value") in this presentation. The "restrike" mode is equal to 2, the "takeover" equal to 1, and the "steady" equal to 0. While a perfect mode is assigned to an integer, a decimal number between 0 and 2 specifies a mixed voltage fluctuation character, i.e. "mode = 1.2" represents a voltage mode consisting of an 80% takeover characteristic and a 20% restrike characteristic.

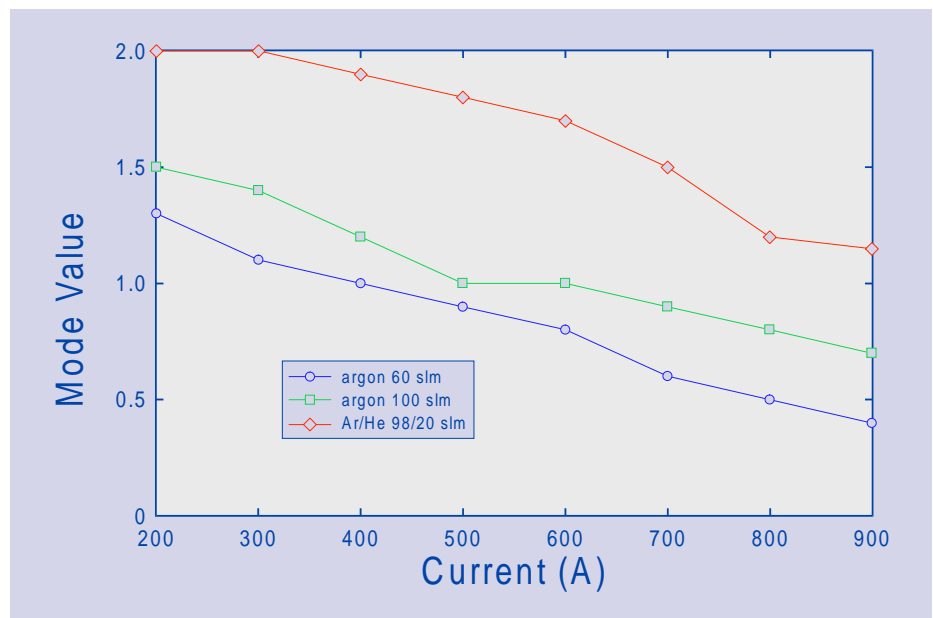
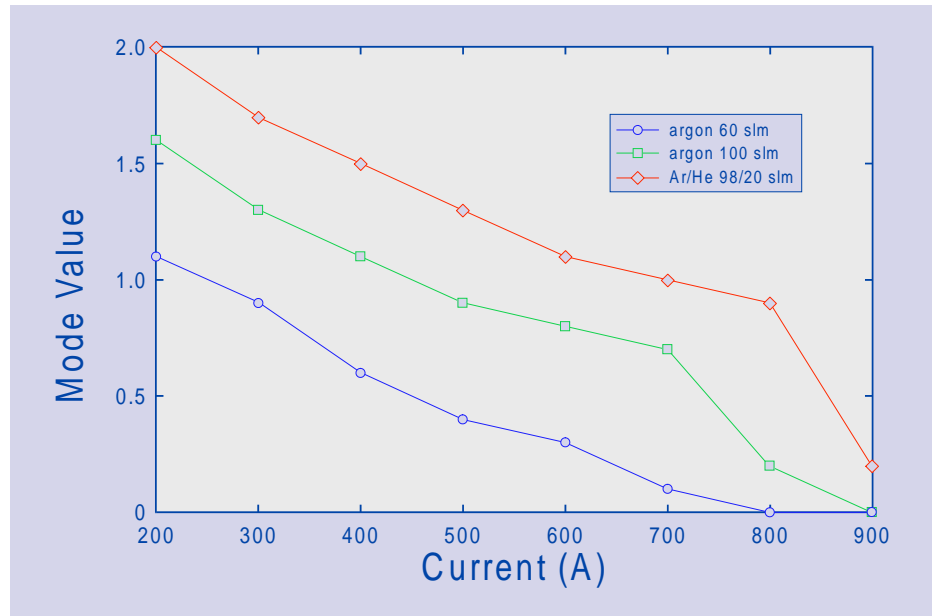
This slide shows a typical end-zone image, and an intensity profile along the line which crosses the arc column center. We define the edge of the cold gas boundary layer to be located at the point where the intensity is half of the highest intensity inside the nozzle channel. Since the radiative energy has a rapid rise between 3,000 K to 6,000 K for an argon based plasma, the above definition will locate the boundary layer edge at a point where the temperature is about 4,500 K. The thickness of the boundary layer, which is the distance from the edge to the nozzle wall, is then converted from a number of pixels to a physical dimension in mm. Since the arc is in a highly fluctuating state, the thickness of the boundary layer has been measured 10 times for each individual experimental condition to obtain an average value and reduce the error. The position of the anode attachment is also identified from the end-zone image if it is visible.



Measurement of DC Plasma Arc Fluctuations (cont.)

J. Heberlein (U. of Minnesota)

The next two slides show the arc operating mode varying with the arc current and the gas flow rate for the straight and swirling arc gas injections, respectively. The results are obtained with argon/helium mixtures. The arc operating mode values decrease with increasing arc current, decreasing mass flow rate, and decreasing secondary gas fraction. For the arc gas injection with swirling flow, there is no steady mode (mode = 0) occurring even with a very large current and a low gas mass flow rate. This is due to the tangential component in the swirling flow which increases the heat transfer from the arc leading to a constriction of the arc column, therefore increasing the thickness of the boundary layer. However, the swirl flow can also randomize the anode attachment by introducing a tangential drag force, which will drive the mode value close to 1 from both directions, even with a relative large mean voltage and fluctuation amplitudes.

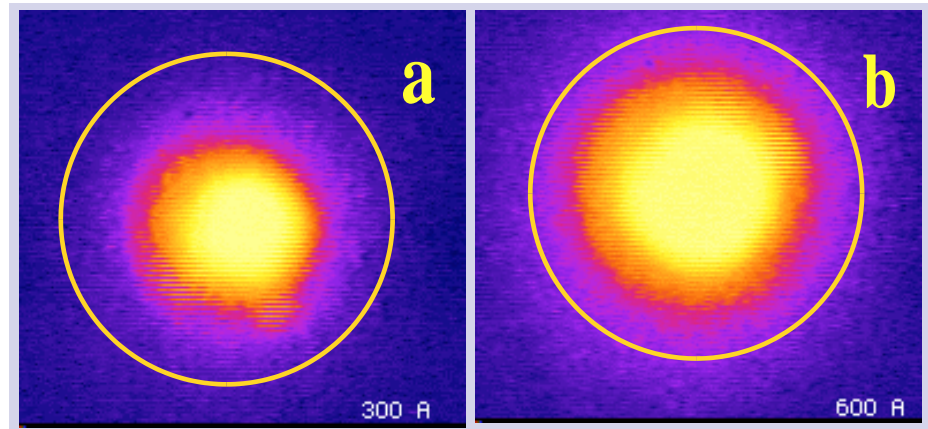
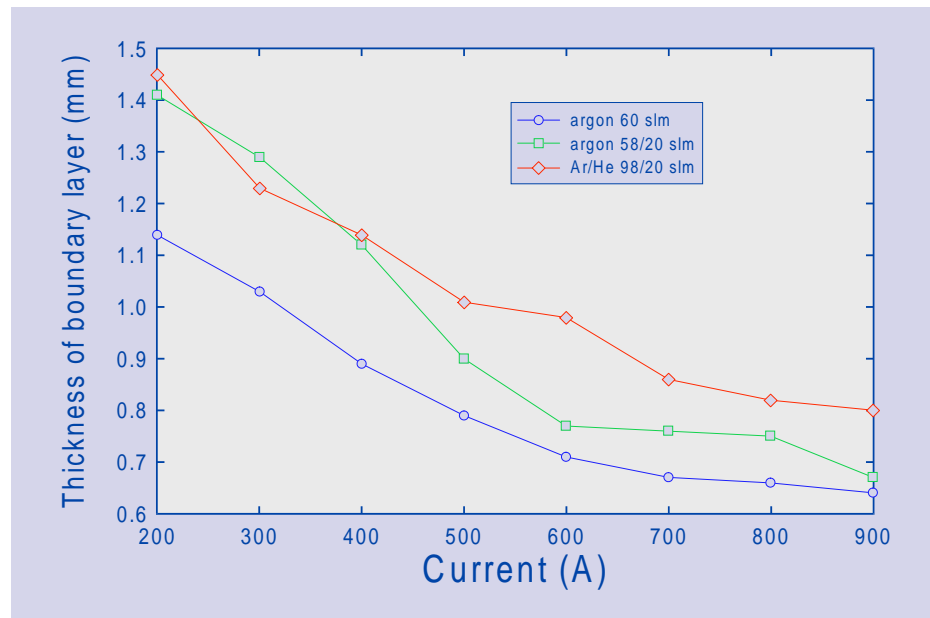


Measurement of DC Plasma Arc Fluctuations (cont.)

J. Heberlein (U. of Minnesota)

These explanations can be confirmed by results obtained with the end-zone image observations. This slide shows the thickness of the cold gas boundary layer changing with current and gas flow rate for swirl injection of the arc gas. The boundary layer thickness increases with decreasing current, increasing gas flow rate and increasing secondary gas fraction. Although occurrence and behavior of an electric breakdown depends on many physical and chemical factors in the anode channel, the thickness of the cold gas boundary layer as we define it using an approximate temperature value could be a good indicator for the characteristics of the arc instability.

This slide shows two end-zone images obtained for the arc operating in a restrike dominant mode and in a takeover dominant mode, respectively. The arc operating in a restrike dominant mode presents a very clearly defined anode attachment, while the arc in a takeover dominant mode shows a more gradual decline of the radiation intensity with an non-distinguishable anode attachment. This difference in the arc cross-section clearly indicates the effect of the thickness variation of the cold gas boundary layer and the associated changes in the gas properties. A thin boundary layer might produce a diffuse anode attachment rather than a constricted anode attachment.



Conclusions Three arc operating modes - "restrike", "takeover" and "steady" have been identified and characterized. Their dependencies on various operating parameters have been presented. The cold gas boundary layer between the arc column and the anode wall is considered to be the most important variable to influence the arc instability modes. The boundary layer thickness has been observed and measured with an end-zone imaging system. The arc operating in the restrike mode has a well-defined anode attachment, while the anode attachment is hardly distinguishable with the takeover and steady modes. The change in operating parameters which results in a decrease in the thickness of the boundary layer will lead to a change of the arc operating from a restrike to a takeover mode, then to a steady mode. However, an increasing fraction of the secondary gas, which usually has a high thermal conductivity, will drag the arc to the restrike mode. The swirl flow component in the arc gas will drive the arc to takeover-like characteristics.

Acknowledgment This work has been supported in part by NSF through the ERC for Plasma-Aided Manufacturing grant EEC-8721545 and through an international collaboration grant NSF/INT-9415715.

Enthalpy Probe

M. Boulos (U. of Sherbrooke)

Enthalpy Probe Techniques for Thermal Plasma Diagnostics

Maher I. Boulos

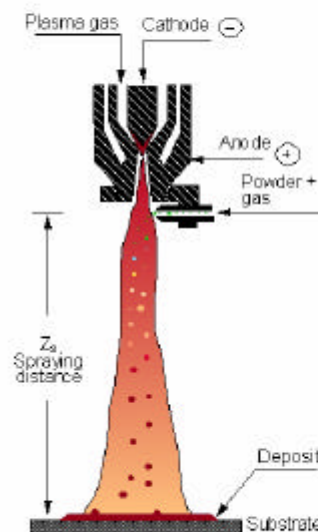
Plasma Technology Research Centre (CRTP)
Université de Sherbrooke (Québec) CANADA J1K 2R1

- ▶ Introduction
- ▶ Basic Concepts
- ▶ Typical Results with D.C. and Induction Plasmas
- ▶ Summary and Conclusion

Thermal Spray Workshops, NIST, Gaithersburg, MD, Nov.19 1998



Introduction: Diagnostics Needs for Plasma Spraying



Independent parameters

Powder parameters

- ▶ d_{p1} , σ_{p1} , d_{p2} , T_{m1} , T_{v1} , H_{m1} , H_{v1} , C_p

Plasma parameters

- ▶ Pressure
- ▶ Composition
- ▶ Power

Powder injection parameters

- ▶ Location
- ▶ Carrier gas flow rate
- ▶ Injection velocity
- ▶ Loading ratio

Substrate parameters

- ▶ Surface preparation
- ▶ Spraying distance
- ▶ Angle of impact
- ▶ Temperature

Dependant parameters

Plasma fields

- ▶ Temperature
- ▶ Velocity
- ▶ Composition

Particle fields

- ▶ Temperature
- ▶ Velocity
- ▶ Size
- ▶ Flux density

Substrate fields

- ▶ Temperature

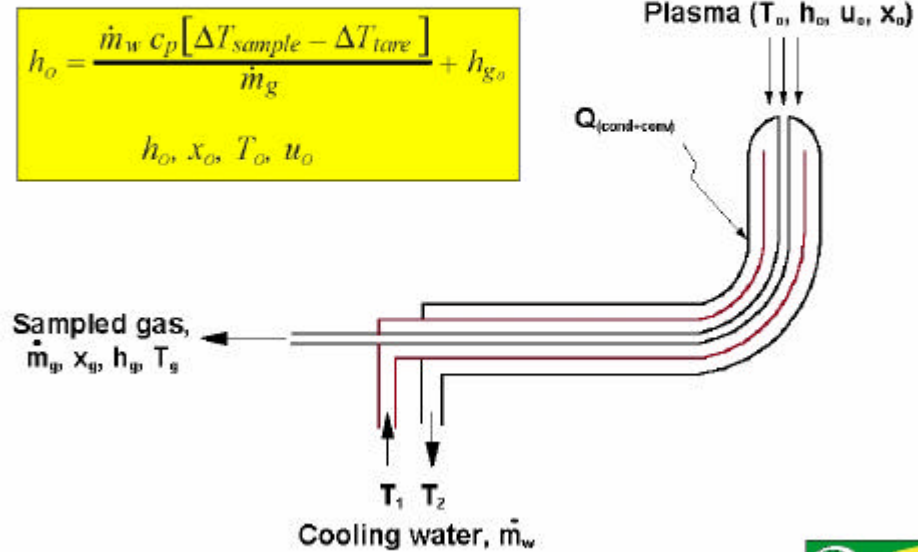


2p.05@sherbrooke.980

Enthalpy Probe
(cont.)

M. Boulos (U. of
Sherbrooke)

Basic Concept of Enthalpy Probe Techniques



Basic Concept of Enthalpy Probe Techniques

Incompressible flow: $U_o = \sqrt{\frac{2(P_o - P_\infty)}{\rho_o}}$

Compressible flow:
Subsonic $\frac{P_o}{P_\infty} = \left[1 + \frac{(\gamma-1)}{2} M^2 \right]^{\frac{\gamma}{\gamma-1}}$

Supersonic $\frac{P_o}{P_\infty} = \left(\frac{\gamma+1}{2} \right) M^2 \left[\frac{(\gamma+1)^2 M^2}{4\gamma M^2 - 2\gamma + 1} \right]$

where $\gamma = c_p/c_v$ and $M = \text{Mach number}$

$$U_o = M_o \sqrt{\gamma R T_o}$$

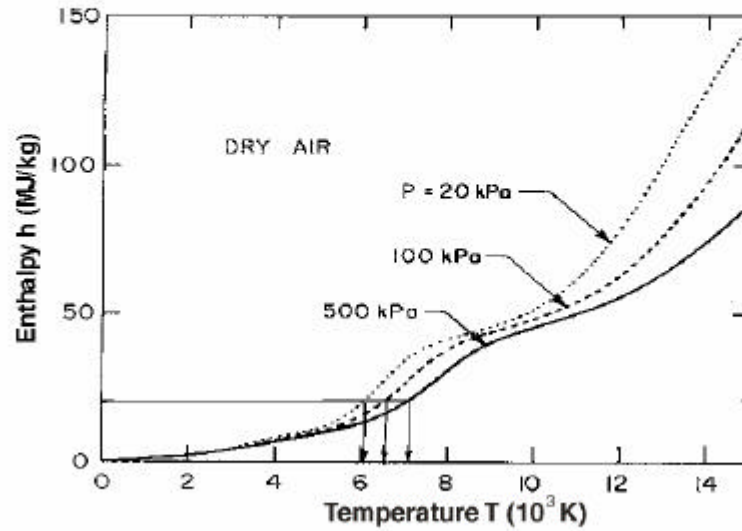


Enthalpy Probe
(cont.)

M. Boulos (U. of
Sherbrooke)

Basic Concept of Enthalpy Probe Techniques

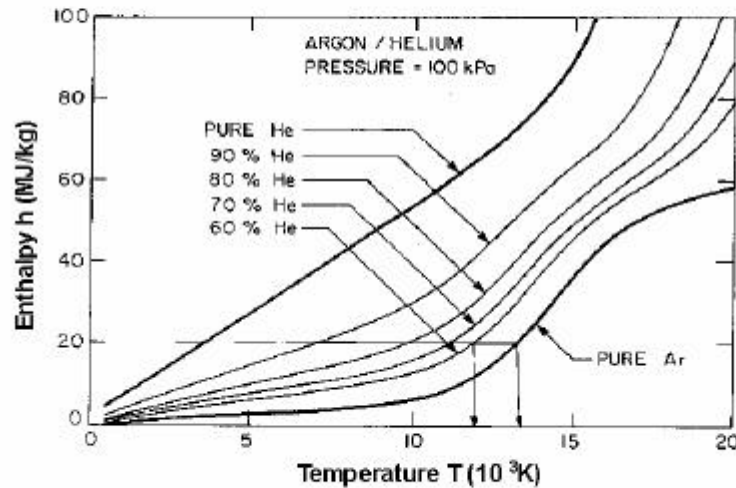
► For dry air



2p.55@shesb.ugrhu.920

Basic Concept of Enthalpy Probe Techniques

► For Ar/He mixtures

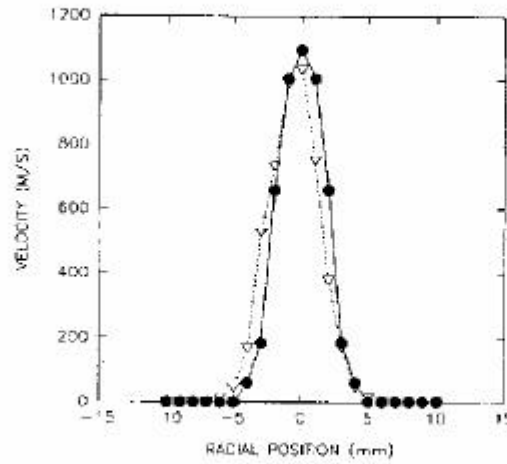


2p.55@shesb.ugrhu.920

Enthalpy Probe
(cont.)

M. Boulos (U. of
Sherbrooke)

Enthalpy Probe Measurements - DC Plasma Jets



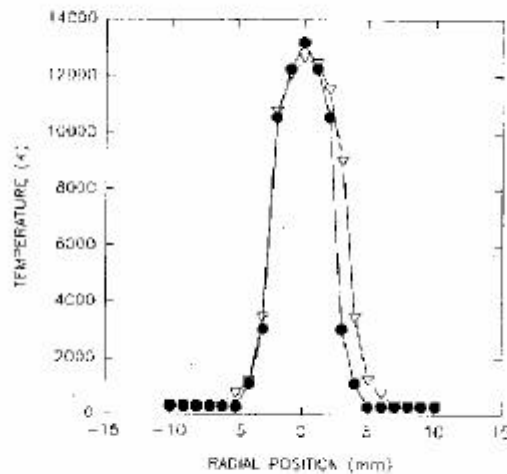
Comparisons of axial velocity Vs radial location for a 900 A operating current: ● laser scattering ▽ enthalpy probe

Fincke *et al.* (1993)



2p. 656@thesherbrooke.ca

Enthalpy Probe Measurements - DC Plasma Jets



Comparisons of axial velocity Vs radial location for a 900 A operating probe: ● laser scattering ▽ enthalpy probe

Fincke *et al.* (1993)

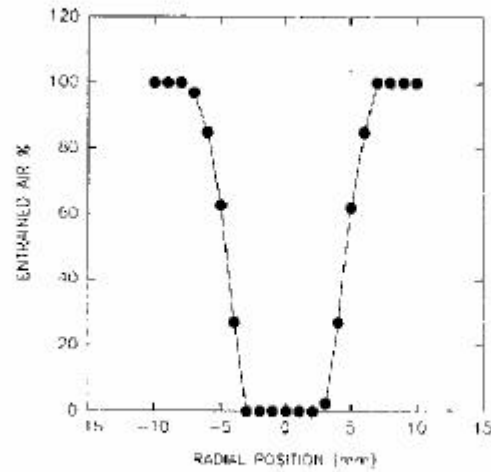


2p. 656@thesherbrooke.ca

Enthalpy Probe
(cont.)

M. Boulos (U. of
Sherbrooke)

Enthalpy Probe Measurements - DC Plasma Jets

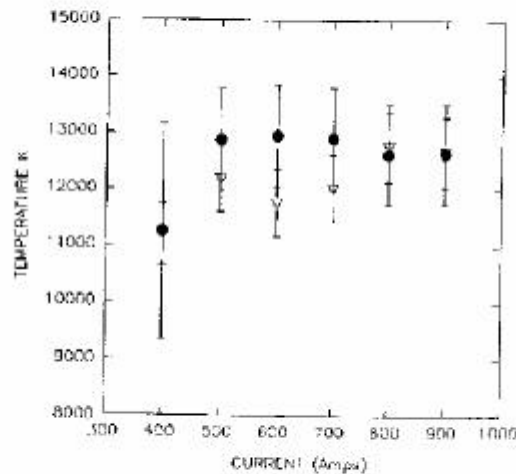


Radial concentration profile of entrained air obtained from enthalpy probe measurements

Fincke *et al.* (1993)



Enthalpy Probe Measurements - DC Plasma Jets



Comparisons of measured centerline temperatures Vs current: ● laser scattering ▽ enthalpy probe

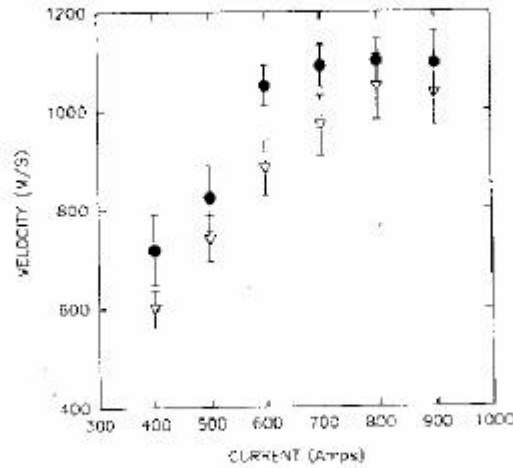
Fincke *et al.* (1993)



Enthalpy Probe
(cont.)

M. Boulos (U. of Sherbrooke)

Enthalpy Probe Measurements - DC Plasma Jets



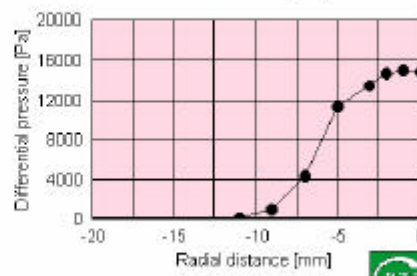
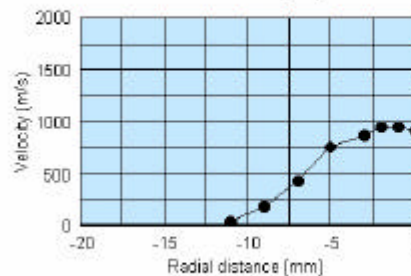
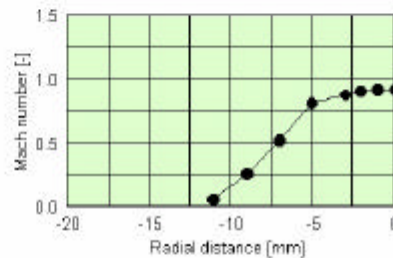
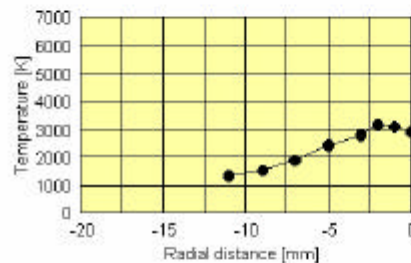
Comparisons of measured centerline velocities Vs current:
● laser scattering, ▽ enthalpy probe

Fincke *et al.* (1993)



Results with the M1.5 Supersonic Induction Plasma Nozzle

► Pure Argon, $P_a = 17.1$ kPa, $P_b = 36.3$ kPa, $P_0 = 25$ kW, $z = 25$ mm

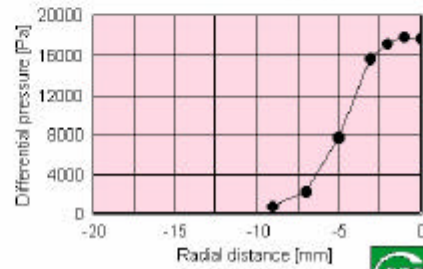
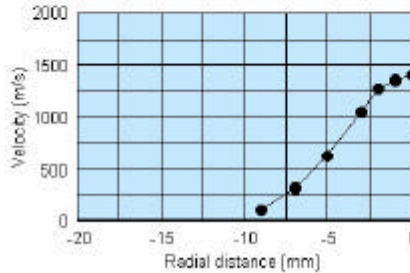
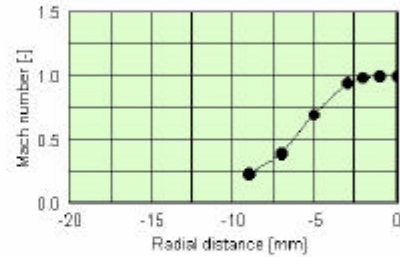
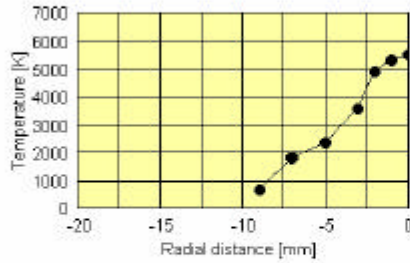


Enthalpy Probe
(cont.)

M. Boulos (U. of
Sherbrooke)

Results with the M1.5 Supersonic Induction Plasma Nozzle

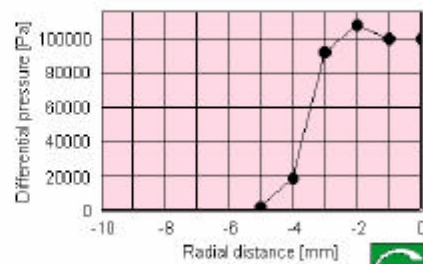
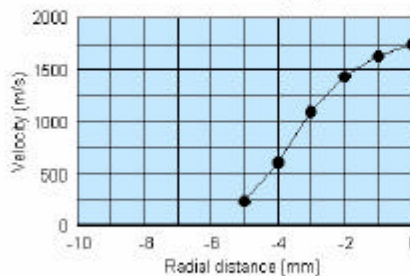
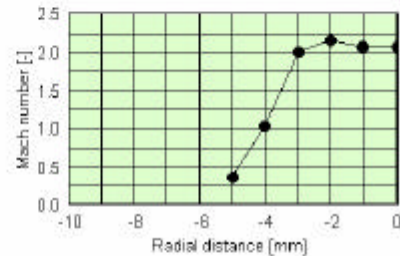
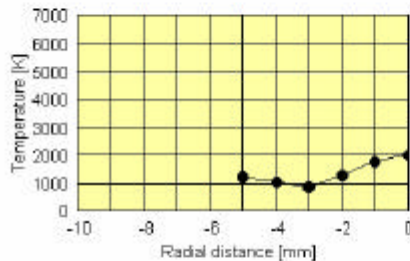
▶ Ar/H₂ (2% H₂), P₀ = 17.1 kPa, P_b = 36.3 kPa, P_e = 25 kW, z = 25 mm



Zip: 76344 Karlsruhe, Germany

Results with the M3 Supersonic Induction Plasma Nozzle

▶ Pure Argon, P₀ = 17.2 kPa, P_b = 212 kPa, P_e = 25 kW, z = 17 mm



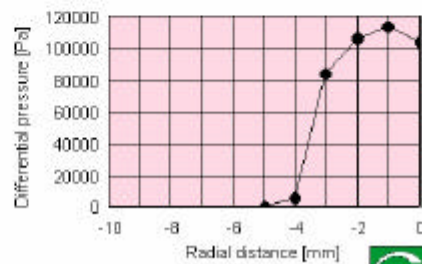
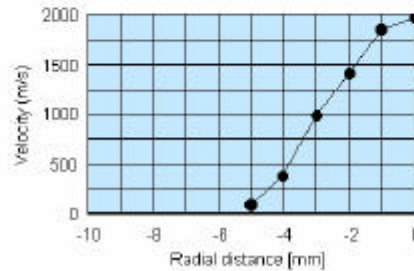
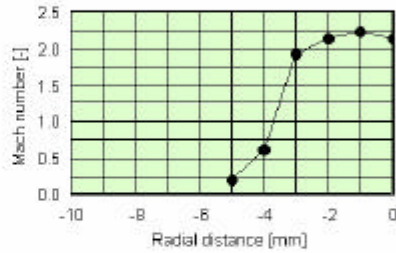
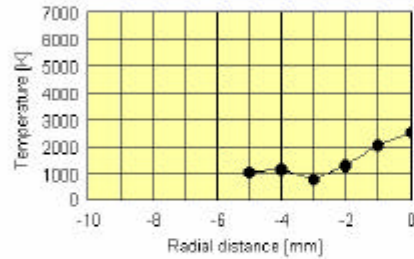
Zip: 76344 Karlsruhe, Germany

Enthalpy Probe
(cont.)

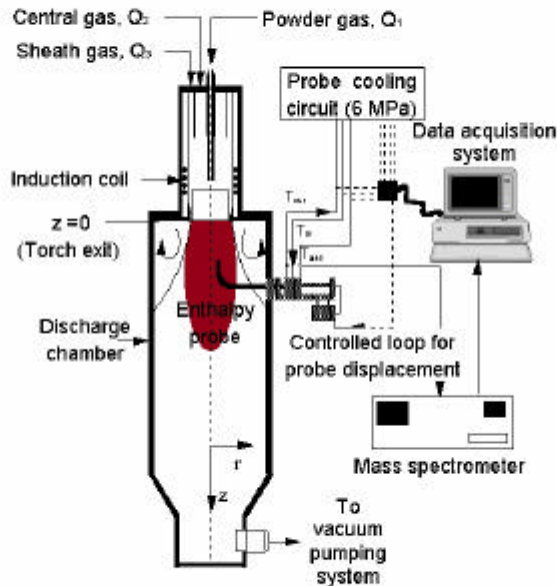
M. Boulos (U. of
Sherbrooke)

Results with the M3 Supersonic Induction Plasma Nozzle

► Ar/H₂ (2% H₂), P_a = 17.3 kPa, P_b = 206 kPa, P₀ = 25 kW, z = 17 mm

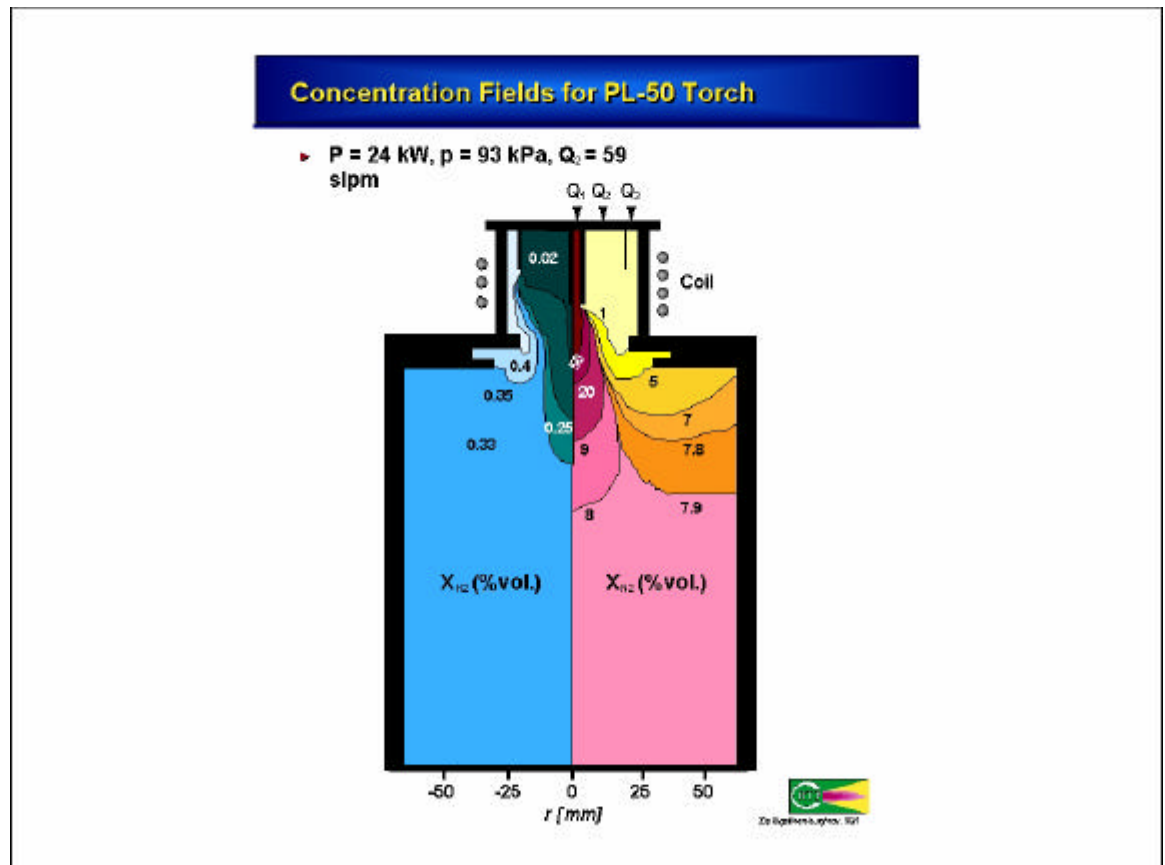
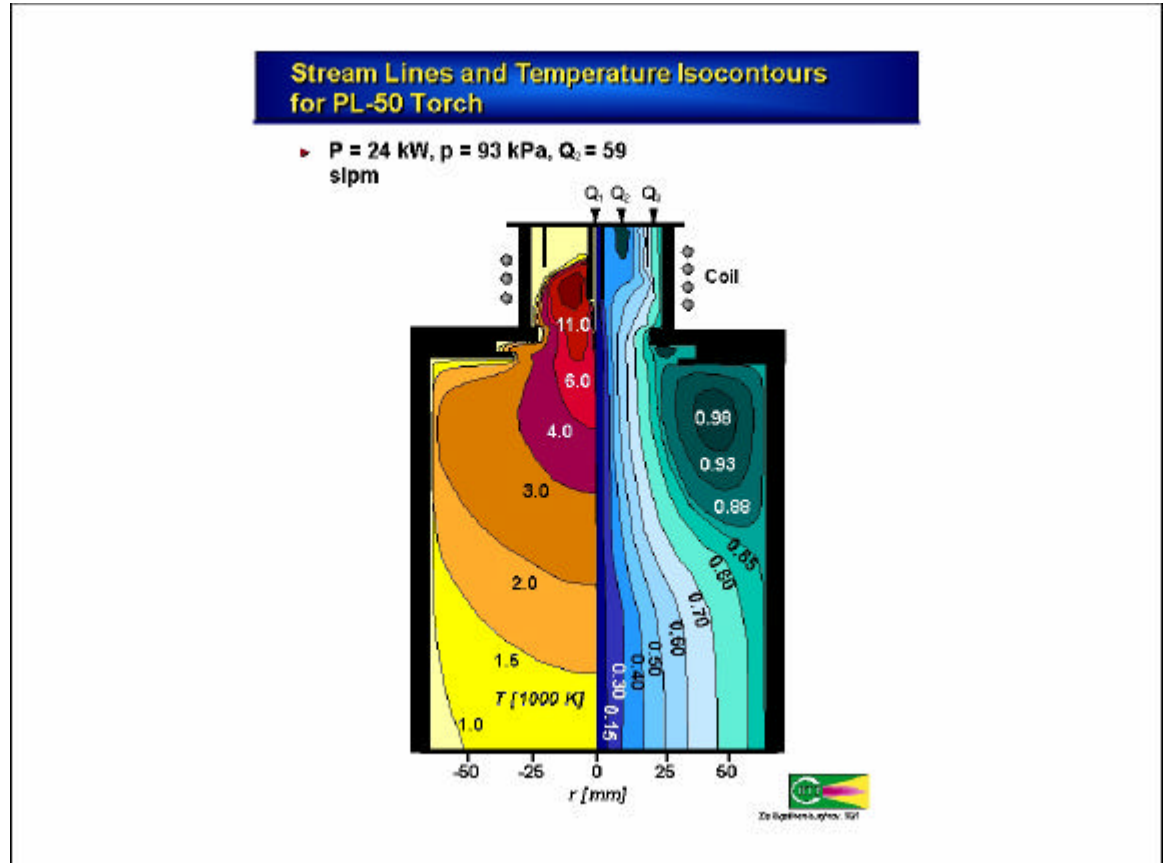


Experimental Set-up for Enthalpy Probe Measurements



Enthalpy Probe
(cont.)

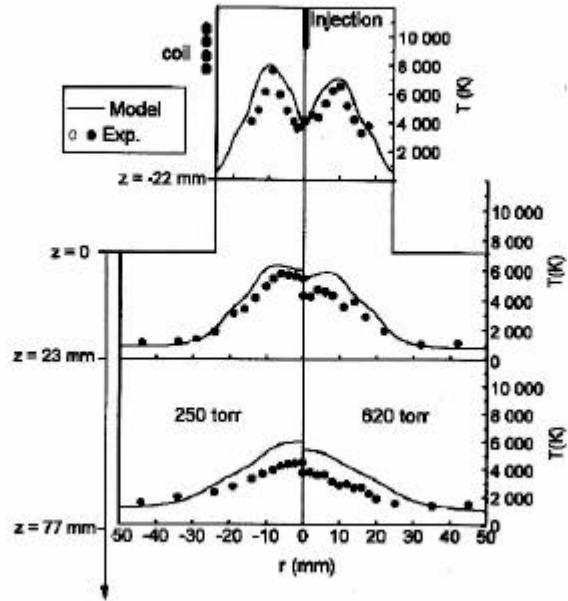
M. Boulos (U. of
Sherbrooke)



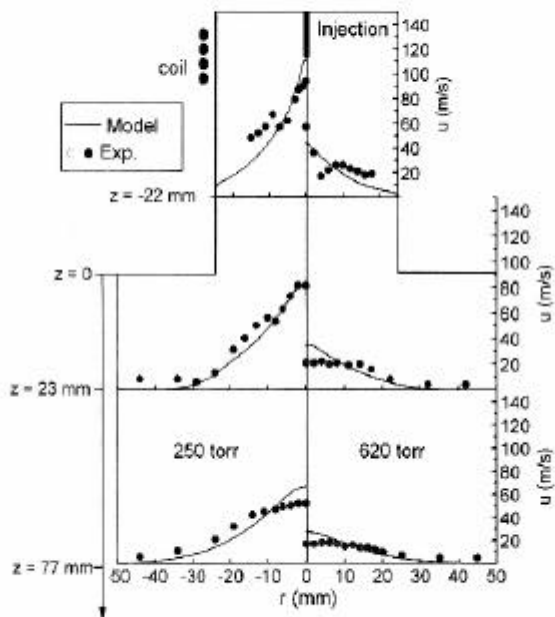
Enthalpy Probe
(cont.)

M. Boulos (U. of
Sherbrooke)

Enthalpy Probe Measurements - RF Induction
Plasma Flow

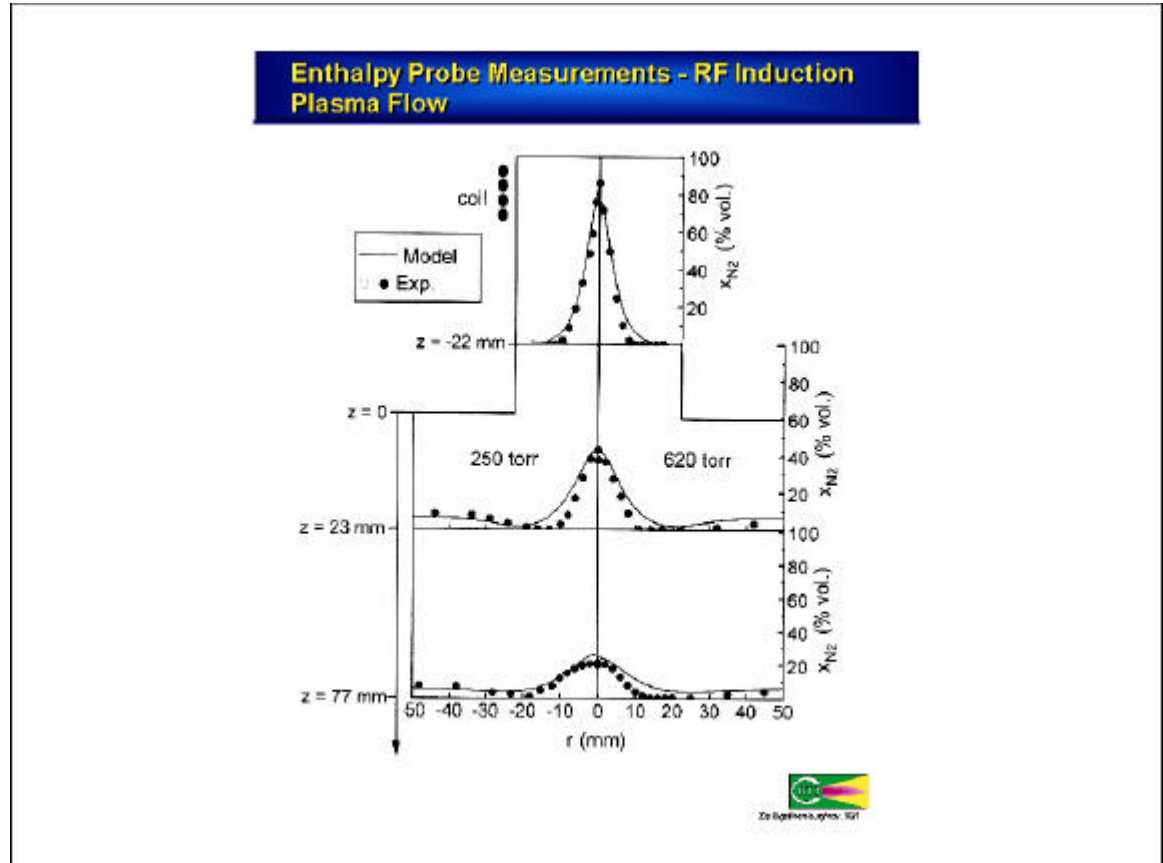


Enthalpy Probe Measurements - RF Induction
Plasma Flow



Enthalpy Probe (cont.)

M. Boulos (U. of
Sherbrooke)



Summary and Conclusions

- ▶ Enthalpy probe technique offers simple means of measurement of the local temperature, velocity and composition of plasma flows under a wide range of conditions

*Impact and
Solidification of
Molten Nickel
Droplets*

W. H. Hofmeister
(Vanderbilt U.)

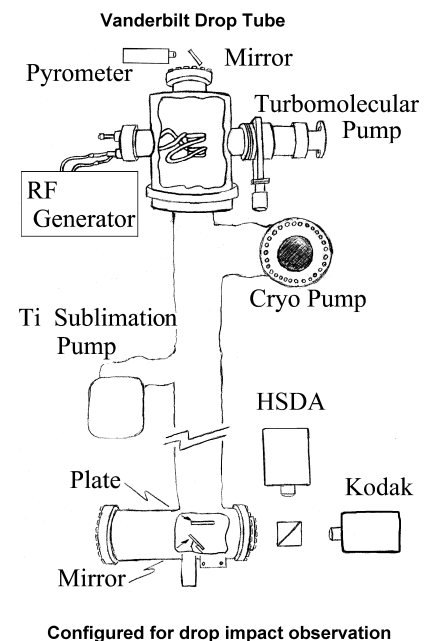
IMPACT AND SOLIDIFICATION OF MOLTEN NICKEL DROPLETS

William Hofmeister
Vanderbilt University

Material in this presentation was published in Solidification 1998, (eds. S. Marsh, et al., TMS, Warrendale, PA, 1998), entitled "Observation of Thermal Profiles during Impact and Solidification of Nickel Drops," by W.H. Hofmeister, R.J. Bayuzick, G. Trapaga, D.M. Matson, and M.C. Flemings, pp. 375-387. Acknowledgments are due to NASA Office of Microgravity Sciences, John Lum, Bob Hyers, Pedro Bastias, James Olive, Prasart Juntawongso, and Alex Altgilbers.

Experiment Schematic

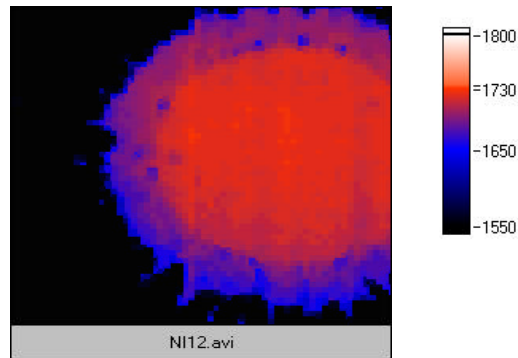
The top chamber is fitted with an electromagnetic levitation coil, a sample exchange carousel, and optical pyrometer. The tube was evacuated and then backfilled with 400 torr ultra high purity helium gas. After melting the temperature of the drop in the coil was regulated by a flow of helium gas over the sample. When the desired temperature was achieved, the levitation power was turned off and the sample allowed to free fall approximately 3.5 meters to the bottom of the tube. The catch chamber at the bottom of the tube was fitted with a 10x10x0.3 cm optically flat quartz plate at the impact site. Below the quartz plate a first surface aluminized mirror was positioned to allow viewing of the splat interface through an 8 inch viewport at the end of the catch chamber. The two thermal imaging systems were positioned to simultaneously view the splat interface via a beam splitting cube. A Kodak Ektapro scanning array camera was operated at 64,000 frames per second and the HSDA96 parallel tapped thermal imaging system was operated at 250,000 frames per second. Both systems were fitted with narrow band pass optical filters centered at 900 nm, and calibrated for temperature measurement using a NIST standard tungsten strip lamp.



*Impact and
Solidification of
Molten Nickel
Droplets (cont.)*

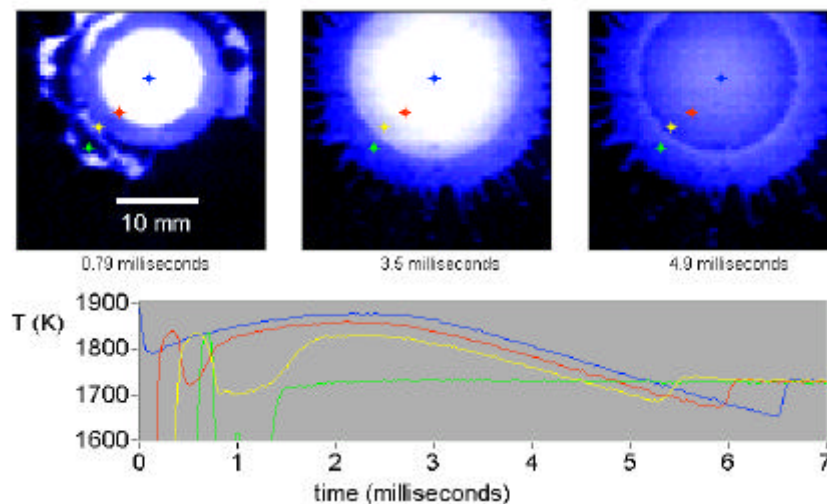
W. H. Hofmeister
(Vanderbilt U.)

Superheated Ni splat



This movie is a temperature corrected, colorized movie of sample 12 which impacted the plate with 175 K superheat. The movie is generated from the Kodak imager.

Time temperature curves from Kodak imager (sample 12)



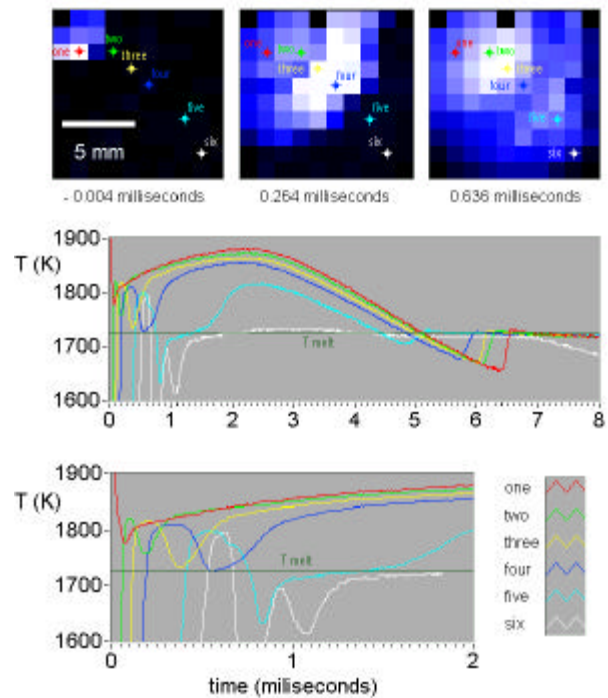
Colored cursors on images correspond to location of time temperature curves.

Impact and Solidification of Molten Nickel Droplets (cont.)

W. H. Hofmeister
(Vanderbilt U.)

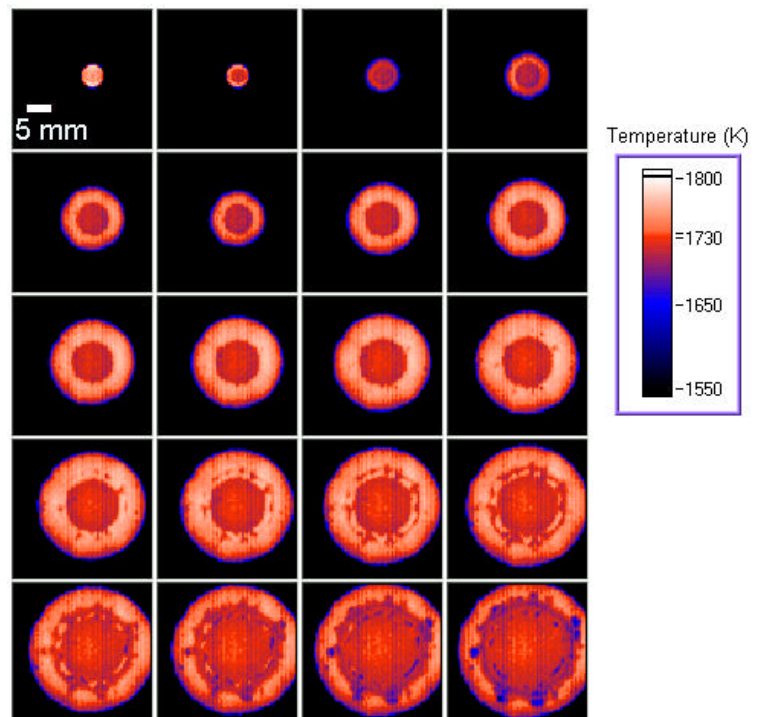
Time temperature curves from HSDA96 thermal imager (sample 12)

The cooling rates on contact were as high as $2.0 \times 10^6 \text{ K s}^{-1}$. The sample spread, then undercooled 70 K before solidification proceeded from the edge inward.



Splat at T_m

Sample 8
Kodak imager
slightly superheated at impact ($< 50 \text{ K}$)

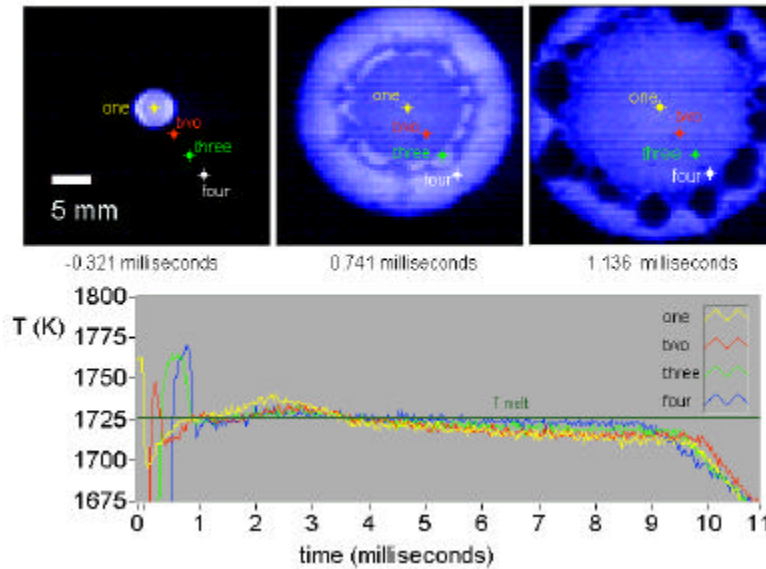


Ni-8 50 microseconds per frame

Impact and Solidification of Molten Nickel Droplets (cont.)

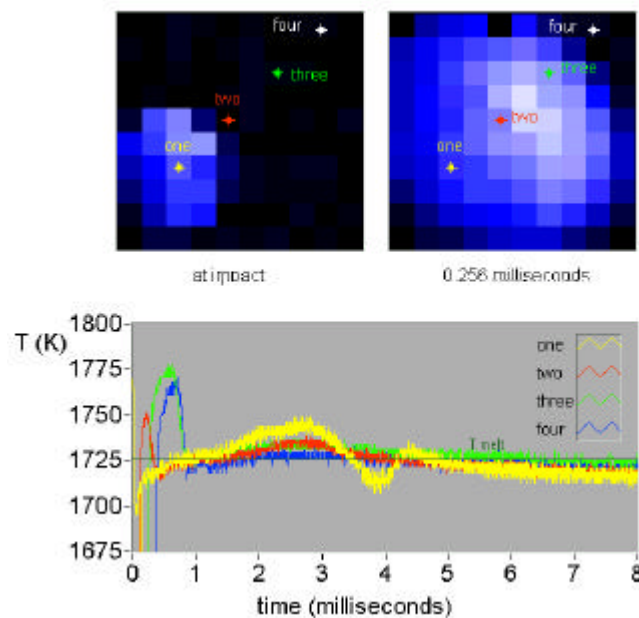
W. H. Hofmeister
(Vanderbilt U.)

Time temperature for Tm splat Kodak imager (sample 8)



Time temperature for Tm splat HSDA96 imager

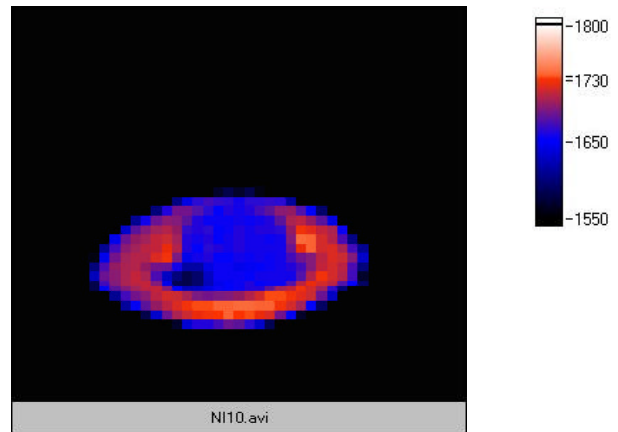
Slight
superheat on
impact.
Negligible
undercooling
before
solidification.
(sample 8)



*Impact and
Solidification of
Molten Nickel
Droplets (cont.)*

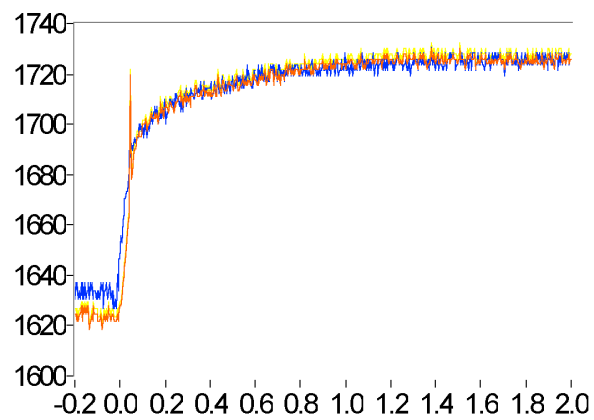
W. H. Hofmeister
(Vanderbilt U.)

Side view of undercooled splat



Sample 10
100 K
undercooled

Time temperature from HSDA96

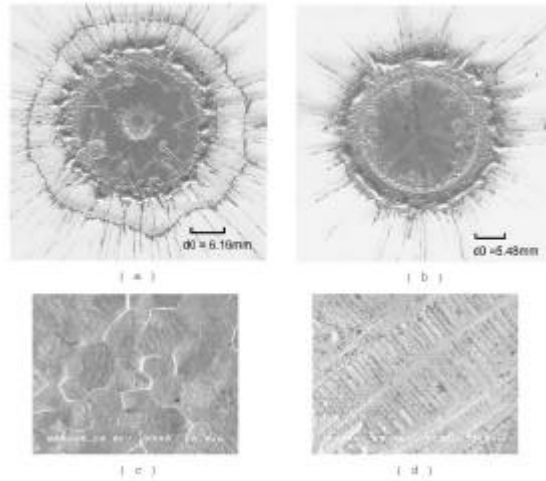


Sample 10 was undercooled close to 100K and solidified on impact with no additional undercooling.

*Impact and
Solidification of
Molten Nickel
Droplets (cont.)*

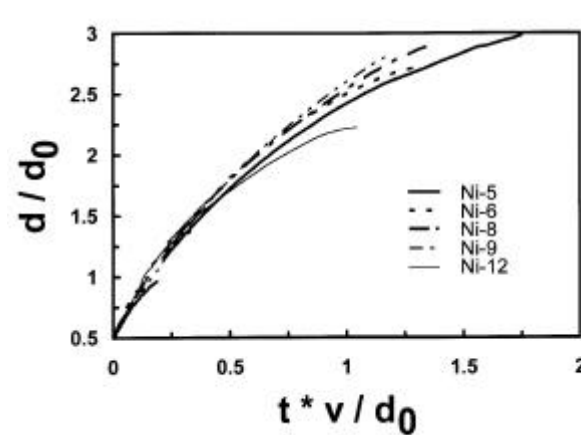
W. H. Hofmeister
(Vanderbilt U.)

Structure of samples 8 and 12



Photos a & c are
from sample 8,
b & d are from
sample 12.

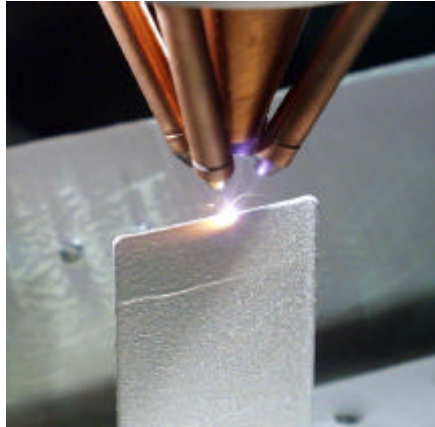
Droplet spreading



*Impact and
Solidification of
Molten Nickel
Droplets (cont.)*

W. H. Hofmeister
(Vanderbilt U.)

High Speed Thermal Imaging for LENS Process Development and Control



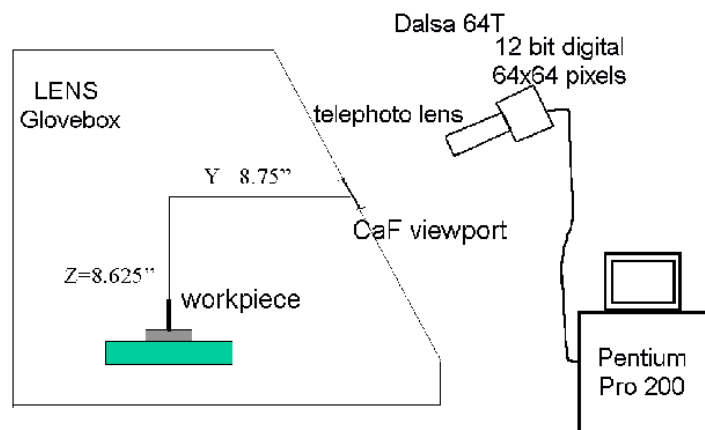
An electronic paper on this subject was published in JOM-e under the title:

“Investigation of Solidification in the Laser Engineered Net Shaping (LENS™) Process” by William Hofmeister, Melissa Wert, John Smugeresky, Joel A. Philliber, Michelle Griffith, and Mark Ensz, July, 1999.

<http://www.tms.org/pubs/journals/JOM/9907/Hofmeister/Hofmeister-9907.html>

This work was sponsored by Sandia National Laboratory, a multiprogram laboratory operated by Sandia Corporation, a Lockheed Martin Company, for the U.S. Department of Energy under contract number DE-AC04-94AL85000.

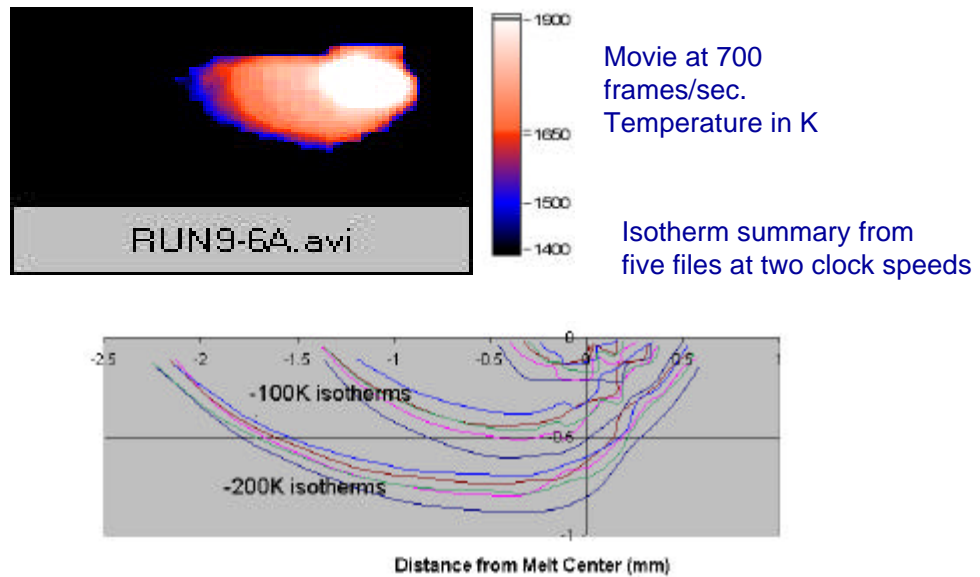
Experimental Set-up



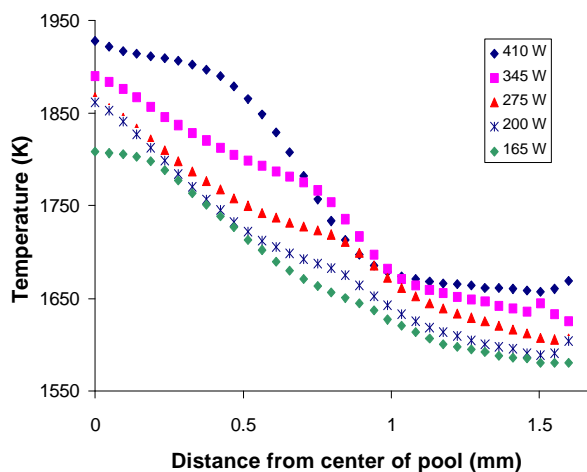
*Impact and
Solidification of
Molten Nickel
Droplets (cont.)*

W. H. Hofmeister
(Vanderbilt U.)

Side view experiments



Temperature Profile from Center of Melt Pool (Coarse Powder)

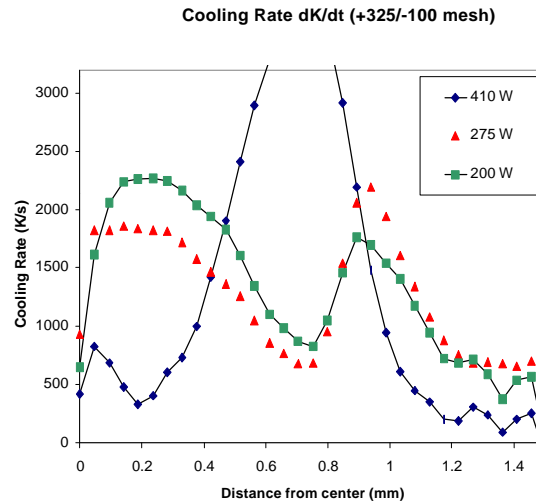


- SS316 powder, -100/+325 mesh
- Stable pool over all powers
- Pool size increases with power
- Superheat lower for coarse powder

*Impact and
Solidification of
Molten Nickel
Droplets (cont.)*

W. H. Hofmeister
(Vanderbilt U.)

Temperature Gradient from Center of Melt Pool (coarse Powder)



- SS316 powder, -100/+325 mesh
- 275W cooling rate is two times 410W cooling rate outside the melt pool

NIST THERMAL SPRAY RESEARCH PROGRAMS

Project Title: Ceramic Coatings Program (*see page 13*)

Project Title: Sensors and Diagnostics for Thermal Spray Processes

Investigators: S. D. Ridder and F. S. Biancaniello

Objectives:

The primary focus of this project is to develop tools for the measurement and control of process conditions for thermal spray systems. This includes off-line analysis tools (e.g. high-speed cinematography, imaging thermography and holography) and real-time sensors suitable for process control. In addition, mathematical modeling techniques will be used to provide predictive calculations of process variables and product characteristics. Appropriate process sensors and controls will then be incorporated into an expert system driven process controller with generic applicability to a wide range of metal processing equipment and computer platforms.

Technical Description:

The focus of the thermal spray project is the development of measurement tools to provide diagnostic and control capabilities for the production of reproducible industrially important spray coatings such as ceramic-based Thermal Barrier Coatings (TBC's) and metallic based diffusion barriers, corrosion protection coatings and wear reducing layers with predictable properties.

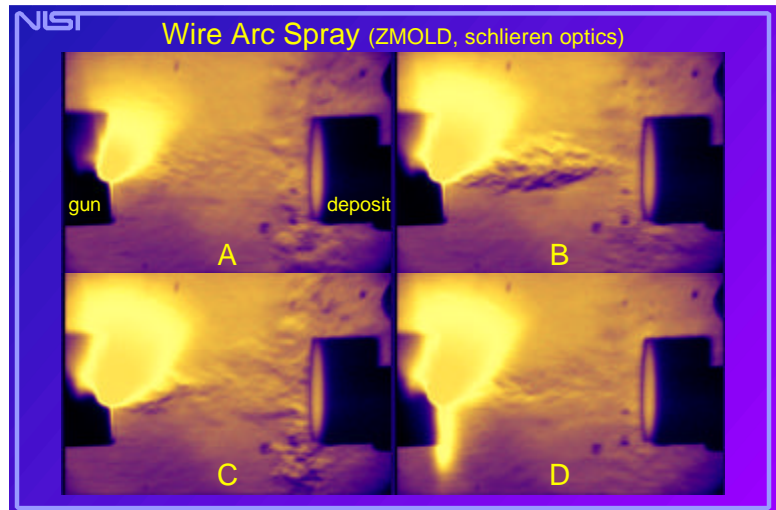
The intended expert-system-driven or intelligent process controller requires the acquisition of an extensive data base that maps the effects of all the process variables or parameters on the resulting coating characteristics. Process parameters must be measured, identified as either dependent or independent variables and reduced using dimensional analysis. A process model must be determined that provides a mapping of the process parameter space to the resulting coating properties and process efficiency. Finally, a control system is developed incorporating the process model, sensors and actuators that provides the necessary heuristics and response time for achieving the product goal. This will ultimately allow US industry to produce the advanced materials that this process can provide with reliable performance and acceptable cost.

In the NIST thermal spray system, independent programmable manipulators are used to move the plasma gun, the substrate and the process sensor. These "robots" provide adequate flexibility for the production and diagnostic monitoring of reproducible coatings on two-dimensional test coupons measuring up to 1 m². High-speed cinematography, schlieren gas flow imaging, multi-exposure laser holography, and high-speed video cameras are currently available and will be further developed to provide diagnostic tools for thermal spray systems (*see page 23.*) A new Near Infra Red (NIR) spectrometer has been purchased and is currently in use to measure the emission spectrum from the DC plasma thermal spray gun (*see page 29.*) CFD modeling capabilities are available to evaluate gas and liquid flow systems. Previous studies of the supersonic flow in gas/metal atomizers have provided new capabilities that enhance the viscous dissipation model within the CFD code (*see page 47.*) This tool could be employed to study fluid flow in thermal spray equipment.

NIST Small Business Innovative Research (SBIR) funds were previously used to develop several of the diagnostic and sensor systems that are now being applied to thermal spray research. SBIR funds are currently sponsoring the development of two new sensor technologies for this program. A new Infra-Red (IR) thermal imaging sensor, currently capable of measuring the temperature of rough, variable emissivity surfaces, is now being modified to provide, in addition, on-line measurement of particle temperature and velocity (*see page 39.*) Another SBIR funded project is investigating emissivity and reflectometry sensors. This research is aimed at providing tools to quantify substrate and coating surface qualities.

Task Outline:

- A) Test methods: *Develop Tools and Procedures for Reproducible Quantitative Analysis*
- 1) **particle size analysis:** sonic sieving of thermal spray powder
 - 2) **surface roughness measurements:** profilometry and confocal metallography
 - 3) **adhesion testing:** 4-point bend testing of coating and substrate
 - 4) **metallography:** specimen preparation of thermal spray coatings
- B) Diagnostic tools: *Develop Tools for Qualitative and Quantitative Measurements of Dynamic Phenomena*
- 1) **schlieren strobe video of thermal spray plumes:** evaluate particle flow and plasma energy fluctuations (see figure on right)
 - 2) **NIR spectrometry:** measure spectrum of thermal spray plasma, use to calibrate imaging pyrometer and to study particle chemistry changes in spray plume
 - 3) **modulation reflectometry:** develop technique to evaluate surface quality before and after coating with thermal spray
 - 4) **thermal imaging of particles and coatings:** validate imaging pyrometer and use to study thermal spray plume and coating
 - 5) **holography to study impact phenomena:** provide data for modeling of particle impacts
- C) Sensors: *Develop Tools for Quantitative Measurements in Real-time for Feedback Control*
- 1) **modulation reflectometry:** provide real-time sensor for measuring substrate and coating surface quality
 - 2) **thermal imaging of particles and coatings:** provide real-time sensor for measuring thermal spray plume and coating characteristics for use in advanced process control system
 - 3) **anode wear sensor:** use time resolved voltage and/or acoustic measurements to monitor anode wear
- D) Processing: *Develop And/or Implement Thermal Spray Equipment to Provide Reproducible Coatings*
- 1) **radial and axial feed DC plasma thermal spray gun**
 - 2) **wire feed DC arc spray gun**
 - 3) **RF plasma spray gun**
 - 4) **process parameter studies:** effects of anode wear and powder size on temperature and velocity and, therefore, coating properties
 - 5) **pure DC powered plasma spray:** study effect of battery supplied current on plasma characteristics
 - 6) **thermal spray process controller:** use new sensors to provide feedback information to control thermal spray gun power, powder feed, and motion.
- E) Modeling: *Develop Tools for Modeling Fluid Flow of Thermal Spray Systems*
- 1) **CFD of radial and axial powder feed plasma spray guns:** study effects of gun geometry, gas flow rates, arc power, and powder feed rate on particle temperature and velocity
 - 2) **CFD of particle impact:** provide particle impact diagnostic data for collaborative work with INEL



Frame sequence from schlieren strobe video of twin wire arc spray.

